Galaxies

Lecture 6: stellar populations in elliptical galaxies; cusp/core and clues to formation

- stellar populations in ellipticals
- Implications of old stars in ellipticals
- Correlation of cusp/core with luminosity
- Clues to elliptical galaxy formation

Stellar populations - overview

- A galaxy may be thought of as a population of stars.
- The distribution of stars can be visualised on the Hertzprung-Russell diagram with axes of either surface temperature versus luminosity or colour versus magnitude.
- The spectral energy distribution (colour) of the galaxy may then be computed as the luminosity weighted integral over the spectral energy distribution (colour) of its constituent stars.

Stellar populations - overview

- Simple stellar populations of single age and chemical composition are best observed in star clusters.
- One can then observe directly how differing stellar ages and chemical compositions determine the integrated properties of a stellar population.
- From this it is a small conceptual leap to understand that the spread of stellar population ages and chemical compositions - *effectively the galaxy star formation history* - are the principle drivers of the observed spectral energy distribution.

Hertzsprung-Russell diagram from HIPPARCOS satellite – bright, nearby stars.

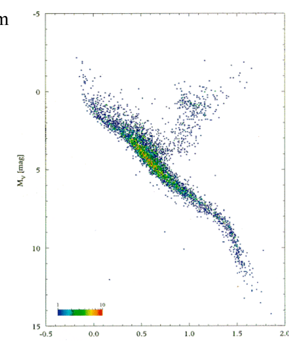

HR diagram: stellar evolution = galaxy evolution

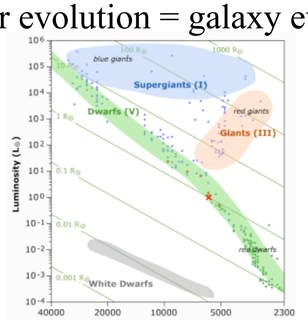

Stellar Populations

•In this sense, we noted that ellipticals are red and spirals are blue.
•From the above discussion we can now understand that
1) spirals are composed of younger, actively forming stellar populations.
2) ellipticals are composed of predominantly old stars with little ongoing star formation

- •Stellar populations in elliptical galaxies are old and simple
- •Combined with the absence of gas and dust in elliptical galaxies we can make some simple statements regarding their *evolutionary history*.

Evolved versus ‘young’ galaxies

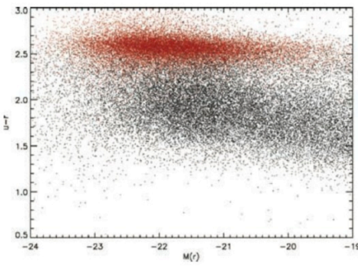

Figure 9. Colour–magnitude diagram for galaxies in the weighted super-clean combined spirals sample. Systems classified as spiral are shown in black, those classified as elliptical in red.

Stellar populations in E’s

- The absence of stars of spectral type A or earlier indicates that typical elliptical galaxies have not experienced major bursts of star formation within the last 5 x 10^{8} years
  - the approximate main sequence lifetime of an A-star.
- (In fact the presence of strong Balmer absorption in the spectra of elliptical galaxies − the signature of a significant A-star population - defines the “E+A” or “k+a galaxy type: a post-starburst elliptical/early-type galaxy.)
- This is consistent with the absence of gas and dust (often correlated with giant molecular clouds and active star forming regions).

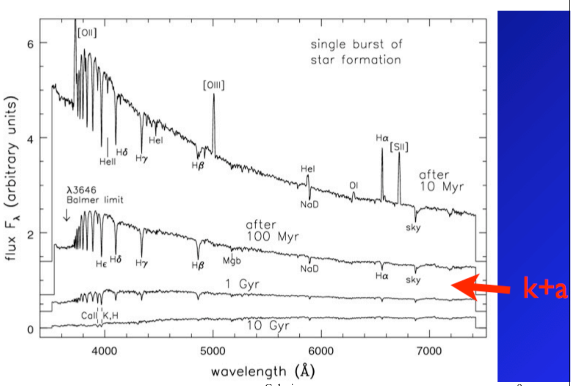

Stellar populations in Ellipticals

- We have seen that fundamental plane and colour magnitude diagram arguments applied to populations of ellipticals point to early, coeval star formation.
- In the absence of young, bright OB stars, the light from ellipticals is dominated by the red giant population, i.e. $L \propto N_{rg}$.
- The number of red giant stars at some time t will be equal to the number of stars with main sequence lifetimes $t - \Delta t_{rg} < t_{ms} < t$.
  - Where Δt_{rg} is the red giant lifetime *(assume constant)*

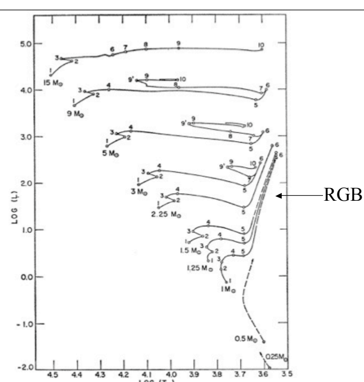

FIG. 3. Paths in the H-R diagram for metal-rich stars of mass $(M/M_\odot)=15$, 9, 5, 3, 2.25, 1.5, 1.25, 1, 0.5, 0.25. Units of luminosity and surface temperature are the same as in Figure 1. Traversal times between labeled points are given in Tables III and IV. Dashed portions of evolutionary paths are estimates.

Stellar populations in E’s

- The luminosity-mass relationship for main sequence stars is $L \propto M^{\alpha}$, with $\alpha \approx 3$ for low mass stars.
- This corresponds to a main sequence lifetime $t_{ms} \propto M/L = M^{1-\alpha}$ if we assume that a fixed fraction of the mass of each star is converted to energy during the main sequence lifetime.
- With this relationship, the range of stellar ages contributing to the red giant population becomes a range of stellar masses, i.e. $M(t_{ms})$ to $M(t_{ms} - \Delta t_{rg}) = M(t_{ms}) + \Delta M$.

Stellar populations in E's

- Defining the stellar initial mass function (IMF) as $dN/dM \propto M^{-1-x}$ as the number of stars in the mass range M to M + dM , then the number of red giant stars can be written as

$$N_{rg} = \frac{\mathrm{d}N}{\mathrm{d}M} \times \Delta M = \frac{\mathrm{d}N}{\mathrm{d}M} \times \frac{\mathrm{d}M}{\mathrm{d}t_{ms}} \; \Delta t_{rg}$$

- Re-writing $t_{ms} \propto M^{-1/\theta}$ with $\theta = 1/(\alpha - 1)$, the number of red giant stars becomes $N_{rg} \propto t^{-1+\theta x}$.
  - Note that we assume that the red giant lifetime is constant and thus acts only as a scaling constant.
- Taking x = –1.35 (the Salpeter IMF) and θ = 1/3, the luminosity of a galaxy dominated by red giant stars becomes $L \propto N_{rg} \propto t^{0.6}$.

Luminosity evolution of E's

- These arguments were first formulated by Gunn, Tinsley and Larson in the mid 1970s.
- The 1980s and beyond saw the advent of the first stellar population synthesis codes for creating evolutionary tracks for integrated stellar populations, e.g. Bruzual and Charlot (1983).
- However, the above analysis approximates fairly well to the luminosity evolution of bright ellipticals: $L \propto N_{rg} \propto t^{0.6}$ (passive evolution: fading)

The Fundamental Plane

- The FP relation can be reconstructed using the following arguments

$$R_e^2 = \frac{L}{2\pi I_e}$$

$$R_e = \frac{M}{c\sigma_e^2}$$

with this secon... a statement of virial equilibrium and ***c*** denoting a combination of physical constants.

The Fundamental Plane

- Dividing these two equations one obtains

$$R_e = \left(\frac{c}{2\pi}\right)\left(\frac{M}{L}\right)^{-1} \sigma_e^2 I_e^{-1}$$

$$\log R_e = 2\log\sigma_e - \log I_e + \log\left[\frac{2}{2\pi}\left(\frac{M}{L}\right)^{-1}\right]$$

$$\log R_e = 2\log\sigma_e - 0.4\Sigma_e + \log\left[\frac{2}{2\pi}\left(\frac{M}{L}\right)^{-1}\right]$$

whi... ...d FP relation.

The Fundamental Plane

- We conclude that

1. Bright ellipticals are in virial equilibrium.
2. To 1st order M/L ratios and structural parameters are very similar.
3. Therefore, their stellar populations, ages and DM properties are very similar.
4. To obtain an exact match to observed FP data requires $M/L \propto M^{0.2}$, i.e. massive ellipticals are slightly older than less massive counterparts.

Ages ~ 10 - 13 Gyr; Z ~ 2-4 Z(solar)

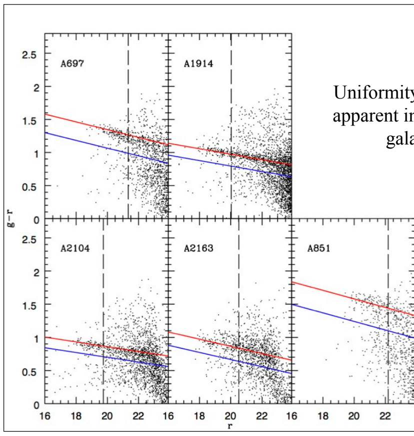

Uniformity especially apparent in clusters of galaxies

Back to Profiles:
more clues to formation

Parameterization of the Surface Brightness Profiles:

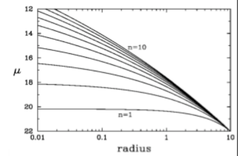

- Sersic law (Sersic 1968): $I(R) = I_e \exp(-b_n[R/R_e)^{1/n} -1])$
- Has a number of attractive features for parameterizing both the small - and large-scale profiles of E/dE galaxies:
  - Accounts for the profiles' curvature on kpc-scales
  - Parameters are robust against radial range of data (Graham et al. 2003)
  - Integrals for r->infinity converge (c.f., Nuker law)

L. Hernquist (6 Nature papers in 1992 on simulations of galaxy formation!)

- One of the drawbacks of the de Vaucouleurs surface brightness distribution is that it does not have an analytic counterpart in 3D density.
- Various density profiles have been suggested that provide a good match to observed surface brightness profiles when projected, e.g. the Hernquist (1990) profile

$$\rho(r) = \frac{M}{2\pi} \frac{r_c}{r(r + r_c)^3}$$

- The Hernquist model is particularly appealing as it arises from the numerical simulation of the merger of two equal mass disk galaxies, each embedded within a dark matter halo.

Hernquist profile (1990)

AN ANALYTICAL MODEL FOR SPHERICAL GALAXIES AND BULGES

Lars Hernquist
Institute for Advanced Study, Princeton, New Jersey
Received 1989 October 23; accepted 1989 December 19

ABSTRACT

A potential-density pair which closely approximates the de Vaucouleurs $R^{1/4}$ law for elliptical galaxies is presented. It is shown that the intrinsic properties and projected distributions of this model can be evaluated analytically. In particular, the distribution function, density of states, and projected surface brightness and velocity dispersion are expressible in terms of elementary functions.

Subject headings: galaxies: photometry — galaxies: structure

Hernquist profile (1990)

I. INTRODUCTION

It has long been recognized that the observed luminosity distribution of many elliptical galaxies and bulges is well represented by the empirical law

$$\log_{10}\left[\frac{I(R)}{I(R_e)}\right] = -3.331\left[\left(\frac{R}{R_e}\right)^{1/4} - 1\right], \qquad (1)$$

where R is the projected radius on the plane of the sky, R_e is the effective radius of the isophote enclosing half the light, and I is the surface brightness (de Vaucouleurs 1948; Kormendy 1977). Although convenient for representing the observable properties of galaxies and bulges, the de Vaucouleurs profile is less useful for theoretical analyses since its deprojected mass density, $\rho(r)$, is not tractable analytically (e.g., Young 1976). This fact motivates interest in density profiles resembling that of the $R^{1/4}$ law but which have simple analytic forms.

Hernquist profile (1990)

The potential, $\varphi(r)$, is found by integrating Poisson's equation. For the density in equation (2)

$$\varphi(r) = -\frac{GM}{r + a}, \qquad (5)$$

Note that $\overline{v_r^2}$ is nowhere divergent. If $r \ll a$,

$$\overline{v_r^2} \sim \frac{GM}{a}\frac{r}{a}\ln\frac{a}{r}, \qquad (11)$$

and so $\overline{v_r^2}$ goes to zero at the center, while $\overline{v_r^2} \sim GM/5r$ in the limit $r \gg a$. If, instead, all stars are on circular orbits, $\overline{v_r^2} = 0$

Hernquist profile (1990)

b) Projected Distributions

The projected surface brightness of the present model can be computed by integrating its luminosity density along lines of sight. Let Υ be the constant mass-to-light ratio. Then the surface brightness is

$$I(R) = \frac{M}{2\pi a^2 \Upsilon (1 - s^2)^2} [(2 + s^2)X(s) - 3] \,, \tag{32}$$

where $s = R/a$, R is the projected radius and

$$X(s) = \frac{1}{\sqrt{1 - s^2}} \operatorname{sech}^{-1} s \quad \text{for} \quad 0 \le s \le 1 \,, \tag{33}$$

$$X(s) = \frac{1}{\sqrt{s^2 - 1}} \sec^{-1} s \quad \text{for} \quad 1 \le s < \infty \,. \tag{34}$$

Cuspy versus cored

- Elliptical galaxies display a range of surface brightness properties from
- luminous, cored galaxies
  - show near constant surface brightness within some core radius
- to less luminous cuspy galaxies
  - the central surface brightness continues to rise to a sharp peak at inner radii.
- Consider next slide comparing the galaxies NGC 1399 (a luminous Elliptical galaxy, Mv = −21.9) and NGC 596 (Mv = −20.9, about half as luminous).
  - Though the inner surface brightness of NGC 1399 is $I(R) \propto R_0$ i.e. constant, we can see that this corresponds to a mass density $\rho(r) \propto r^{-1}$ (Hernquist or de Vaucouleur profiles).
  - NGC 596 displays $I(R) \propto R^{-0.5}$ and thus $\rho \propto r^{-1.5}$ and possesses and even steeper central mass density profile - modified Sersic.

Cores/Cusps

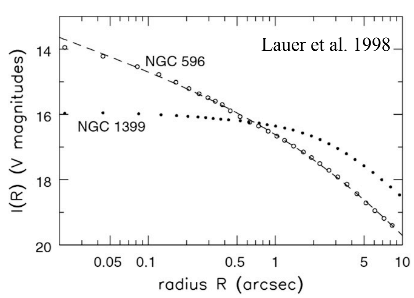

Cuspy versus cored

- Recall that $1 L_\odot pc^{-2} = 26.4\ M_V\ arcsec^{-2}$.
- Therefore, the central surface brightness of NGC 1399 of $I_V(0) = 16$ corresponds to a stellar surface density of dex [(26.4 − 16)/2.5] = 14, or 450 $L_\odot pc^{-2}$.
- The central stellar density of NGC 596 is approximately $5 \times 10^5\ L_\odot pc^{-2}$.
  - Recall that the central stellar surface density of a spiral galaxy such as NGC 7331 reaches only 350 $L_\odot pc^{-2}$.
- These surface brightness trends were first quantified by Kormendy (1977). Luminous galaxies are increasingly core dominated according to the relation $\mu_e = 20.2 + 3 \log R_e$ or $M_B = -19.3 - 2 \log R_e$.
- Taking $\mu_e = -2.5 \log I_e$ and $M_B = -2.5 \log L_B$, one obtains $I_e \propto R_e^{-1.2} \propto L^{-1.5}$ and $L_B \propto R_e^{0.8}$ (and notice that $L \propto I_e R_e^2$ as expected).

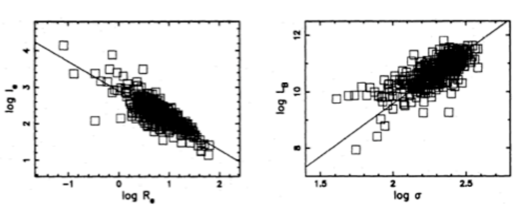

Kormendy (1977) Faber & Jackson (1976)

Cuspy versus cored

- At this point we emphasize again that this relation holds for bright elliptical galaxies. As we shall see, faint ellipticals appear to follow a different linear relation.
- The variation in the central surface brightness properties certainly points to ***variations in their evolutionary histories.***
- Indeed, the debate as to whether bright, cored ellipticals and faint, cuspy ellipticals are separate populations or not still continues actively.
- We will consider this further below. However, at this point we can note

1) within the hierarchical view of galaxy formation that sees massive galaxies constructed from the accretion of smaller sub units,
2) the presence of lower surface density cores in bright galaxies may well arise from the increased energy present in stellar orbits resulting from past mergers.

Reconciling bright and faint ellipticals

- Morphological classification and magnitude cuts lead to the definition of giant and dwarf ellipticals as bulge-dominated systems with $M_V < -18$ and $M_V > -18$ respectively.
- In addition, dwarf spheroidal galaxies form an ill-defined class of very faint spheroidal (i.e. not a disk and not irregular) galaxies with $M_V > -11$ or so.
- Plotting such objects on 2D scaling relation diagrams (e.g. Kormendy) reinforces the idea that Es, dEs and dSphs are physically distinct classes of objects.
- As such we need to explain their origins.

- Ellipticals, dSphs, and globular star clusters are not all obviously an extension of the same spheroid sequence … (dSphs later lecture)

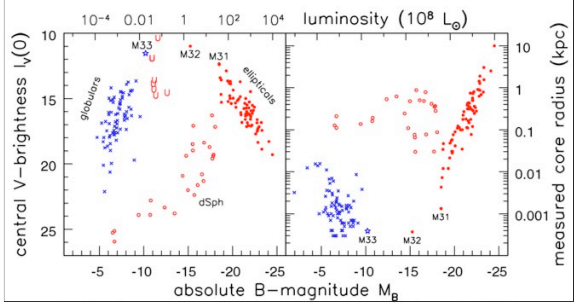

Reconciling bright and faint ellipticals

- However, an alternative view is to consider them as essentially a single class of galaxy with a continuum of slowly changing physical properties.
- Put another way, if one is to classify them as separate galaxy class, where should you draw the line?
- Is an elliptical galaxy with MV = −18.2 physically distinct from an elliptical with MV = −17.8?
- One manifestation of this continuum of physical properties is the variation of central (i.e. $R \approx 0.02R_e$) surface brightness properties as a function of magnitude.

Reconciling bright and faint ellipticals

Taking a sample of bulge dominated galaxies from either the Virgo of Fornax clusters one observes that bright ($M_V < -18$) galaxies display a central luminosity deficit with respect to a single de Vaucouleurs/Sersic model, i.e. an approximately constant surface brightness core.

This core is modeled as a power law of slope α with a smooth transition to a larger scale Sersic profile -- the so-called core-Sersic model.

A Modification of the Sersic Model

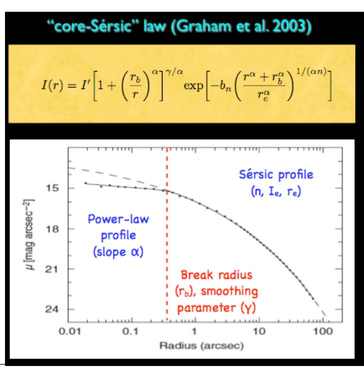

Motivation for the Core-Sersic Parameterization: VCC1978 (M60)

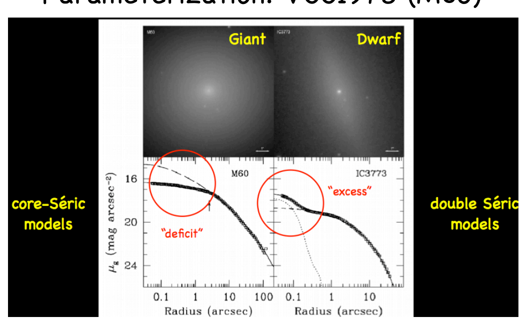

Reconciling bright and faint ellipticals

- At fainter magnitudes (MV > −18), galaxies display a central luminosity excess with respect to a single model fit, i.e. a bright nuclear region fit with an additional Sersic component (a double Sersic model).
- Viewing the sample of galaxies as a function of magnitude one observes that the trend from central deficit to central excess galaxies is relatively (there is some scatter) smooth and continuous.

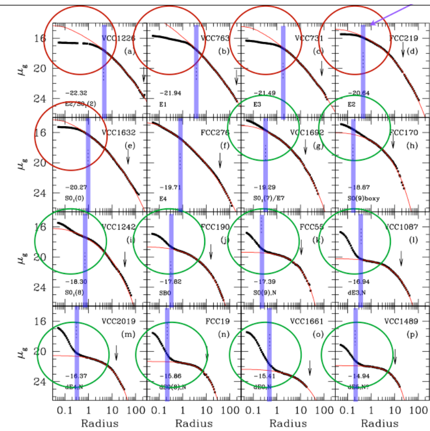

Reconciling bright and faint ellipticals

- Finally, one can plot all of the parameters normally considered in 2D scaling relations, e.g. $\mu 0$, Sersic n, Re , μe , $\langle\mu\rangle$e , as a function of magnitude.
- This reveals a smooth, continuous variation of galaxy properties from giants, through dwarfs, to dwarf spheroidals.
- Certainly if one selected any pair of these properties, e.g. μe and Re (the Kormendy relation), one would compute different linear relations for dwarfs and giants and perhaps conclude that they represented different classes of galaxy.
- Clearly though the changing gradient of quantities such as μe versus M_B do reflect different physical histories as a function of brightness (mass) and we consider these below.

Scaling Relations of RS Galaxies

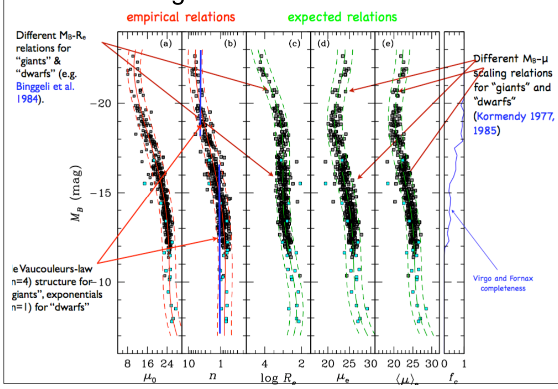

Mergers

- Although the scaling relations extend continuously over a factor of 10^6 in mass, the most massive galaxies in the Universe appear to be ellipticals or spheroids. Why should this be the case?
- Stars in an (idealized) equilibrium system should form in a disk and stay in a relatively disk-like structure.
- At the same time, the stars in mergers (either the pre-existing ones or those formed during the merger) should undergo *violent relaxation* and be redistributed in spheroidal components.
  - violent relaxation: rapid evolution of a stellar system that has formed out of equilibrium. Orbits can rapidly due to the rapid changes in the underlying gravitational potential. [See Chap. 4 of Binney & Tremaine 1987.]

Mergers

- CDM (cold dark matter) cosmologies are "bottom up" in the sense that the larger systems are formed hierarchically from repeated mergers of low-mass ones.
- Simulations predict that most massive (spheroidal) galaxies should indeed have experienced many mergers in their lifetime, including several major mergers after star formation was largely complete.

Mergers: stellar disks

- Mergers of (equal-mass) stellar disks generally give rise to roughly spheroidal-like profiles (i.e., ≈ $R^{1/4}$-law surface brightness profiles).
- But these simulations fail to reproduce the central structure of spheroidal galaxies: i.e., the central (phase space) densities are too low. Suggests that gas is required.
- phase space density: f(r,v,t) = the number of stars at r with v at time t in the range d^3r and d^3v.

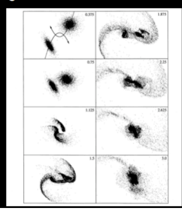
Barnes (1992)

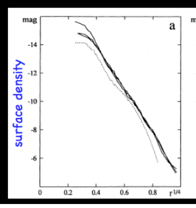

Mergers: addition of gas

- If gas is added to the simulations, some gas undergoes a rapid inflow from angular momentum loss caused by gravitational and hydrodynamic torques (which generally depend on the alignment/orbits/structure of the progenitors).

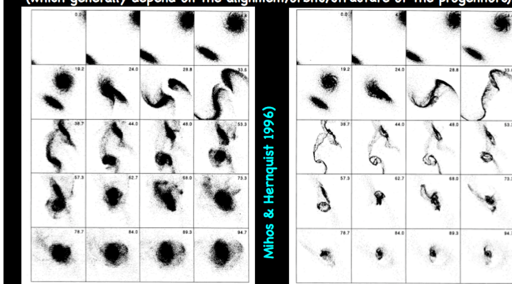

Cote et al. (2007)

The Astrophysical Journal, 437:L47–L50, 1994 December 10

DENSE STELLAR CORES IN MERGER REMNANTS

J. Christopher Mihos and Lars Hernquist[1]
Board of Studies in Astronomy and Astrophysics, University of California, Santa Cruz, CA 95064;
hos@lick.ucsc.edu, lars@lick.ucsc.edu
Received 1994 August 15; accepted 1994 September 26

ABSTRACT

We use numerical models which include star formation to analyze the mass profiles of remnants formed by mergers of disk galaxies. During a merger, dissipation in gas and ensuing star formation leave behind a dense stellar core in the remnant. Rather than joining smoothly onto a de Vaucouleurs profile, the starburst population leads to a sharp break in the surface density profile at a few percent of the effective radius. While our results are preliminary, the lack of such signatures in most elliptical galaxies suggests that mergers of gas-rich disk galaxies may not have contributed greatly to the population of present-day ellipticals.
Subject headings: galaxies: elliptical and lenticular, cD — galaxies: evolution — galaxies: interactions — galaxies: starburst — galaxies: structure

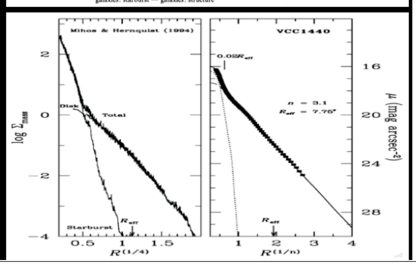

Data hadn't caught up with galaxy formation predictions!

45

Formation of Elliptical Galaxies

Formation of Elliptical Galaxies: basic principles

- How do ellipticals form? In a hierarchical universe massive galaxies are predicted to be the result of the successive mergers of less massive galaxies (White and Rees 1978).
- The weak dependence of the M/L ratios of bright ellipticals on their mass indicates that star formation – potentially associated with the merging/mass assembly process – occurred earlier in more massive galaxies.
- This is reasonable insofar that galaxies (or pre-galactic clumps) in dense regions of the universe would be expected to merge faster and earlier, leading to the production of more massive galaxies.
- Merging produces an incoherent mix of stellar orbits.

Formation of Elliptical Galaxies: basic principles

- As we have seen, long two-body relaxation times preserve the memory of individual encounters in the form of stellar streams, tidal tails and stellar shells.
- However, violent relaxation – stellar encounters in a rapidly changing potential – results in more complete orbital mixing.
- The products of N-body simulations recreating the merger of massive disk dominated galaxies produce slowly rotating, pressure-supported bulge dominated galaxies
- Hernquist-like 3D density distributions indicate that they would result in de Vaucouleurs-type surface brightness distributions (Hernquist 1992).

Formation of Elliptical Galaxies: basic principles

- The central surface brightness profiles of bright ellipticals are “core-like”, i.e. flattening toward the centre. This suggests that they formed via “dry” or gas-poor merging.
- This is a collisionless process – little angular momentum is lost via two-body encounters – and the additional orbital angular momentum of the merging galaxies results in a “puffing up” of the central stellar distribution.

Formation of Elliptical Galaxies: basic principles

- However, as one moves to fainter ellipticals there is a relatively smooth trend to observe high-surface brightness stellar nuclei.
- This suggests an increasing importance of “wet” or gas-rich mergers as one considers lower mass ellipticals.
- Gas-rich mergers are collisional and the orbital angular momentum of the merging galaxies can be dissipated away. This allows the gas to accumulate in the centres of such systems, potentially triggering dense, nuclear starbursts.

Formation of Elliptical Galaxies: basic principles

- Bright ellipticals and faint ellipticals form a single family; they are not fundamentally different objects. This can be seen from plots (previous slides) showing the continuity of scaling relations of red-sequence selected galaxies (ellipticals).

Formation of Elliptical Galaxies: basic principles

- The relations linking bright and faint ellipticals are not linear. Put another way, if you tried to define linear scaling relations (e.g. the Kormendy relation) for bright and faint ellipticals you would compute different gradients and assume that the ob jects are different.
- However, it is clear that different physical effects have played a role in the evolution of bright and faint ellipticals and that there appears to have been a relatively smooth transition between competing effects as a function of luminosity (mass).

Formation of Elliptical Galaxies: basic principles

- Elliptical galaxies dominate the galaxy populations in the centres of rich clusters. However, the Butcher-Oemler effect indicates that the ellipticals we observe in rich clusters today have undergone relatively recent transformation.
- This suggests that merging/interactions, accentuated by ram pressure stripping, have played a role in their formation.

Elliptical Galaxies

Lectures 7: the isothermal sphere, King profile

- Collisionless Boltzmann Equation
- Isothermal sphere and King model
- M/L ratios and DM

Myths of Elliptical Galaxies?

- Our view of Elliptical galaxies has changed greatly : In the 1970s, Ellipticals were thought to be :
- Diskless bulges with deVaucouleurs ($R^{1/4}$) profiles and constant density (King) cores.
- Oblate spheroids flattened by rotation
- Void of gas and dust
- Contain a single ancient population of stars
- Relaxed dynamically quiescent systems
- To a large extent, **all** of the above are now thought to be wrong.

Profiles

- Early (pre-1975) work suggested that I(R) turned over in a **flat core** of constant density
- This was naturally understood in terms of isothermal and King models (see below)
- However, the **serious** influence of atmospheric seeing, had not been appreciated.
- For all but the most luminous ellipticals, the existence of flat cores was shown to be **incorrect** using Hubble Space Telescope imaging.

Isothermal and King Profiles

- Historically, isothermal and King models were used to understand "flat cores":
- Because they yield simple physical results, it is worth looking at them.
- They assume a self-gravitating spherical system with isotropic velocity dispersion.
- They have a Boltzmann distribution in star energy (potential + kinetic)

Isothermal and King Profiles

- Their projected light, I(R), turns over in a **flat core**, with known dynamical properties:
  - Within $3r_0$ it approximates the modified Hubble law: $I(R) = I(0) / [1 + (R/r_0)^2]$
  - It has a central density $\rho(0) = 9\,\sigma(0)^2/4\,\pi G r_o^2$
  - It has core M/L ratio = $\rho(0)/j(0)$ where $j(0)=0.495\, I(0)/r_o$
- At large R, isothermal models have $j(r) \sim R^{-2}$ with divergent mass.
- King models introduce a cutoff in energy that truncates the outer profile yielding finite mass.
- **Important Note:** These models in general do **not** make good fits to Elliptical galaxies.
- However, they yield quick estimates of $\rho(0)$ and M/L.

Isothermal profiles

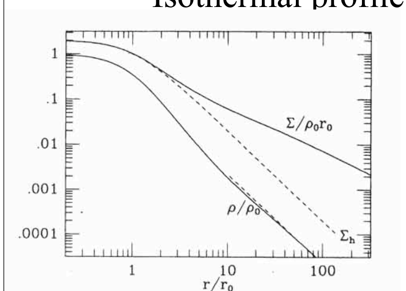

Figure 4-7. Volume (ρ/ρ_0) and projected ($\Sigma/\rho_0 r_0$) mass densities of the isothermal sphere. The dashed line at bottom right shows the density profile of the singular isothermal sphere. The dashed curve labeled Σ_h shows the surface density of the modified Hubble law (4-128).

Isothermal profiles, showing both space and projected density (= luminosity for constant M/L).

The inner regions ($r < 3r_0$) closely match the modified Hubble profile (dashed line).

King profiles

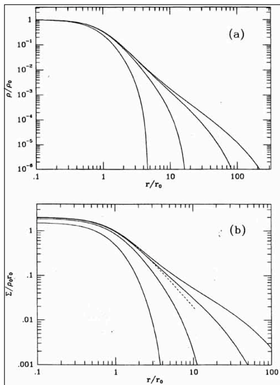

Figure 4-9. (a) Density profiles of four King models: from top to bottom the central potentials of these models satisfy $\Psi(0)/\sigma^2 = 12, 9, 6, 3$. (b) The projected mass densities of these models (full curves), and the projected modified Hubble law (dashed curve).

- A series of King profiles with different concentrations (specified here by the central potential).
- The central regions are similar to the isothermal sphere.

Collisionless Boltzmann Equation

- We first consider **collisionless** dynamics: "Collision", here, means star-star **deflection**, not direct impact
- For the collisionless case, stars are assumed to move in a **completely smooth** potential
- For galaxies this is **almost always** a very good approximation

The Distribution Function (DF) : f(r, v, t)

- A system is fully described by its **distribution function** (DF) or **phase space density** : f(**r, v**, *t*)d^3**r**d^3**v** = number of stars at **r** with **v** at time *t* in range d^3**r** and d^3**v**
- Knowledge of the DF is a holy grail, since it yields complete information about the system In practice, however, we only observe certain **projections** of the DF (eg Σ(R), V_p(R), σ_p(R))
- Recovering the DF directly from observations is essentially impossible.
- To proceed, we need to introduce **further constraints** on the DF
- an obvious example is f(**r**, **v**, t) > 0 everywhere and always, ie we cannot have -ve # stars!
  - However, there are other constraints :

Collisionless Boltzmann Equation

- Look for a **continuity equation,** since
- no stars created/destroyed : flow conserves stars
- stars do not **jump** across the phase space (ie no **deflective** encounters)
- View the DF as a moving fluid of stars in 6-D space (**r, v**), ie x,y,z,v_x,v_y,v_z stars move/flow through the region as their positions and velocities change

CBE

- Consider a 1-D example using x and v_x
- recall f is a number **density**
- focus on a small element of phase space at x and v_x with size dx by dv_x

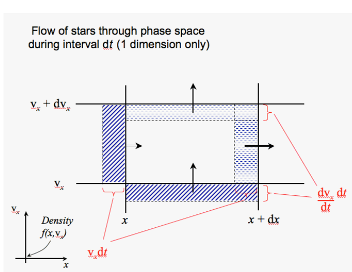

CBE

- In interval dt, net flow in x is :

$$v_x dt\, dv_x\, [f(x, v_x, t) - f(x + dx, v_x, t)] \;=\; -v_x\, dt\, dv_x \frac{\partial f}{\partial x}\, dx$$

- the net flow due to the velocity gradient is

$$dx\, \frac{dv_x}{dt} dt\, [f(x, v_x, t) - f(x, v_x + dv_x, t)] \;=\; -dx\, dt\, \frac{dv_x}{dt} \frac{\partial f}{\partial v_x} dv_x$$

- the sum of these equals the net change to f in the region, ie, at x, v_x of size dx dv_x

$$dx\, dv_x \frac{\partial f}{\partial t} dt \;=\; -dt\, dx\, v_x \frac{\partial f}{\partial x}\, dv_x - dx\, dt\, \frac{dv_x}{dt} \frac{\partial f}{\partial v_x}\, dv_x$$

CBE

- dividing by dx dv_x dt, we get

$$\frac{\partial f}{\partial t} + v_x \frac{\partial f}{\partial x} + \frac{dv_x}{dt}\frac{\partial f}{\partial v_x} = 0$$

- but since

$$\frac{dv_x}{dt} = a_x = -\frac{\partial \Phi}{\partial x}$$

- we have

$$\frac{\partial f}{\partial t} + v_x \frac{\partial f}{\partial x} - \frac{\partial \Phi}{\partial x}\frac{\partial f}{\partial v_x} = 0$$

- adding the y and z dimensions, which are independent, we finally have

$$\frac{\partial f}{\partial t} + \mathbf{v} \cdot \nabla f - \nabla \phi \cdot \frac{\partial f}{\partial \mathbf{v}} = 0 \qquad \text{The CBE!}$$

CBE

- The CBE describes how the DF changes in time. It is a direct consequence of :

1 conservation of stars
2 stars follow smooth orbits
3 flow of stars through **r** defines implicitly the location **v** (= d**r**/dt)
4 flow of stars through **v** is given explicitly by -grad(Φ)

CBE

- What we **observe** are :
  - **mean** velocities : < v >
  - velocity **dispersions** : (which is related to < v^2 >)
  - stellar **densities** : n (also ρ for mass density, or j for luminosity denisty)
- 0th moment in v: $\int$ f(**r, v**) d^3v = n(**r**) = ρ(**r**)

which could, in principle, define Φ (impose this cdt later)

- 1st moment in v: mean velocity = <v_i(**r**, t)>
  = (1/n) $\int$ v_i f(**r, v**) d^3v
- These first two moments of CBE give us the Jeans equation …

Jeans equation

- Using the 1-D x axis as example, simply integrate the CBE over all v_x. We obtain (0th moment in v_x) :

$$\frac{\partial f}{\partial t} + v_x \frac{\partial f}{\partial x} - \frac{\partial \Phi}{\partial x}\frac{\partial f}{\partial v_x} = 0 \longrightarrow \frac{\partial n}{\partial t} + \frac{\partial\big(n\langle v_x\rangle\big)}{\partial x} = 0$$

- (term in Φ goes to 0 with integral of *f* as *v*->infinity)
- where n = n(x,t) is the space density and <v_x> is the mean drift velocity along x
- This is a simple continuity equation for the number of stars along the x axis.

Jeans Equation

- Now multiply the CBE through by v_x and again integrate over all v_x
- on rearranging and using 0th moment above, we obtain (1st moment in v_x) :

$$\frac{\partial f}{\partial t} + v_x \frac{\partial f}{\partial x} - \frac{\partial \Phi}{\partial x}\frac{\partial f}{\partial v_x} = 0 \longrightarrow$$

$$\frac{\partial\langle v_x\rangle}{\partial t} + \langle v_x\rangle\frac{\partial\langle v_x\rangle}{\partial x} = -\frac{\partial \Phi}{\partial x} - \frac{1}{n}\frac{\partial(n\sigma_x^2)}{\partial x}$$

- where σ_x^2 is the velocity dispersion about the mean velocity, it arises from $\langle v_x^2\rangle = \langle v_x\rangle^2 + \sigma_x^2$

Applications of Jeans Equation

The Jeans equation, when combined with observations, has a number of applications (some of which we'll examine next week in context of the Milky Way and Local Group of galaxies, including dSph's):

- deriving M/L profiles in spherical galaxies
- deriving the flattening of a rotating spheroid with isotropic velocity dispersion
- analysis of asymmetric drift
- surface density (and volume density) in the galactic disk

Profile Analysis

- Taking moments of the CBE lost almost all detailed information from the DF
- Rather than working with the full DF, the Jeans equation works with just n, <v> and <v^2>
- Can we reintroduce the full DF and regain a more complete description of a system ?
- **yes**, by introducing two new powerful constraints :
  – demand that the system is in **steady state** (in equilibrium, independent of time)
  – demand that the DF **generate the full potential** -- via Poisson's equation (ie: not just act as a tracer population)

Self-Consistency -> profile analysis

- an important step is to **require** that the DF **also** yields the potential $\Phi(\mathbf{r})$

$$4\pi G \int f(\mathbf{r},\mathbf{v})\, d^3\mathbf{v} \;=\; 4\pi G\rho(\mathbf{r})$$
$$= \nabla^2\Phi(\mathbf{r}) \qquad \text{Poisson's equation}$$

- In spherical form: (eg for a DF of the form f (E, |L|)

$$\frac{1}{r^2}\frac{d}{dr}\left(r^2\frac{d\Phi}{dr}\right) \;=\; 4\pi G \int f(\tfrac{1}{2}v^2+\Phi\,;|\mathbf{r}\times\mathbf{v}|)\,d^3\mathbf{v} \qquad (*)$$

- This is now a fundamental equation describing spherical equilibrium systems.
- Solutions not only have self consistent Φ and f, but f also satisfies the steady state CBE.
- **Such a solution now describes a self-consistent, physically plausible stellar dynamical system.**

Spherical Isotropic Systems : DF = f(E_r)

Take f = f(E_r) adopting the following variables

- **relative potential** : $\Psi \;=\; \Phi_o - \Phi$
- **relative energy** : $E_r \;=\; -E + \Phi_o \;= \Psi - 1/2\, v^2$
- note : both Ψ and E_r are more +ve for more bound stars deeper in the system (smaller r)
- choose Φ_o so that f > 0 for E_r > 0 (bound)

Spherical Isotropic Systems : DF = f(E_r)

- (*) takes the form [recall $d^3v = 4v^2\, dv$]

$$\frac{1}{r^2}\frac{d}{dr}\left(r^2\frac{d\Psi}{dr}\right) \;=\; -16\pi^2 G\int_0^{\sqrt{2\Psi}} f(\Psi-\tfrac{1}{2}v^2)\,v^2\,dv$$
$$= -16\pi^2 G\int_0^{\Psi} f(E_r)\,\sqrt{2(\Psi-E_r)}\,dE_r$$

- These now describe a spherical, non-rotating, isotropic velocity dispersion system.
- They will be our starting point in constructing specific spherical models below

Model building with distribution functions (DFs)

- begin with the simplest cases : equilibrium, non-rotating, spherical systems, ie, DF = f(E_r)
- (1) Choose a DF which is a function of energy : f(E_r) = f(Ψ - 1/2v^2)
  – Can show that f(E_r) is already a solution to the steady state CBE,
  – so our solutions will naturally satisfy the basic phase space continuity condition
- (2) Integrate the DF over v to find $\rho(\Psi)$
- (3) Solve Poisson's equation to find $\Psi(r)$
- (4) Combine $\rho(\Psi)$ and $\Psi(r)$ to give the mass distribution : $\rho(r)$

Isothermal Sphere

- Consider an **exponential or isothermal** (Boltzmann) DF as first guess at representing spherical stellar system

$$f(E_r) \;=\; \frac{\rho_1}{(2\pi\sigma^2)^{\frac{3}{2}}}\, e^{E_r/\sigma^2}$$

- Recall, more +ve Ψ & E_r means more bound.
- Also, note f(E_r) > 0 for E_r < 0: there are unbound stars! .... we anticipate problems at large radii.
- substituting Ψ - 1/2v^2 for E_r and integrating f(E_r) over v gives $\rho = \rho_1 \exp(\Psi / \sigma^2)$

Isothermal Sphere

- Plugging this into Poisson's equation gives :

$$\frac{d}{dr}\left(r^2 \frac{d\ln\rho}{dr}\right) \;=\; -\,\frac{4\pi G}{\sigma^2}\,r^2\rho$$

- This is, in fact, the equation for a hydrostatic sphere of isothermal gas, with σ^2 = kT/m

- consider the solutions …

Singular Isothermal Sphere

- For the central boundary condition $\rho(0)$ = infinity, we have $\rho(r) = \sigma^2 / (2\pi\, G\, r^2)$
- this is the **singular isothermal sphere**: $\rho \sim r^{-2}$
- Circular velocity : V_c = const = σ sq(2)
- Dispersion velocity : $\langle v^2 \rangle = 3\sigma^2$ everywhere (isothermal); 1-D : $\langle v_r^2 \rangle = \sigma^2$
- But the model has infinite density at r = 0, and has infinite mass as r goes to infinity!

Density; potential; rotation & image for SIS :

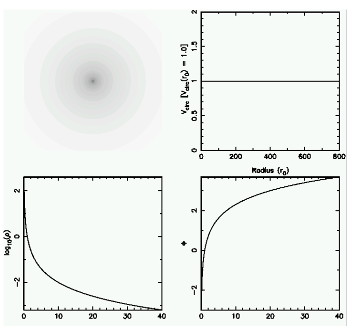

General Isothermal Sphere

- Choose as central boundary conditions at r = 0 :
- $\rho(0) = \rho_o$ finite central density
- $(d\rho/dr)_{r=0} = 0$ flat central density profile
- Integration of Poisson's equation with these boundary conditions yields $\rho(r)$

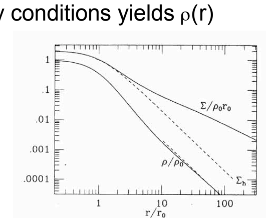

General isothermal sphere

- We find a **constant** near-nuclear density : $\rho(r) \sim \rho_o$ within a radius $r_o = 3\,\sigma / (4\,\pi\, G\, \rho_o)^{1/2}$
- This is a **core** and r_o is called the King (or core) radius $I(r_o) = 0.5013\, I(0)$, so r_o is appropriately defined
- r_o is also the scale length of the r^{-2} envelope (see below): big cores are in big galaxies
- Circular velocity : $V_c = -\,\sigma\,(d \ln \rho / d \ln r)^{1/2}$

General isothermal sphere

- When plotted as $\log(\rho / \rho_o)$ vs $\log(r / r_o)$, there is only **one** isothermal profile
- At **small** radii (e.g. r < few r_o) the **density law** resembles the Hubble density law : $\rho(r) \sim (1 + (r / r_o)^2)^{-3/2} = \rho_H(r)$
  I(R) fits ~OK to the centers of many Elliptical galaxies
- At **large** radii (e.g. r > 15 r_o) the system resembles the SIS : $\rho(r) \sim (r / r_o)^{-2}$ and $V_c = \sigma$ sqrt(2)
- this is **different** from the Hubble density Law:
  - projected light profile **does not** fit Ellipticals well in the outer parts (too flat)

General Isothermal Sphere

- The scale length and central density together define the dispersion : $\sigma^2 \sim \rho_o r_o^2$
- for a given central density, hotter galaxies are larger
- for a given core radius, hotter galaxies are denser
- basically, stars are bound and must not escape
- Quantitatively : $\sigma^2 = (4/9) \pi G \rho_o r_o^2$
  - To simplify calculations, use $G = 4.5 \times 10^{-3}$ in units of pc, km/s, and Msun
- Eg: for $\sigma = 100$ km/s, $r_o = 100$ pc
  we have $\rho_o = 159$ Msun pc^{-3}

General Isothermal Sphere

- A good isothermal core match to the centers of Ellipticals can be used to estimate central M/L
- obtain r_o and I(0) from isothermal fits to I(R), and measure σ
  - (express I(0) in units of Lsun pc^{-2} to allow simplified calculations with $G = 4.5 \times 10^{-3}$)
  - $j(0) = 0.5\, I(0) / r_o$
  - $\rho(0) = 9 \sigma^2 / (4\pi G r_o^2)$
  - $M/L = \rho(0) / j(0)$

This method is called "core fitting" or "King's method"

Typical values for ellipticals cores are ~10-20 solar M/ L suggesting ***minimal/no dark matter***

General Isothermal Sphere

- There is a problem with all isothermal models: **they have infinite total mass**
- It is easy to see why the system is at least infinite in extent :
  - at any given radius, stars have isotropic dispersion
  - at this radius at least some stars are therefore moving **outward**
  - but further out the dispersion is **still** σ, and stars are moving outward
- the system must have infinite extent
- Ultimately, this arises because $f(E_r) > 0$ for negative E_r, i.e. the model includes **unbound stars**.
- To rectify this problem, we attempt to modify things slightly by removing the unbound stars:

King model

- Suppress stars at large radius (ie as E_r -> 0, we want $f(E_r)$ -> 0) modify the exponential DF :

$$f(E_r) = \frac{\rho_1}{(2\pi\sigma_0^2)^{\frac{3}{2}}} \left(e^{E_r/\sigma_0^2} - 1\right)$$

- Repeating the same analysis as before, we get for Poisson's eqn :

$$\frac{d}{dr}\left(r^2 \frac{d\Psi}{dr}\right) = -4\pi G \rho_1 r^2 \left[e^{\Psi/\sigma_0^2} \mathrm{erf}\left(\frac{\sqrt{\Psi}}{\sigma_0}\right) - \sqrt{\frac{4\Psi}{\pi\sigma_0^2}}\left(1 + \frac{2\Psi}{3\sigma_0^2}\right)\right]$$

King model

- Solve this by integration, choosing boundary conditions at r = 0 :
- $\Psi(0) = q\, \sigma_o^2$ (q > 0, large q = deep central potential)
- $d\Psi / dr = 0$ (as before)
- Inner regions : like isothermal, with core (King) radius ~ r_o (defined as before)
- Outer regions : (r) decreases & approaches 0 at r_t
- note : velocity **range** at Ψ is 0 -> Ψ sqrt(2)
- so density = int(f d^3v) = 0 at r_t = **tidal** or **truncation radius** = **edge** of sphere
- larger $\Psi(0)$ (larger q) -> larger r_t & $M_{tot} = M(r_t)$
- Alternative parameter to $\Psi(0)$ or q is **concentration** $c = \log_{10}(r_t / r_o)$

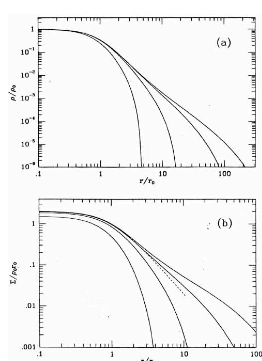

Figure 4-9. (a) Density profiles of four King models: from top to bottom the central potentials of these models satisfy $\Psi(0)/\sigma^2 = 12, 9, 6, 3$. (b) The projected mass densities of these models (full curves), and the projected modified Hubble law (dashed curve).

King Profile

- Single sequence of King models by varying (equivalently) : $\Psi(0)$; q; c
- Empirically, we find :
- c = 0.75 - 1.75 (q = 3 - 7) fit GCs very well
- c > 2.2 (q > 10) fit some Ellipticals quite well
- c = 1.7 (q = 8) fits Hubble law well
- c = inf (q = inf) is the isothermal sphere

King profile

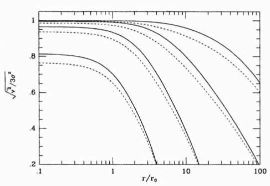

Figure 4-11. The RMS velocity at a given spatial radius r (full curves) and the RMS line-of-sight velocity at projected radius R (dashed curves) for the King models shown in Figures 4-9. Velocities are given in units of $\sqrt{3}\sigma$.

- King models are **not** isothermal : $\sigma^2 = \langle v^2 \rangle = \sigma_o^2$ within r_o but drops at larger radii

  However, as with isothermal models, for each c (or q) we have a range of King models each of different σ_o, subject to $\sigma_o^2 \sim \rho_o r_o^2$

  Eg, for given r_o, high ρ_o has high σ_o

Galaxies

Lecture 8: violent relaxation; dark matter

- Violent relaxation and formation of Ellipticals
- Dark matter
  - Basic evidence
  - Rotation curves
  - DM in Ellipticals?

Violent Relaxation

- Recall that collisional relaxation timescales for galaxies are >>H_0
- We will see that simulations of galaxy formation suggest gas quickly forms a disk as it collapses and cools in a dark matter halo
- Form elliptical galaxies from merging disks
- Merger involves 'violent relaxation' of the potential, and most of the signatures of rotating stars/gas in the disks can be erased

Violent Relaxation

- Our previous discussion focussed on **static systems**, since they are relatively tractable.
- Varying potentials are usually intractable and require a numerical approach.
- There are, however, a few situations which can be treated semi-analytically
- Paradoxically, one of these is when the potential is maximally fluctuating
- This is the case of **violent relaxation**

Violent Relaxation

- For galaxies, 2-body encounters are negligible and evolution is determined by the CBE (Lec 7)
- For a static potential, energy (E) of a star is conserved and the DF doesn't change
- Isolated galaxies in steady state do **not**, therefore, evolve dynamically (we're ignoring gas & 2-body processes here)
- For a galaxy to change, there needs to be a **changing potential**
- For each star, $dE / dt = d\phi / dt$ at the star

Violent Relaxation

• Collapse of collisionless system accompanied with changes of the gravitational potential $\phi(\mathbf{x},t)$, giving rise to an additional relaxation process.
• Let $\varepsilon = 1/2\, v^2 + \phi$ be the specific energy for a given star

$$\frac{d\varepsilon}{dt} = \frac{\partial\varepsilon}{\partial v}\cdot\frac{dv}{dt} + \frac{\partial\varepsilon}{\partial\phi}\frac{d\phi}{dt} = -v\cdot\nabla\phi + \frac{d\phi}{dt}$$

$$= -v\cdot\nabla\phi + \frac{\partial\phi}{\partial t} + v\cdot\nabla\phi = \frac{\partial\phi}{\partial t}$$

where $d\mathbf{v}/dt = -\mathrm{grad}(\phi)$

• Thus a time-dependent potential of a collisionless system can induce a change in the energies of the stars involved.

Violent relaxation

- The DF evolves and the structure of the galaxy changes
- This occurs during (i) inhomogeneous collapse, and (ii) encounters (collisional relaxation time)
- These are brief traumatic times : "galaxy changes are by **revolution** rather than by **evolution**" (Binney & Tremaine)

Violent Relaxation

- In collapse of large cold system, ϕ changes rapidly
- stars gain and lose energy, which broadens f(E)
- energy is **redistributed** via **collective interactions**
- this acts like a **relaxation process**
- Note : the **total** energy remains constant : this is a **non-dissipational** process
- energy is **not** radiated away, as with dissipational (gaseous) collapse
- If the total energy is initially zero (eg, diffuse system at rest), then following collapse: some stars will be strongly bound, but some must also have been ejected.

Violent Relaxation

- Note : scattering is independent of the star's mass
- fundamentally **different** from 2-body (collisional) relaxation
- **no** segregation by mass (eg, heavy stars **don't** sink to center, as in Globular Clusters)
- **Phase mixing** (later slides) helps smooth out lumps fairly quickly
- distribution is ~smooth after ~few collapse times
- violent relaxation timescale is ~few x dynamical (collapse) timescale

$t_{ff} = (3\pi/32G\rho)^{1/2}$

Quick derivation of t_{ff}

For particles at radius $r = R$;

$$\frac{1}{2}mv^2 = \frac{GmM}{R} \quad \Rightarrow \quad v\_esc = \sqrt{2GM/R}$$

$$\tau_{dyn} \approx \frac{R}{v} = \sqrt{\frac{R^3}{2GM}}$$

noting that average density $\overline{\rho} = 3M/4\pi R^3$

$$\tau_{dyn} \approx \frac{1}{3\sqrt{G\overline{\rho}}}$$

Violent Relaxation

- If relaxation is **complete**, then fully random scattering occurs
- results in isotropic velocity field and Boltzmann-like f(E)
- Usually, however, the density distribution becomes smooth **before** scattering is complete
- relaxation ceases and is **incomplete**
- residual anisotropies & phase-space substructures remain (some memory of ICs)

Violent Relaxation

- N-Body example : van Albada 1982
- start with ~ homogeneous sphere with low σ
- 1st infall -> dense centre
- settles into ~ $R^{1/4}$ law
- σ drops with radius
- β (anisotropy) is 0 at nucleus, -> 1 at edge
  (most scattering occurred at small radius on 1st infall
  most stars have low angular momentum)
- N(E) dE spreads out, most stars have E ~ 0, few are deeply bound

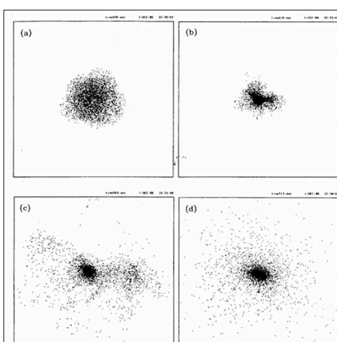

Figure 4-19. Four stages of a collapse simulation. (a) Initially the 5,000 particles have small random velocities and are approximately homogeneously distributed within a roughly spherical boundary. (b) Gravity causes the system to fragment into sublumps that fall together to form a tight minimum configuration. (c) The kinetic energy built up during the infall phase enables the system to reexpand to a centrally concentrated configuration larger than the initial configuration. (d) After a series of pulsations of ever-decreasing intensity, the system settles to a quasi-steady state. (Plots kindly supplied by T. S. van Albada: for details see van Albada 1982.)

Violent relaxation

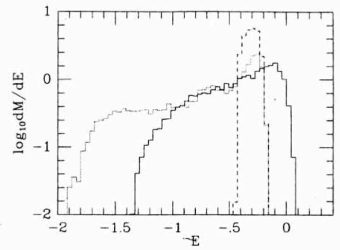

Figure 4-20. The evolution of the differential energy distribution of the model shown in Figure 4-19. The corresponding times are: $t = 0$ (dashed and then dash-dot curve); after one initial free-fall time (dotted and then dash-dot curve); after violent relaxation has ceased (full curve). Energy is measured in units of GM/R_e, where M is the system's mass and R_e is the effective radius of the $R^{1/4}$ model that best fits the final configuration (see Figure 4-22). (After van Albada 1982.)

Violent relaxation

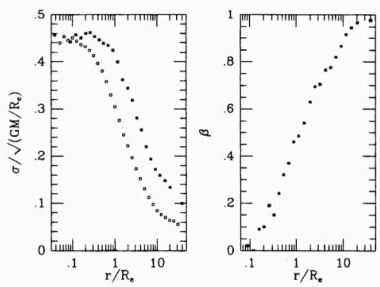

Figure 4-21. Left panel: radial velocity dispersion (filled squares), and projected velocity dispersion (open squares) in the final configuration of the simulation shown in Figure 4-19. Right panel: anisotropy parameter $\beta \equiv 1 - \sigma_\theta^2/\sigma_r^2$ in this system. The velocity dispersions have been scaled to those of the best-fitting $R^{1/4}$ model (see Figure 4-22). (After van Albada 1982.)

Violent relaxation

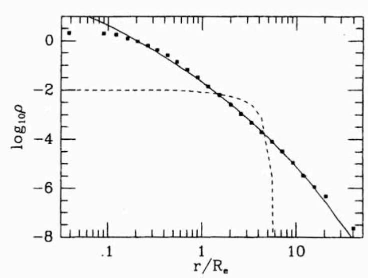

Figure 4-22. The radial density profile of the final configuration of the simulation shown in Figure 4-19 (squares), together with the simulation's initial density profile (dashed line) and the density profile of the best-fitting $R^{1/4}$ model (full curve). The initial and final simulation profiles have been scaled to the effective radius R_e of the latter model. (After van Albada 1982.)

Violent relaxation

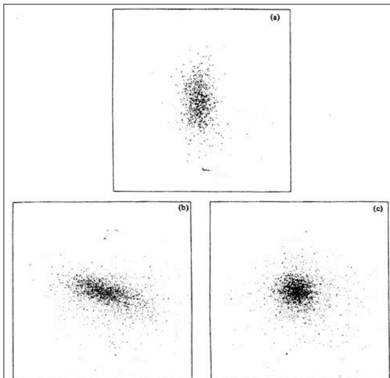

Figure 4-23. Three orthogonal projections of the final configuration to which 25,000 particles settled after they had been released from a cold, elliptical initial configuration. (From Wilkinson & James 1982.)

Violent relaxation

Violent Relaxation

- If the initial distribution is hotter
  -> less concentrated
- If the initial distribution is rotating slowly
  -> less concentrated & rotating oblate figure
- If the initial distribution is rotating faster -> even less concentrated & prolate/bar figure
- If the initial distribution is ellipsoidal -> rotating ellipsoid, anisotropic everywhere

Dark Matter in galaxies

Dark Matter

- Dark matter in galaxies was first revealed by the study of their rotation curves,
  - i.e. a resolved measurement of circular velocity as a function of radius.
- The rotation curve provides a dynamical measurement of the projected galaxy mass.
- Observed rotation curves were flat at large radii - a result inconsistent with a mass profile obtained by scaling the galaxy light profile by a suitable ***stellar mass to light ratio.***

Dark Matter for Ellipticals?

- More obvious from extended rotating disk (eg, in spiral galaxies).
- Typical values for ellipticals cores are ~10-20 solar M/ L suggested ***minimal/no dark matter***
- Best evidence for DM in ellipticals actually comes from gravitational lensing rather than direct stellar velocity measurements

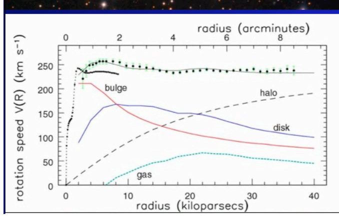

DM revealed by rotation curves

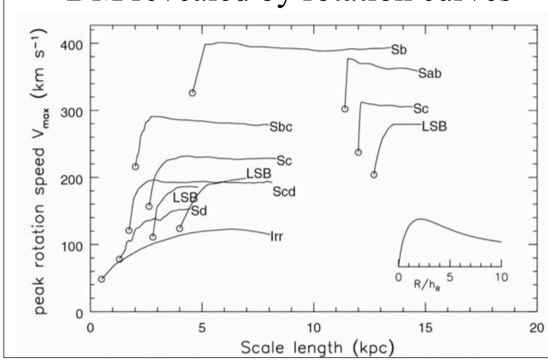

DM revealed by gravitational lensing

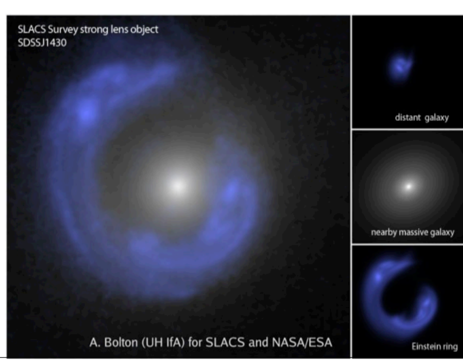

structural outline of a galaxy

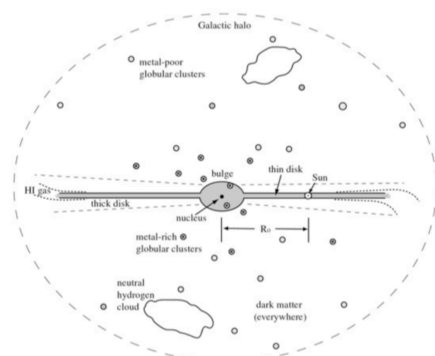

DM in general

- The data called for large amounts (up to 40x more than the stellar mass) of dark matter at large galactic radii - the dark matter halo.
- The incidence of flat rotation curves is ubiquitous across spiral galaxies of differing morphological type.
- This indicates that the presence of a dark matter halo is common to all spiral galaxies.
- Elliptical galaxies also exist in dark matter haloes. The clearest evidence for dark matter in elliptical galaxies is provided by gravitational lensing whereby the dark halo distorts the light from a background galaxy.

DM - Mass to light ratios

- The B-band luminosity of the Sun is $L_{\odot,B} = 4.7 \times 10^{25}$ W. The mass of the Sun is $M_\odot = 2 \times 10^{30}$ kg.
- Therefore the B-band mass-to-light ratio of the Sun is $M_\odot / L_{\odot,B} \approx 4.25 \times 10^{4}$ kg W^{-1} .
- The mass-to-light ratio of the Sun provides a basic unit, i.e. one solar mass of stars liberating one solar mass of B-band luminosity possesses $\langle M/L_B \rangle = 1$.

DM

- Over the spectral sequence of stars (OBAFGKM) the mass-to-light ratio varies from $\langle M/L_B \rangle \sim 10^{-3}$ for the bright, massive O stars to $\langle M/L_B \rangle \sim 10^{3}$ for faint, low mass M stars.
- The average value of the stellar mass-to-light ratio within 1 kpc of the Sun (the Solar neighbourbood) is
  $\langle M/L_B \rangle = 4$.
- From the earlier LF analysis the total luminosity density of stars is $j_{\star,B} = L_B /\mathrm{Vol} = 1.2 \times 10^8\ L_{\odot,B}\ \mathrm{Mpc}^{-3}$.
- Assuming that the mean stellar mass-to-light ratio in the solar neighbourhood is representative of this larger volume then the mean stellar mass density is
  $\rho_\star = \langle M/L \rangle\, j_{\star,B} \approx 5 \times 10^{8}\ M_\odot\ \mathrm{Mpc}^{-3}$.

DM

- If we go further and assume that the stellar mass density in the local volume is representative of the universe as a whole then the normalised stellar mass density of the universe is

$$\Omega_{\star,0} = \frac{\rho_{\star,0}}{\rho_{c,0}} \approx \frac{5 \times 10^8 \mathrm{M}_\odot \mathrm{Mpc}^{-3}}{1.4 \times 10^{11} \mathrm{M}_\odot \mathrm{Mpc}^{-3}} \approx 0.004$$

- So normal stars make up only 0.5% of the density required to generate a spatially flat universe.

DM

- Consideration of BBN and CMB analyses indicates that $\Omega b = 0.04$
- we immediately confront the fact that most of the baryons in the universe do not exist in the form of “normal” stars.
- additional baryons in galaxies exist as
  - low-mass stars such as brown dwarfs,
  - stellar remnants such as faint white dwarfs
  - diffuse clouds of hot gas: the warm/hot interstellar medium (WHISM).
- On the scale of galaxy clusters, the dominant structures in the universe, most of the baryons exist in the form of a X-ray emitting plasma.

Rotation Curves: Spiral galaxies; (disky Ellipticals)

- The Milky Way galaxy is a spiral galaxy. The Sun moves around the Galactic centre on an approximately circular orbit of radius R = 8.5 kpc and velocity v = 220 kms^{-1} .
- If the orbit is stable then the outward centripetal acceleration is balanced by the inward acceleration due to gravity, i.e.

$$\frac{v^2}{R} = \frac{GM(R)}{R^2}$$

$$\text{or} \quad v = \sqrt{\frac{GM(R)}{R}}$$

where M (R) is the mass of the galaxy contained within a radius R.

- A flat rotation curve indicates $M(<R) \propto R$.
- What density profile does this imply?

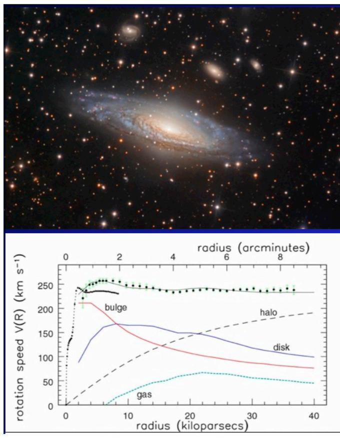

DM revealed by rotation curves

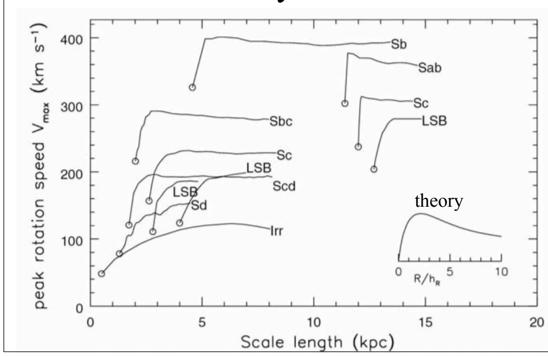

Rotation curves

- one can write the mass enclosed within a sphere of radius R as

$$M(R) = \frac{v^2 R}{G} = 9.6 \times 10^{10} \mathrm{M}_\odot \left(\frac{v}{220 \mathrm{kms}^{-1}}\right)^2 \left(\frac{R}{8.5 \mathrm{kpc}}\right)$$

where the values scale the mass enclosed to that within the Sun's location within the Galaxy.

- If we assume
  - a maximum radius for the halo of matter surrounding the Galaxy
  - a assymptotic velocity value

  we can determine the halo mass,
- i.e. taking v = 220 kms^{-1} and R_{halo} = 100 kpc we obtain M_{halo} = 1.1 x 10 ^{12} M⊙ (*all other estimates agree)*

structural outline of a galaxy

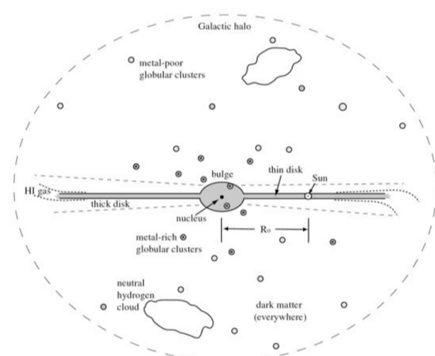

Rotation curves

- For an exponential, thin disk, one can show that :

$$\begin{aligned} V_c^2(R) &= R\frac{\partial \Phi}{\partial R} \\ &= 2\frac{GM_d}{R_d} y^2 \left[I_0(y)K_0(y) - I_1(y)K_1(y)\right] \quad (y = \frac{R}{2R_d}) \\ &\simeq 0.767 \frac{GM_d}{R_d} \frac{0.44(R/R_d)^{1.3}}{1 + 0.235(R/R_d)^{2.3}} \qquad R < 4R_d \end{aligned}$$

- Where I_n and K_n are modified Bessel functions of the first and second kind.
- This rotation curve has peak: V_{max} at R_{max} ~ 2.2 R_d
- for R > 3 R_{max} V_c(R) falls ~ $R^{-1/2}$ (Keplerian)

Rotation curve of the thin exponential disk:

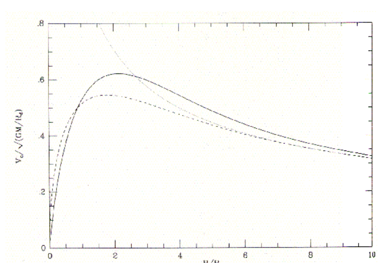

Figure 2-17. The circular-speed curves of: an exponential disk (full curve); a point with the same total mass (dotted curve); the spherical body for which $M(r)$ is given by equation (2-170) (dashed curve).

see: Binney, Tremaine (1994) *Galactic Dynamics*, p. 78

Rotation curves

- The B-band luminosity of the Galaxy is $L_{MW\,B} = 2.3 \times 10^{10}\, L_{\odot\,B}$ and therefore

$$\langle M/L_B \rangle_{MW} \approx 50 \langle M/L_B \rangle_{\odot} \left(\frac{R_{halo}}{100 \text{ kpc}} \right)$$

- So how big is the halo of the Milky Way?

History

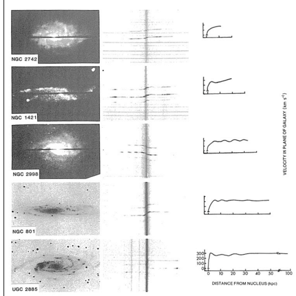

- 1970s & 80s (Rubin et al): **~flat** out to ~ 2 - 3 R_d concluded dark matter (**careful** : exponential disk still ~flat here)
- Kent (1986) images **same** galaxies and derives rotation curves directly from light profile
  - they **match** the observed rotation curves !
  - dark matter **not required**; bulge + disk with normal M/L suffices

Large HI (neutral Hydrogen) disks

- Fortunately, HI extends **well beyond** the optical disk
- while Hα goes to 2-3 R_d (~0.75 R_{25}), HI often goes to > 5 R_d

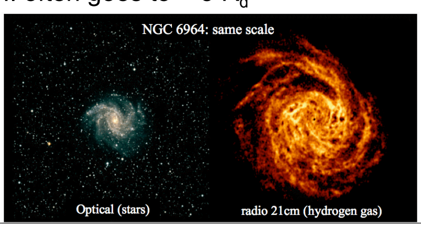

HI (neutral Hydrogen) gas

- V_{rot} rarely declines; still flat or rising **well beyond the disk**
- It is necessary to invoke an invisible **halo**
- Since $\phi = \phi_d + \phi_h$ and $V_c^2 = r\, d\phi/dr$, then: $V_c^2 = V_d^2 + V_h^2$
- Use the observed rotation, V_c, and the (predicted) disk rotation, V_d, to infer the halo contribution, V_h, and its potential.
- Typically, bulge + disk accounts for inner rotation curve with reasonable M/L_B ~ 3 - 5
- If this is forced to fit the inner rotation, it is a called "maximum disk" model
- Dark matter **halo** needed at larger radii, giving total M/L_B ~ 30
  - ~5 times more dark matter than normal matter in stars + gas
  - This is a **lower limit** since V_{rot} still constant/rising!

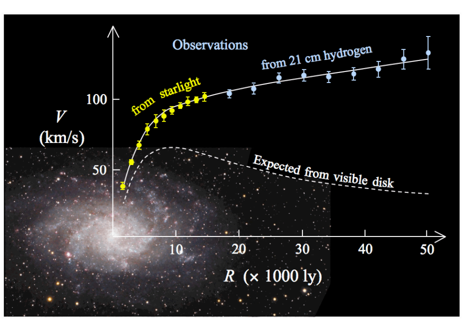

- Historically important paper: van Albada et al (1985) analysis of NGC 3198 :

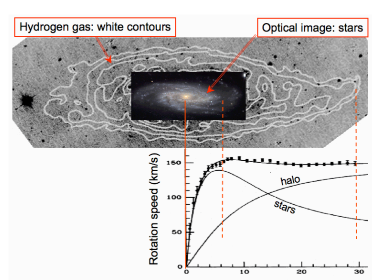

Rotation curves

$$\langle M/L_B \rangle_{MW} \approx 50 \langle M/L_B \rangle_{\odot} \left(\frac{R_{halo}}{100 \text{ kpc}} \right)$$

- So how big is the halo of the Milky Way?
- Assume the outermost globular clusters and satellites such as the Large and Small Magellanic Clouds are bound to the Milky Way then the halo extends to ~75 kpc
- then $\langle M/L_B \rangle_{MW} \approx 40 \langle M/L_B \rangle_{\odot}$.

Rotation curves

- If the Milky Way extends some four times further, i.e. to 300 kpc, almost halfway to M31,
  …. then we obtain $\langle M/L_B \rangle_{MW} \approx 150 \langle M/L_B \rangle_{\odot}$.
- This implies that the Milky Way contains some 10 to 40 times more mass than can be accounted for by its visible stars.
- Should the Milky Way be typical in this respect then we can write the normalised mass density in galaxies as
- $\Omega_{gal} = (10 \rightarrow 40)\Omega_{*} \approx 0.04 \rightarrow 0.16$.
- Although this simple prediction contains many assumptions we are therefore forced to contemplate the fact that some fraction of the dark halos surrounding galaxies is composed of ***non-baryonic dark matter.***

DM

- It is now generally accepted that galaxies reside within large halos of dark matter.
- Two sketches of a galaxy with its associated dark matter halo, with optical galaxy superimposed at correct scale.
- Left: simple picture, of a smooth dark matter distribution -- possibly mildly oblate or triaxial.
- Right: n-body simulation of a more realistic halo, with significant substructure. It is still unclear whether the substructure is present in real halos -- certainly, if it is, then not all sub-clumps contain dwarf galaxies …

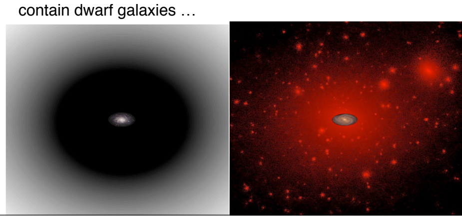

DM in ellipticals

- Recall, that typical values for ellipticals cores are ~10-20 solar M/L from isothermal sphere modeling
- suggests ***minimal/no dark matter***
- However, note that if σ_r **increases** at large R, we **know** σ_θ is increasing
  – in this case Dark Matter is clearly **present**.
- In practice, the most distant tracers of the potential are GCs and PN
- They **do** suggest DM halos are present (next slide)
- However, better methods exist: gravitational lensing

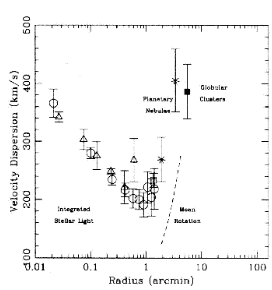

Figure 2. Velocity dispersion σ vs $\log r$ for (i) integrated light of NGC 1399 (open symbols), (ii) the globular cluster in NGC 1399 (filled square) and (iii) our PNs velocity measurements (stars). The dotted curve shows the rotational velocity for our solid body rotation fit to the velocity of the PNs. For comparison, the surface brightness of NGC 1399 at a radius of 3 arcmin is $\mu_B = 24.5$ mag arcsec^{-2}.

see: Arnaboldi, Freeman (1997) *ASP Conf.*, **116**, 54

DM revealed by gravitational lensing

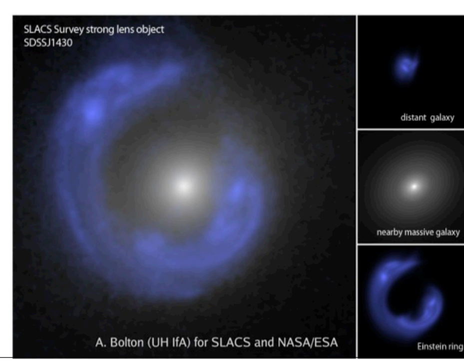

Dark Matter Halo Structure

- At largest measured radii V_{rot} is ~flat, so (r)~ r^{-2} in this region
- Unknown beyond this, but must drop faster to keep total mass finite.
- Difficult to constrain the **inner** parts Bulge + "maximum disk" fits yield plausible M/L (~ 3-5), suggesting DM not important here
- Halo contribution clearly drops at small radii, but functional form not well constrained.
- N-body codes which follow hierarchical assembly of DM halos yield a particular form: The Navarro-Frenk-White (NFW) 2-parameter broken power-law profile:

$$\rho(r) = \frac{\rho_0}{(r/a)(1+r/a)^2}$$

- This has $\rho(r) \sim r^{-1}$ in the center and $\rho(r) \sim r^{-3}$ at r >> a.

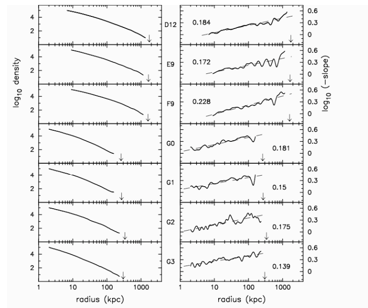

Fig. 3.— Nonparametric estimates of the density $\rho(r)$ (left panel) and the slope $d \log \rho / d \log r$ (right panel) for the ten N-body halos of Table 1. The virial radius r_{vir} is marked with an arrow. Dashed lines in the right hand panels are linear fits of $\log(-d \log \rho / d \log r)$ to $\log r$; regression coefficients are also given.

DM halo profile

- Or a slightly better 3-parameter fit is the "Einasto Profile":

$$\rho(r) = \rho_e \exp[-d_n[(r/r_e)^{1/n} - 1]]$$

- This is identical to the Sersic profile for **projected** light. In this case, d_n ~ 3n - 1/3 + 0.0079/n, ensures that r_e contains half the total mass. n ~ 7 -> 4, decreasing systematically with halo mass (cluster -> galaxy halos).
- Both these give rotation curves that rise to a peak and slowly decline
- They are approximately flat in the regions measured by optical or HI rotation curves.

The "NFW" form for dark matter halos

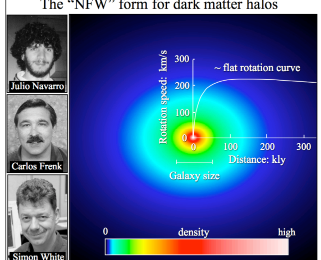

- The density of a NFW dark matter halo is shown color coded, along with its circular rotation curve.
  This results from fits to n-body codes that follow the cosmological evolution of dark matter, and its hierarchical merging to form dark matter halos.
  Perhaps surprisingly, no matter what the size of the halo, roughly the same **universal density law** arises, from dwarf galaxy mass, through galaxy mass, to cluster mass.
  Although the rotation curves ultimately decline, they appear flat over a large region which is sampled by the HI disks.

Disc-halo conspiracy

- There is an intriguing property of these rotation curves:
- After a rapid rise, most rotation curves are ~flat **at all radii** :   in regions where V_c is determined by disk matter, **and**   in regions where V_c is determined by dark matter○How do these two **different** regions know they should have the **same** rotation amplitude ??
- This is not currently understood, but indicates something important about galaxy formation ○Notice that a related puzzle also underlies the Tully-Fisher relation
- V_{max} is set by the halo, while M_l is set by the luminous matter○Indeed, the theoretical origin of the TF relation is not yet fully understood.

Spiral Galaxies

Lecture 9: disks, spirals (thick disks)

- Disk galaxies in detail
- Formation and physical explanation come later: hydrodynamics of gas

Disk galaxies appear to be more complex than ellipticals

- Wide range in morphological **appearance**:
  - eg classification bins : simple E0-6 compared with all the spiral types
  - not just smooth, considerable fine-scale details
- Wide range in stellar **populations**:
  - old, intermediate, young and currently forming
  - ongoing chemical enrichment
- Wide range in stellar **dynamics**:
  - "cold" rotationally supported disk stars
  - "hot" mainly dispersion supported bulge and halo stars
- Significant **cold ISM**:
  - note : the cold and warm components are **dissipative**, and therefore :
  - influences dynamical evolution (eg helps spiral formation)
  - influences stellar density distribution (eg creates dense cores & black holes)

Basic Components

- **Disks :**
  - Metal rich stars and ISM
  - Nearly circular orbits with little (~5%) random motion & spiral patterns
  - Both thin and thick components
- **Bulge :**
  - Metal poor to super-rich stars
  - High stellar densities with steep profile
  - V(rot)/σ ~ 1, so dispersion support important.
- **Bar :**
  - Flat, linear distribution of stars
  - Associated rings and spiral pattern

Basic Components

- **Nucleus :**
  - Central (< 10pc) region of very high density (~10^6 Mpc^{-3})
  - Dense ISM &/or starburst &/or star cluster
  - Massive black hole
- **Stellar Halo :**
  - Very low SB; ~few % total light; little/no rotation
  - Metal poor stars; GCs, dwarfs; low-density hot gas
- **Dark Halo :**
  - Dark matter dominates mass (and potential) outside ~10 kpc
  - Mildly flattened &/or triaxial

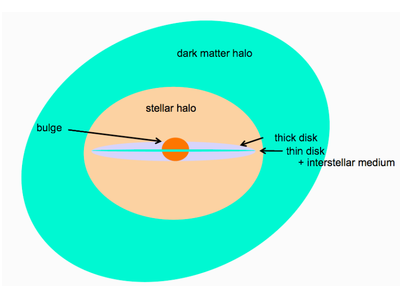

3-D Shapes - Disks

- Distribution of (projected) b/a :
  - Approximately **flat** over wide range, from 0.3 to 0.8
  - Rapid rise at b/a ~ 0.1 - 0.3; and rapid fall at b/a > 0.8
- Interpretation :
  - Randomly oriented thin circular disks give N(b/a) = const -> observed N(b/a) consistent with **mostly flat circular disks**
  - Drop at low b/a due to bulge. Note: slower rise for big bulge S0s, and faster rise for small bulge Scs.
  - Minimum b/a ~ 0.05 - 0.1 for ~bulgeless Sdm -> **disks can be highly flattened**
  - drop at high b/a ~ 0.8 caused by **non-circular disks** -> dark matter potentials slightly oblate/triaxial

- Distribution of axial ratios, q = b/a, for 4800 S0s (left) and 13,500 spirals (right) from the APM southern survey.
- Note that random orientations of circular flat disks would have a **flat** distribution in q = b/a.
- Deviations at low b/a are due to the presence of a bulge (boosting the minor axis) and at the high end because many spiral disks are slightly

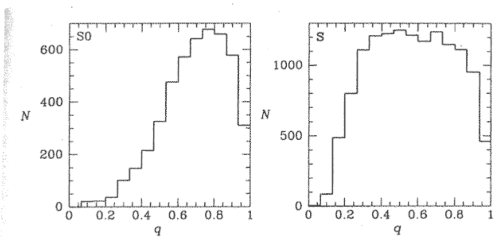

Figure 4.46 The distribution of apparent axial ratios of the APM galaxies. The left-hand panel shows the data for 4782 S0 galaxies, the right-hand panel for 13482 spiral galaxies [After Lambas, Maddox & Loveday (1992) from data kindly supplied by S. Maddox]

3-D Shapes - Disks

- Warps: starlight almost always flat (if undisturbed)
- however, HI is often **warped**, with warp starting beyond D_{25}
- 180 degree symmetry: "integral sign" when seen edge-on.
- 75% of warped galaxies have **no** significant companion (isolated system): stationary feature, probably a response to gas orbiting in non-spherical dark matter halo potential misaligned with disk

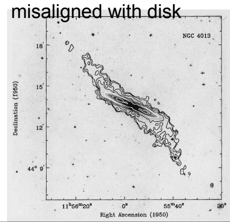

- (left) As with NGC 4013 this galaxy is isolated (though it does have a faint tidal stream), and yet it's neutral hydrogen shows an integral sign warp (the main disk HI has been removed for clarity).
- (right) It is thought that the warp in this disk is a transitory response to a merger - a gas rich galaxy has recently merged with the more massive spheroidal galaxy, and the gas is in the process of settling down into a steady flat disk

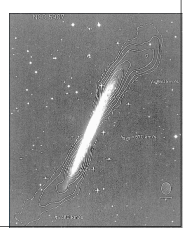

3-D Shapes - Bulges

- Not as easy as ellipticals because of other components
- Study edge-on spirals to minimise contamination
- Results :
  - oblate spheroids, flattened by rotation -> probably similar to low-luminosity ellipticals

3-D Shapes - Bars

- Axis ratios from 2.5 to 5.
- Probably **flat**, since they aren't visible in edge-on spirals
- However, "peanut" bulges thought to be thickened (unstable) bars seen edge-on

NGC 5746 is a nearly edge on spiral with a "boxy" or "peanut" shaped bar.

Bars and Associated Structures

(Buta et al 1996, Barred Galaxies, ASP Conf Ser, Vol 91)

- strong bars observed in ~1/3 of spirals, weak bars in ~1/3
- fraction of total luminosity in bar typically 10-30%
- isophotes typically “boxy”, profiles can be fitted by power laws or exponential functions
- inner, outer rings closely associated with presence of bar
- some bars contain bulges or bars within bars
- bars rotate in rigid pattern with pattern (precession) speed co-rotating with disc at end of bar (density wave)
- bars appear to fall into two distinct classes, strong and weak

Bars in spirals

Stronger bars
(smaller bar axial ratio)
make stronger shocks.

Note the tendency
to make "inner rings"
when the bar is strong.

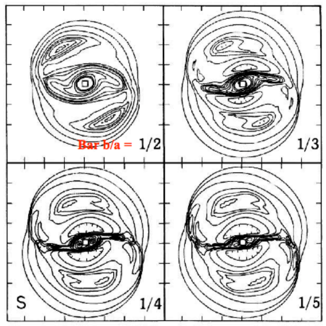

FIG. 4.—The steady state gas density distribution as a function of the bar axial ratio (b/a). Details are the same as for Fig. 3. The sequence proceeds from rounder bars (high b/a) to more elongated bars (low b/a).

Bars in spirals

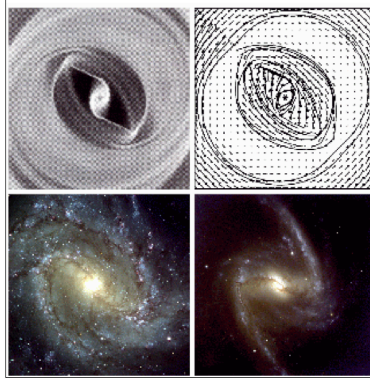

14

Bars: molecular gas in spiral galaxy centres

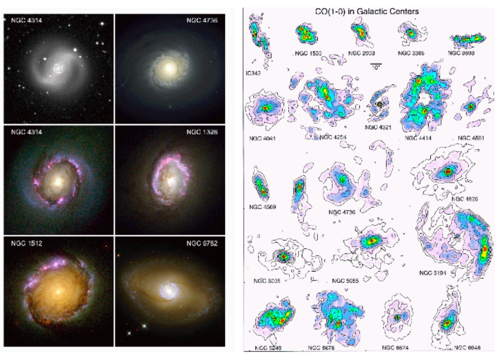

15

NGC5850 (wozniak et al. 1995, A&AS, 111, 115)

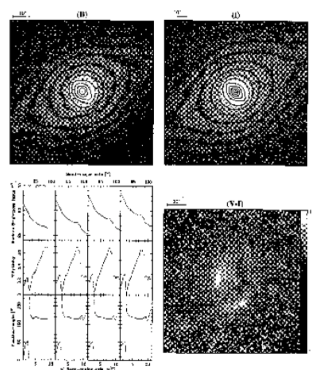

Bars in bars

16

Peanut Bars

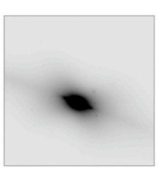

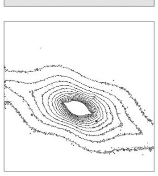

- HST image of NGC 128 with its contour diagram clearly showing the "peanut" shape of the bulge.

  Three galaxies with peanut bulges, with major axis long-slit spectra showing the gas velocities below (from the [NII] 6584 emission line). This study by (Bureau & Freeman 1999) confirms that ~all the peanut bulge objects in their sample are caused by bars that have undergone vertical instabilities and buckled.

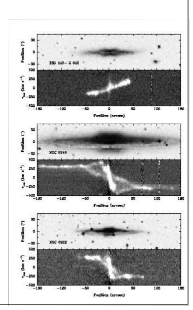

Galaxies

Disk Surface Photometry

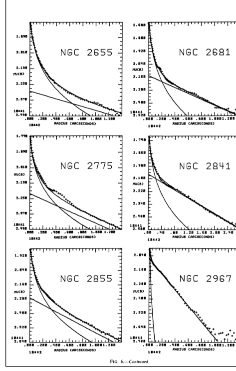

- Model as two components: bulge and disk
- 1d fits to elliptically-azimuthally averaged light profile
- 2-D fits to full image: better, since bulge & disk have different ellipticities

Galaxies

18

- Full 2-D bulge-disk separation for NGC 214. Left is a B image of the galaxy. Center is the best-fitting combination of bulge (deVaucouleurs) and disk (exponential) components, projected by the same inclination angle. Right shows the residual image, which shows non-axisymmetric feature, such as spiral arms. The oval is the region over which the fit was done. Tick marks are 10 arcseconds. [Fig 4.49 in BM, data from R. de Jong].
- In principle, 2D fits are better since the disk and bulge have different intrinsic shapes and so project differently. In practice both 1D and 2D decomposition is often rather uncertain.

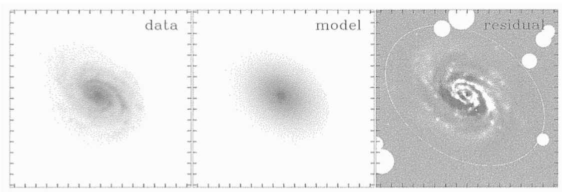

Radial Profiles - disk

$$I(R) = I(0)\, exp\,(-R/R_d)$$
$$\mu(R) = \mu(0) + 1.086\,(R/R_d)$$

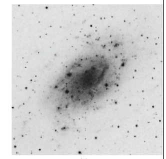
(a)

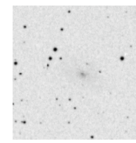
(b)

- Exponential fits well
- R_d is the disk **scale length**, ie $I(R_d) = 1/e\ I(0)$
- Typically, $R_d \sim 0.25\ R_{25} \sim 2$ - 5 kpc (R_{25} is 25th mag/ss isophote)
- wavelength dependent, reflecting radial trends in color (metal abundance and/or age)
- In practice, disk light falls sharply beyond 3 - 5 R_d
- $R_d > R_e$ always (eg MW : $R_d \sim 5$ kpc, $R_e \sim 2.7$ kpc)
- Integrating to infinity: $L_{tot} = 2\ \pi\ R_d^2\ I(0)$
- $\mu_B(0) \sim 21.65$ +- 0.3 mag/ss (Freeman 1970 "Law" of ~const $\mu(0)$ for normal spirals)
- However, a few Low Surface Brightness (LSB) galaxies have much fainter μ (0)

Disc Truncations, Transitions

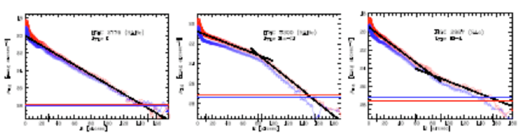

Figure 1. The three main disk types: Type I, Type II, and Type III *(from left to right)*. Azimuthally averaged, radial SDSS surface brightness profiles in the g'- *(triangles)* and r'- *(circles)* band overlayed by r'-band exponential fits to the individual regions: single disk; inner and outer disk.

Pohlen 2007

Radial Profiles - bulge

$$I(r) = I(R_e)\ exp\left(-7.67\left[\ (R/R_e)^{1/4} - 1\ \right]\right)$$
$$\mu(r) = \mu(R_e) + 8.325\left[\ (R/R_e)^{1/4} - 1\ \right]$$

- deVaucouleurs $R^{1/4}$ Law, in flux or mag units
- Effective radius, R_e, contains half the light; [Note: $I(R_e) = I_e$, etc]
- $R_e \sim 0.5$ - 4 kpc (larger for early Hubble types)
- $I(0) = 2140\ I(R_e)$
- Integrating to infinity: $L_{tot} = 7.22\ \pi\ \ R_e^2\ I_e$

Bulges of spiral galaxies

- work over past decade shows that "bulge" structures are mucn more diverse than previously appreciated
- Massive Bulges (most S0-Sa galaxies)
  - luminosity profiles are well fitted by an $r^{1/4}$ law
  - structure similar to elliptical galaxies, with typically higher flattening
  - primary origin presumed to be similar to ellipticals (primordial collapse and/or galactic mergers)
- Intermediate/Late-Type Spirals
  - lower-mass "bulges" actually prove to be steep-profile inner disks, with Sersic indices n = 1-2; "pseudobulges"
  - primary origin probably secular evolution of discs + bars

Kormendy & Kennicutt 2004, Ann Rev Astr Ap, 42, 603

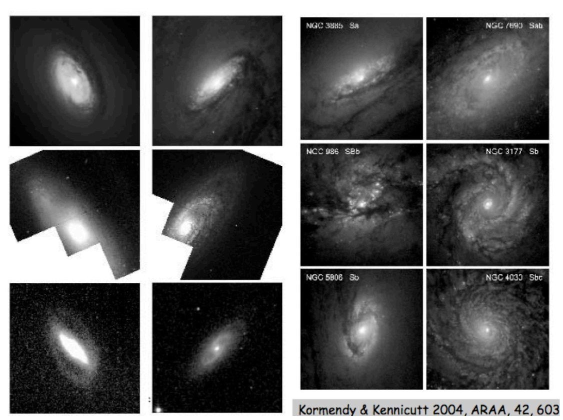

Kormendy & Kennicutt 2004, ARAA, 42, 603

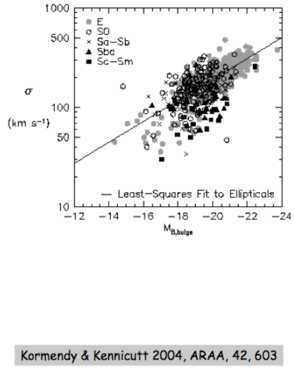

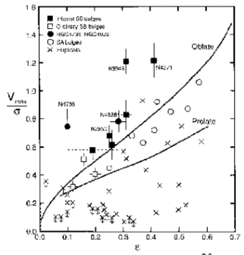

Bulge/disc properties

- B/D ratio correlates with galaxy type (as expected!), but with a large dispersion
- interpretation: SFR, arm structure, etc only loosely correlated with spheroid/disk fraction

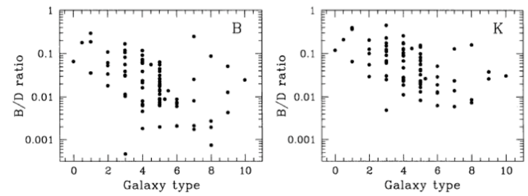

Fig. 20. The bulge to disk ratio as a function of morphological type, using the results from the 2D fit of Paper II.

de Jong 1996, A&A, 313, 45

Radial Profiles - stellar halo

- MilkyWay and M31 have **resolved** halos with metal poor stars, and globular clusters
- Both of these systems contain significant **substructure** -> tidally stripped dwarf galaxies and globular clusters.
- However, M33 does **not** have a significant stellar halo (? D.Trethewey thesis)
- Extremely difficult to see as integrated light in other galaxies
- Stacking ~1000 SDSS edge on galaxies shows extended red light out to μ_i ~ 29 mag/ss:
  - Implied density: $\rho(r) \sim r^{-\alpha}$ with $\alpha \sim 3$.
  - Consistent with moderately flattened spheroid: c/a ~ 0.6
- Overall, still unclear yet:
  - How much of stellar halo is in form of tidal streams
  - How many galaxies have stellar halos .

- 165 pointings of the Wide Field Camera on the INT in V and i yield 7 million stars with photometry that identifies RGB stars in M31 halo -- out to 80kpc (6 degrees). As for the MW, the M31 halo seems to have significant substructure. (Irwin et al. 2005)
- The result of stacking (after first scaling by R_d) 1047 edge on spirals galaxies from the SDSS (Zibetti et al 2005). The i-band contours in surface brightness are 29.5, 28.5, 27.5, 25.5, 23.5, 21.5 mag/ss. The excess light reveal a stellar halo. Data fro the other bands suggest it is quite red in color. These authors conclude that the data support the early formation of halos by the merger of dwarfs

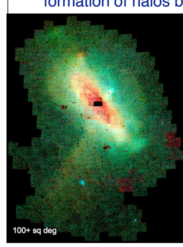

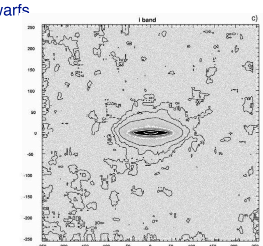

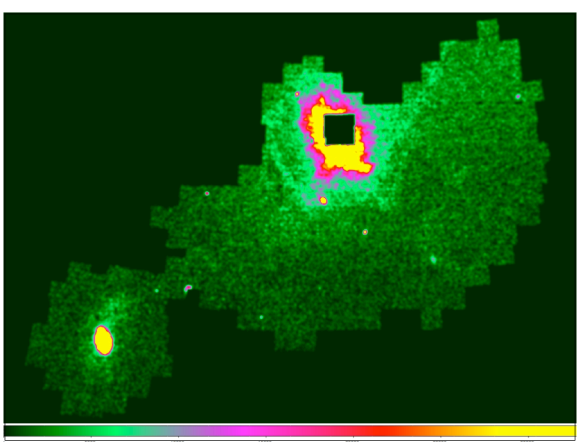

Vertical Disk Structure

$$I(z) = I(0)\, exp\,(-|z|/z_o)$$

- Studies of edge on disks suggests **exponential** distribution
- Where z_o is the **scale height** of the disk, ie $I(z_o) = I(0) / e$
- At large z_0, excess light sometimes reveals a second "Thick Disk" of larger z_0 (see below for further discussion of vertical disk structure)

- Light profiles perpendicular to the disk of IC 2531 in UBVRI at several distances from the nucleus (from Wainscoat, Freeman & Hyland 1989).
- Note the straight lines on these magnitude-distance plots, showing an exponential brightness profile.

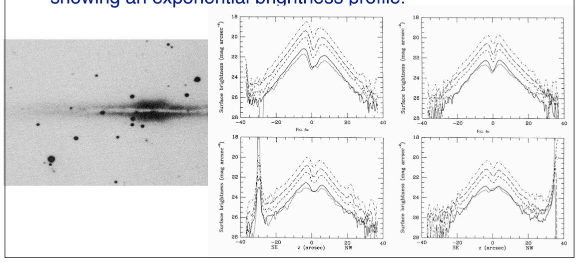

- **Discs: vertical structure**
  - best measurements for Milky Way, from star counts
  - counts near Galactic plane well fitted with exponential function

    $\rho(z) = \rho_0 \, e^{-z/z0}$
  - scale height z_0 is a strong function of stellar type and age, reflecting dynamical heating of stars
    - $z_0 \sim 100$ pc for youngest stars
    - ~ 400 pc for old disk population
  - counts at high z-height show a significant excess, attributed to a second "thick disc"

Kuijken & Gilmore 1989, MNRAS, 239, 605

good fit to double exponential:

$\rho(z) = \rho_0 \, e^{-z/z0} + \rho_1 \, e^{-z/z1}$

$\rho_0 = 0.96 \quad z0 = 250$ pc

$\rho_1 = 0.04 \quad z0 = 1000$ pc

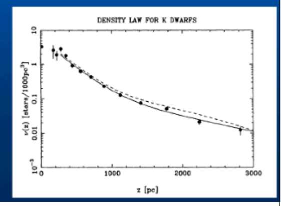

- **Discs: vertical structure**
  - several photometric studies of external galaxies, classic study *van der Kruit & Searle 1982, A&A, 110, 61; 79*
  - vertical light profiles well fitted by sech function:

    $\rho(z) = \rho_0 \, \mathrm{sech}^2 (z/z')$ [sech z = $2 / (e^z + e^{-z})$]

    (for large z this is exponential with scale height $z0 = z'/2$)
  - disks well fitted with typical scale length $z_0 \sim 300$ pc
  - stellar scale height is roughly constant with radius, despite exponential falloff in disk surface density
  - most disks show sharp outer edges
  - some evidence for second (thick) disk components, with $z0 \sim 1$ kpc
    - but presence and properties of thick disk appear to vary widely
    - thick disks more common in galaxies with massive bulges

Examples (Barteldrees & Dettmar 1994, A&AS, 103, 475)

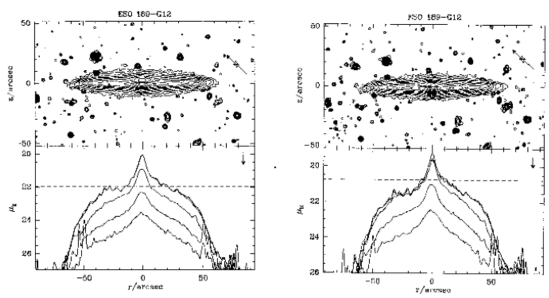

Newly discovered thick disc in Andromeda (M31)
http://www.ast.cam.ac.uk/~mlmc2/M31thickdisc.html

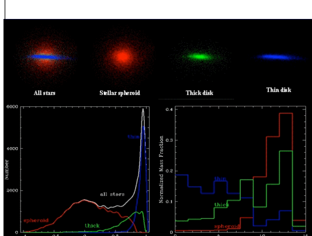

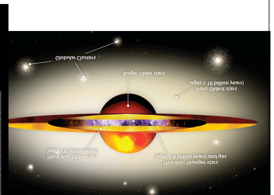

Structure of the Milky Way

Table 1. The Galaxy: Some Vital Statistics

Solar Orbit	$V_0/R_0 = 29 \pm 1$ km s^{-1} kpc^{-1} $V_0 = 220 \pm 10$ (R_0/8 kpc) km s^{-1} $R_0 = 8.0^{+0.5}_{-1.0}$ kpc
Mass	M (<10 kpc) = $(1.0 \pm 0.2) \times 10^{11}$ $M_\odot$ M (<100 kpc) = $(7 \pm 2.5) \times 10^{11}$ $M_\odot$
Luminosity (bol)	$L = 3^{+2}_{-1} \times 10^{10} L_\odot$ $M_V \sim -20.5 \pm 1.0$ $\quad M_H \sim -23 \pm 1$
Stellar Mass	$M_* \sim (4 \pm 2) \times 10^{10} M_\odot$
Interstellar Mass	$M_{ISM} \sim (7 \pm 3) \times 10^9 M_\odot$ $M_{ISM}/M_* \simeq 0.2$
Total Visible Mass	$M_{vis}/M_{tot} \sim 0.5$ $(R \leq 10$ kpc) ~ 0.07 $(R \leq 100$ kpc)
Star Formation Rate	$SFR = 2 \pm 1 \, M_\odot$ yr^{-1} $SFR/<SFR>_{past} \sim 0.7 \pm 0.3$

Best constraints come from modeling of near-IR all-sky data (DIRBE instrument on COBE)

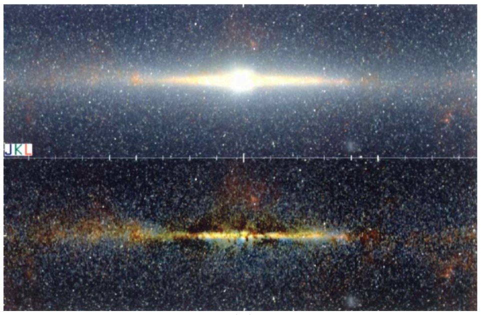

Freudenreich 1998, ApJ, 492, 495

- **Method**
  - measure projected light distribution at 2 - 5 μm
  - correct for dust extinction and emission
  - deproject to 3D
    - fit multi-parameter model, minimize residuals with data
    - use physical, dynamical constraints to remove model degeneracies
    - best measurements for Milky Way, from star counts
- **Results**
  - strong evidence for a bar (+ bulge, disk)
    - bulge/bar light fraction ~ 20% (+-10%)
    - bar radius 3-5 kpc
    - bar axis 15-40° from line of sight to Galactic center
    - shape of bar/bulge strongly triaxial
    - strong molecular/HII ring in disc may coincide with end of bar
  - Sun is ~15 pc above Galactic midplane
  - DIRBE confirms presence of thick disk (primary evidence from star counts --> next section)
  - spiral arms detected, with pitch angle ~10-15°

Freudenreich 1998, ApJ, 492, 495

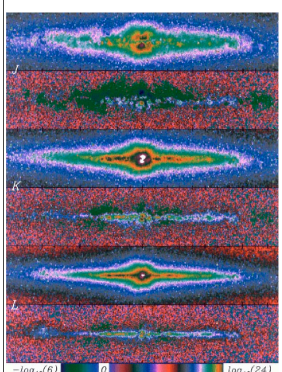

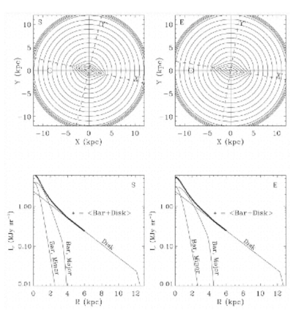

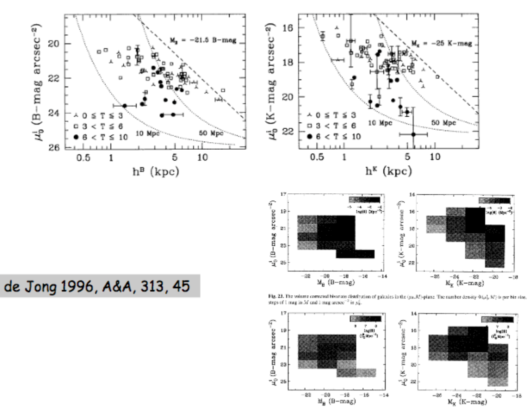

de Jong 1996, A&A, 313, 45

Stellar Velocities in the Disk

- Already looked at gas velocities in disk in context of dark matter and mass
- Disks are **faint** - stellar LOSVD (Line Of Sight Velocity Dispersion) is difficult to measure
- Also, brighter central regions are confused by bulge component
- Nevertheless, some results are emerging.

(1) Rotation

- For disk stars, $V_{los} >> \sigma_{los}$ so stars are **cold** and have ~ circular orbits
- Usually, V_{stars} follows V_{gas} which is close to V_c

- Typically, star orbital rotation velocity can be **slower** than the gas
- this is called **asymmetric drift** and indicates a higher stellar dispersion
  - support beginning to be shared with dispersion
  - stars at r likely to be at apogee, so have $V < V_c$
- In S0s, ~30% have **counter-rotating** gas disks
  - A few spirals even have two counter-rotating **stellar** disks
  - both indicate external origin postdating primary disk formation

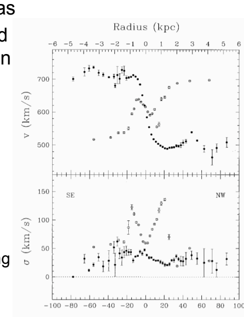

Vertical Stellar Dispersion

- Face-on galaxies yield σ_z : the vertical stellar dispersion
- As a function of radius, σ_z decreases exponentially, with scale length $2R_d$
- This agrees with simple stellar dynamics theory:
- An isothermal disk gives $\sigma_z^2 = 2 \pi G z_o \Sigma_M$ where Σ_M is the surface mass density and z_o is the scale height
- Hence $\sigma_z \sim \Sigma_M^{1/2} \sim I(r)^{1/2} \sim \exp(-R/2R_d)$, as found.
- Consider the Milky Way disk: observations near the solar neighborhood: The inferred mass density within the disk suggests dark matter does **not** dominate the disk.

Vertical Stellar Dispersion

- So it turns out there are **several components** of different z_o and σ_z
  - gas and dust, $z_o \sim$ 50 pc ; $\sigma_z \sim 10$ km/s
  - young thin disk, $z_o \sim$ 200 pc ; $\sigma_z \sim 25$ km/s
  - old thick disk, $z_o \sim$ 1.5 kpc ; $\sigma_z \sim 50$ km/s
- The astrophysical origin of this is thought to be σ_z increasing with **age**
  - stars born "cold" from molecular clouds with $\sigma_z \sim$ sound speed, and corresponding small z_0
  - stars gradually "heated" by scattering off DM clumps and spiral arms, and/or
  - heating of the disk over time by satellite passage and/or minor mergers

2-D Velocity Fields: Spider Diagrams

- A circular disk tilted by angle i (0 = pole on) projects to an ellipse.
- The photometric major axis (PMA) of this ellipse is called the **line of nodes**
- Contours of projected velocity, V_{los}, give a **spider diagram**
  - **Kinematic Major Axis** (KMA): line through nucleus **perpendicular** to velocity contours
  - **Kinematic Minor Axis** (KMI): V_{los} contour at V_{sys} through the nucleus

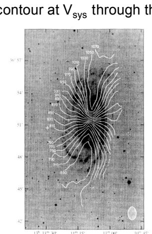

These spider diagrams reveal much about the detailed form of the disk velocity field:

- **Circular velocity** in an inclined circular disk:
  - KMA aligned with photometric major axis (PMA)
  - KMI aligned with photometric minor axis (PMI)
- **Flat** V(r) (beyond initial rise) gives:
  - V_{los} contours are approximately **radial** at large R
  - If V(r) **declines** past V_{max}, then V_{los} contours close in a loop.
- **Solid body** i.e. $V_c(r) \sim r$ in near-nuclear regions, gives:
  - equally spaced contours across nuclear KMA, with spacing 1/slope
- **Warped** disks have:
  - Twisted V_{los} contours in outer parts
    - Note: model galaxies as a set of rings with different V(r), PA(r), i(r)
- **Bars** often show:
  - evidence of **radial motion** over bar region
- **Oval disks** (e.g. arising from non-axisymmetric halo)
  - KMI and KMA not perpendicular
  - KMA not aligned with PMA, and KMI not aligned with PMI
- **Spiral arms** yield:
  - small perturbations to V_{los} contours near arm positions

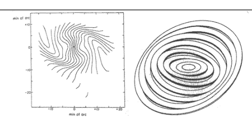

Figure 8.36 A tilted ring model of M83 (right) and the spider diagram predicted by this model (left). [After Rogstad, Lockhart & Wright (1974)]

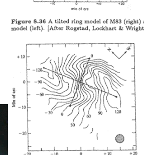

Figure 8.37 The observed spider diagram of M83. [After Rogstad, Lockhart & Wright (1974)]

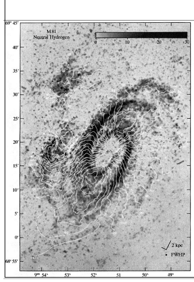

Disk Scaling Relations

- There are a number of correlations, "Scaling Relations", between the global parameters of galaxies:
  - Luminosity; Size; Surface Brightness; Rotation Velocity;
- They are important for several reasons:
  - They reveal the internal properties of galaxies
  - They must arise naturally in theories of galaxy formation.
- In the case of disk galaxies, the most important is between V_{rot} and Luminosity:

V_{max} and the Tully-Fisher Relation

- V_{max} = maximum rotation velocity (inclination corrected), derived from:
  - Major axis optical (often Hα) rotation curves (**half** the full amplitude)
  - HI 21 cm integrated (single dish) profile width, W_{20}: W_{20} / sin i = $2V_{max}$

- Rotation amplitudes, V_{max} are usually measured in one of two ways.
- Long slit optical spectra aligned with the galaxy major axis trace out the rotation curve, allowing the amplitude to be measured.

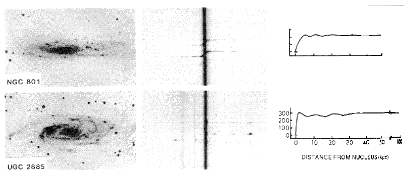

Figure 10-1. Photographs, spectra, and rotation curves for five Sc galaxies, arranged in order of increasing luminosity from top to bottom. The top three images are television pictures, in which the spectrograph slit appears as a dark line crossing the center of the galaxy. The vertical line in each spectrum is continuum emission from the nucleus. The distance scales are based on a Hubble constant $h = 0.5$. Reproduced from Rubin (1983), by permission of *Science*.

see: Binney, Tremaine (1994) *Galactic Dynamics* p.600

Disk Scaling Relations

- Tully & Fisher (1977) recognised that V_{max} correlates with galaxy luminosity
- $L \sim V_{max}{}^{\alpha}$ $\alpha \sim 3 - 4$
- As for the Faber-Jackson relation, the T-F relation stems from virial equilibrium: $V_c^2 \sim M/R$ and $L \sim I(0)\, R^2$
  $L \sim (M/L)^{-2}\, I(0)^{-1}\, V_c^{4}$
- T-F relation holds if $(M/L)^{-2}\, I(0)^{-1} \sim$ const (roughly true)
- Usually, choose **longer** wavelengths (eg I & H bands rather than B & V):
  - smaller scatter on the T-F relation, and slightly steeper gradient (α larger)
- This is because, at ~1-2microns :
  - L is less sensitive to star formation and dust
  - L tracks older population which dominates mass and has a more homogeneous M/L ratio

TF with wavelength

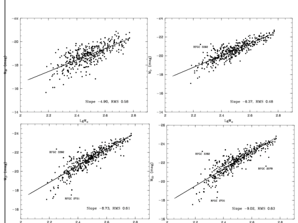

- A sample of edge on galaxies with luminosities measured in 4 bands: B I J H.
- Both the slope and scatter of the relation decreases to the longer wavelengths (the y-range is different in the four plots).
- The B images are sensitive to different amounts of star formation and reddening,
- near-IR images are relatively insensitive to reddening and track the old population which dominates the mass (i.e. it has a much more consistent mass-to-light ratio).

Disk Scaling Relations

- The T-F relation is one of the key methods of **distance determination**
  - First calibrate on nearby galaxies with Cepheid distances
  - this yields the following relations :

$$M_B^{0,i} = -7.41\,(\log W_R^i - 2.5) - 20.04 \ \pm 0.04$$

$$M_R^{0,i} = -8.09\,(\log W_R^i - 2.5) - 21.05 \ \pm 0.04$$

$$M_I^{0,i} = -8.55\,(\log W_R^i - 2.5) - 21.51 \ \pm 0.04$$

$$M_H^{0,i} = -10.39\,(\log W_R^i - 2.5) - 22.22 \ \pm 0.08$$

Cepheid calibration of TF

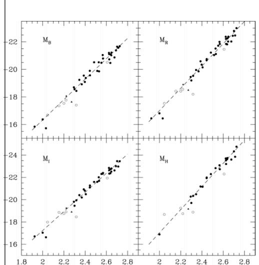

- The zero-point of the Tully Fisher relation needs to be calibrated using galaxies with accurate known distances
- namely, those with measured Cepheid's.
- This was one of the tasks for the HST Key Project to measure H_0.
- The relations shown here in 4 bands also exhibit the systematic decrease in scatter and slope from blue to red bands. But here, the y-axis -- the luminosities -- are now properly calibrated.

Ex-gal distance scale

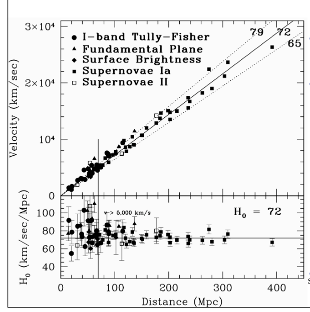

- The now famous culminating figure from the HST Key Project to measure H_0.
- Cepheids were used to measure the distance to nearby calibrator galaxies,
- which in turn calibrated the Tully Fisher relation.
- This is one of the primary methods for constructing the more distant Hubble diagram (which also includes distance measurements using the Fundamental Plane, Surface brightness fluctuations, and supernovae type Ia).
- (see lecture on ex-gal distance scale)

Galaxies

Lecture 10: the interstellar medium

ISM

- Like the Earth, galaxies have an **atmosphere** -> a gaseous component held "down" by gravity
- this atmosphere fills the space between stars, hence: **interstellar medium** (ISM)
- by mass, the ISM is usually not very important: $M_{ISM} \sim 1\% \; M_{stars}$
- The **average** midplane density is ~1 cm^{-3} columns ~$3 \times 10^{21} cm^{-2}$/kpc (~0.005 gm cm^{-2}/kpc)

ISM

- The ISM contains:
  - starlight; gas; dust; cosmic rays; magnetic fields
  - Near the sun they all have similar energy density pressure 1 eV cm^{-3}
- The element mix is the usual:
  - H/He/others: 74/24/2 (% by mass);
  - 90/10/0.01 (% by number)
- Of the "others", ~10-50% have condensed out as solid particles: **"dust"**.

ISM

- Despite its low mass, the ISM is ultimately very important, for several reasons:
- It plays a crucial role in the star <-> gas cycle
  - in spirals and irregulars, it facilitates ongoing (& current) star formation
  - it is a repository for element buildup and is therefore integral to chemical evolution
- Because it can cool, its collapse is **dissipational** (lose energy over time - lost energy converts to heat - radiation mechanisms allow cooling)
  - stars can form !! hot gas -> cold gas -> stars
  - new generations of stars "cool" spiral disks, allowing arm formation
  - globally, gas can migrate inwards to smaller radii, which implies:
    - galaxies are smaller than dark matter halos !
    - galaxies have steep density gradients
    - galaxy nuclei can have very high densities, including a SMBH

ISM

- Being **atomic/molecular**, its emission & absorption provides enormous *diagnostic information*. For example:
  - Doppler motions reveal galaxy dynamics
  - abundance measurements allow study of chemical evolution
  - physical conditions: density; temp; pressure; turbulence; columns; mass, can all be derived
  - some emission lines can be seen (relatively) easily at cosmological distances (e.g., nebular lines line Hα, [OII])
  - high redshift QSO absorption lines reveal halo & disk evolution.
- The ISM can dominate a galaxy's integrated SED (spectral energy distribution): starlight dominates the UV-NIR; but the ISM dominates outside this range.
  - Mid-IR to Sub-mm is dominated by emission from **dust**
  - Soft X-rays come from the **hot ISM phase** (though X ray binaries can be important)
  - cm-radio comes either from **HII regions** or a **relativistic magneto-ionic plasma**
  - certain emission lines (eg Lyα; [CII]158um) can be **major coolants**

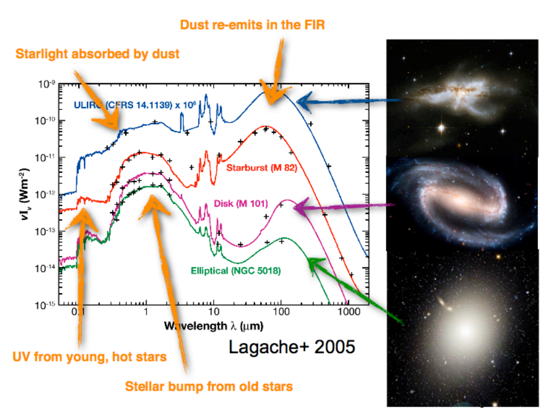

ISM

- The ISM is energized primarily by **stars** (starlight, winds, supernovae)
  - UV starlight photoionizes atoms & dissociates molecules; photo-ejected electrons heat gas
  - SN shocks heat/ionize/accelerate gas & are largely responsible for the ISM's complexity.
- The ISM can be highly **inhomogeneous**, with several **phases**
  - These phases are (roughly): hot/warm/cold, with low/medium/high density
  - In a wide range of conditions these phases have **similar pressures** -> $P/k = nT \sim 10^4 \sim 1$ eV cm^{-3}.
  - However, in dynamic situations, pressure balance is no longer applicable.
- The ISM contains **cloud** and **intercloud** components with density contrast ~ 10^2-10^5
  - these clouds are not like terrestrial clouds; by analogy, more like blocks of wood or lead hanging in the air.

ISM

- The ISM is a **dynamic environment**, with **mass exchange** between phases
- cooling facilitates: hot -> warm -> cold -> stars.
- Supernovae explosions inject energy which accelerates the gas and continuously rearranges the geometry
  - e.g. a disk ISM will "boil" & "bubble" with gas cycling out & back above the disk.
- sporadically, tidal encounters & their resulting starbursts can:
  - add fresh, unenriched (low metallicity) gas
  - energize and evacuate large regions
  - cycle gas out into the halo, some of which may return later.
  - radically alter the ISM, e.g. spiral + spiral -> elliptical.

ISM

- What about the **distribution** of ISM (particularly in spiral disks)?
- **Globally** the scale height depends on the phase's temperature/velocity dispersion and $\nabla\phi$
  - colder phases are confined closer to the plane
  - hotter &/or more turbulent phases are thicker
  - in disks, the ISM flares at large radii and is thinner at small radii
  - However, high local energy density can affect this distribution by driving vertical blow-out.
- **Locally**: the ISM is highly complex & "foamy"
  - SN evacuate complex interconnected "superbubbles"
  - between are sheets & clouds of denser colder gas.
- The Milky Way can act as a **template** for studying other galaxy ISMs
  - As usual, the proximity of the MW's ISM offers important insights
  - Hence, MW ISM studies are now extensive & comprise a major area within astronomy

ISM Components & Their Observational Signatures

- While ultimately ISM gas spans all conditions, in practice much resides in one of several **components**
- These components are distinguished by their **phase** (n,T,X_e) and their **location**
- Note that overall, the intercloud/cloud fraction by mass is ~50 : 50, but by volume it is ~98 : 2

Component	Temp K	Density midplane cm^{-3}	Pressure nT K cm^{-3}	X_e ionization	FF filling %	<h> thickness pc
Intercloud						
Hot HII (HIM)	10^6	0.002	2000	1	50:	3000:
Warm HII (WIM)	8000	0.15	1200	1	20	1000
Warm HI (WNM)	8000	0.3:	2400	0.5	30:	500
Clouds						
Cold HI (CNM)	120	25	3000	0.1	2	100
Cold H_2 (CNM)	15	200	3000	10^{-4}	0.1	75

ISM Components & Their Observational Signatures

- Three other important components add to the mix :
- **Dust**: 1nm - 1um solid particles found in essentially all phases
  - ~50% heavy elements are in dust (~100% of the refractories)
- **Magnetic fields**: generally a few μGauss in both ordered and random components
  - energy density: $B^2/8\pi \sim 10^{-12}$ erg cm^{-3}~1 eV cm^{-3}
  - field compression in superbubble expansion: effects on ISM structure
- **Cosmic Rays**: relativistic electrons & protons, created in SN shocks
  - these diffuse throughout the galaxy and permeate all phases (some even hit the earth)
  - they are a primary heating source in dark molecular cloud cores (which are otherwise shielded).
  - the most energetic electrons + magnetic fields -> radio synchrotron
  - proton collisions with nuclei -> diffuse gamma emission
  - equipartition with **B** field likely, so suspect ~1 eV cm^{-3}

ISM Components & Their Observational Signatures

- All observations involve either emission or absorption
- these, in turn, depend on **Emission Measure** (EM) and **column density** (N)
  - Emission processes are usually **collisional**, so are ~ n^2
  - surface brightness is therefore ~ $\int \langle n^2 \rangle\, dl$ (pc cm^{-3})$^{-2}$ **Emission Measure** (EM).
  - Absorption processes, in contrast, are ~ $\int \langle n \rangle\, dl$ cm^{-2} **Column Density** (N).
- For ionized gas, the relevant density is usually n_e The table shows EM & n_e for various systems:

- Note, for a typical crossection ~ a_{Bohr} ~ 10^{-16} cm^{-2}, N ~ 10^{14} cm^{-2} gives τ ~ 1% with $I/I_0 = e^{-\tau}$.
- This is easily measurable with suitable background source
- low density gas invisible in emission can often be studied in absorption.

Medium	n_e cm^{-3}	Size pc	EM pc cm^{-6}	Emission Visibility	N_e cm^{-2}	Absorption Visibility
Young Nova	10^7	10^{-3}	10^{11}	v. bright!	3×10^{22}	thick
PN	10^4	10^{-1}	10^7	bright	3×10^{21}	good
HII Region	10	10^2	10^4	fine	3×10^{21}	good
Diffuse ISM	10^{-1}	10^3	10	difficult	3×10^{20}	good
Halo	10^{-3}	10^4	10^{-2}	invisible	3×10^{19}	fine

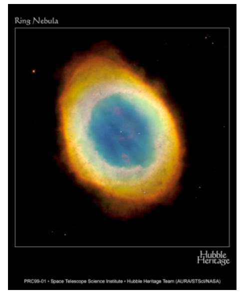

M87
Expanding for 610 yrs
Diameter of 1.3 lyr

Twin jet nebula, M2-9

Planetary Nebula -- brief (~10,000 yrs), but spectacular, fate of giant stars which become unstable & throw off significant fraction of their mass

Can see them with a small telescope!

Bipolar examples: may form because of streams of material ejected along the axis of the poles.

Planetary Nebula (PN).

The intricacy of the "Cat's Eye Nebula" structure may be caused in part by material ejected from a binary central star.

- Note some useful conversions: E_{eV} ~ $1240/\lambda_{nm}$ ~ T_K / 7740 per particle.
- so @ T > 10^5K, H & He are fully ionized, and kT ~ EUV - soft X-ray

Transition ΔE eV	wavelength range	Cause
10^{-6}	21 cm	electron spin flip in atomic H
10^{-2} - 10^{-3}	FIR - mm	molecular rotation
0.1 - 0.01	NIR - FIR	gas molecular vibration; bond bending in dust
0.03 - 0.003	MIR - sub-mm	phonons in dust @ T ~ 1000-10 K
1 - 10	UV - NIR	outer shell electron transitions in atoms and molecules
10 - 10^3	EUV - X-ray	inner shell electron transition; 50 - 500 km s^{-1} post shock gas

Warm *Ionized* Gas

- This gas has T ~ 8000K and resides in:
  - star forming HII regions (n_e ~ 1 - 100+ cm^{-3})
  - diffuse ionized gas (n_e ~ 0.01 - 1 cm^{-3})
- In both cases, equilibrium occurs when:
  - ionization rate = recombination rate (ionization balance)
  - heating = cooling (thermal balance)
- **ionization** is from stellar UV photons; **recombination** occurs naturally **heating** is from photo-ejected electrons; **cooling** is via emission lines
- Note that in these circumstances the ionization degree **does not** reflect the temperature
  - e.g. at 8000K, O->O^+->O^{2+} cannot occur by collisions (it is too cold)
  - but a weak radiation field ~50eV (250A) photons can ionize up to O^{2+}.

Warm *Ionized* ISM

- HII regions
  - directly trace massive star formation
  - primarily traced by hydrogen recombination lines (Hα, Pα, Brγ) or thermal radio continuum
- Diffuse ionized gas
  - characteristic density 0.01 - 0.1 cm-3
  - in spiral galaxies gas is primarily photoionized by UV radiation escaping HII regions
    - early-type galaxies (spheroids) may possess completely diffuse phase, that is primarily heated by shocks
  - in some galaxies (e.g., NGC 891) medium comprises significant fraction of ISM mass, energy budget
  - sometimes associated with diffuse neutral phase

Examples of WISM

A starbursting 'disc' galaxy

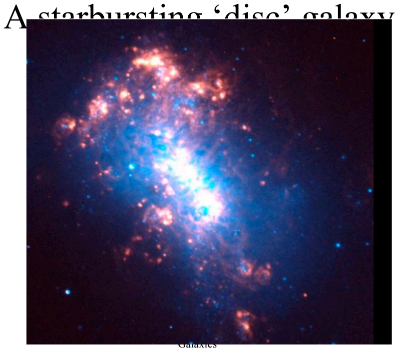

Hα equivalent width variation with Hubble T-type

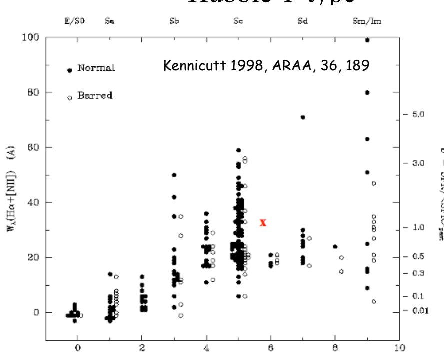

Ratio of recent to past star formation

Hydrogen Recombination Radiation

- electrons are captured by protons and the resulting cascade emits photons.
  - the rate is $\alpha\, n_e n_p$ cm^{-3} s^{-1}, where α is a recombination coefficient (units are cm^3 s^{-1}).
- Usually, the gas is optically thick to Ly-α, which is trapped, termed **case B**:
  - every Lyman line photon is scattered locally many times, ultimately being converted to Ly-α and a higher-series photon, while all of the higher-series photons are emitted with no further scattering.
  - the **total** recombination rate is then α_B = 4.52 & 2.58 x 10^{-13} cm^{3}s^{-1} (for 5000 & 10,000 K)
  - While for just Hβ it is $\alpha_{H\beta}$ = 5.38 & 3.01 x 10^{-14} cm^{3}s^{-1} (for 5000 & 10,000 K)

- The table gives some useful Hydrogen line wavelengths and relative strengths (Case B; T = 10^4 K):
- Note that the Lyα- flux is often difficult to predict:
  - it is resonantly scattered and absorbed by dust,

Series (lower level)	α wav ratio/Hβ	β wav ratio/Hβ	γ wav ratio/Hβ	δ wav ratio/Hβ	Series Limit wav
1: Lyman	1216 A$_{vac}$ 23	1026 A$_{vac}$??	973 A$_{vac}$??	950 A$_{vac}$??	912 A$_{vac}$
2: Balmer	6563 A 2.86	4861 A 1.00	4340 A 0.47	4101 A 0.26	3646 A
3: Paschen	1.87 μ 0.339	1.28 μ 0.163	1.09 μ 0.090	1.00 μ 0.055	0.82 μ
4: Brackett	4.05 μ 0.080	2.63 μ 0.045	2.16 μ 0.028	1.94 μ 0.018	1.45 μ

Atomic (neutral) Gas

- *Most information comes from measurements of 21 cm HI line*
  - *single-dish measurements of several thousand galaxies*
    - *integrated HI flux --> HI masses*
    - *integrated line profiles --> radial velocities, rotation velocities*
  - *aperture synthesis mapping*
    - *detailed HI distributions*
    - *rotation curves, detailed 2D velocity fields*
    - *(nearby galaxies) cloud/inter-cloud structure of atomic ISM, temperature distributions*
- *Additional constraints from interstellar absorption lines in UV and visible*

HI Distribution

- gas is much more extended --> typically $R_{HI} \sim 1.5\text{-}5\ R_{25}$
  - star formation has proceeded over only part of the disc
  - HI kinematics can be used to trace the gravitational potential at large radii (tens of kpc)

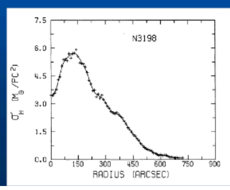

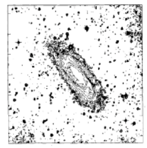

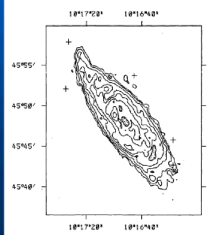

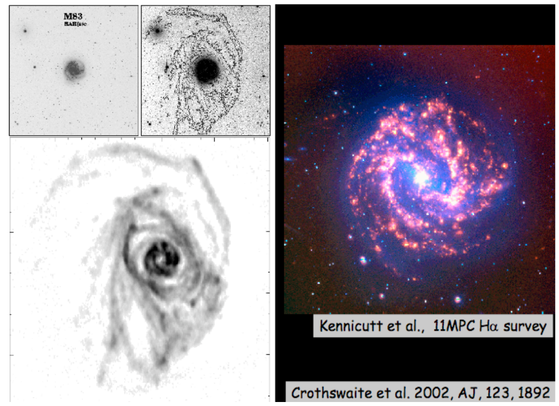

M81 Group HI (VLA)

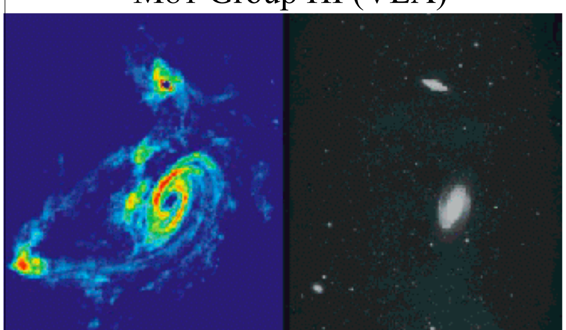

Yun et al. 1994, Nature, 372, 530

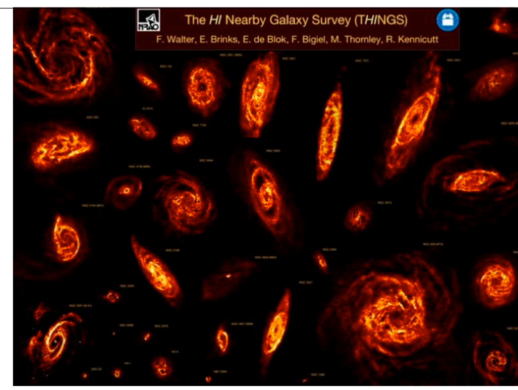

HI Kinematics

- Usually most HI rotates at roughly constant velocity ("flat rotation curve")
  - integrated HI line profile has characteristic "double-horned" shape
  - provides precise measurements of radial velocity and linewidth

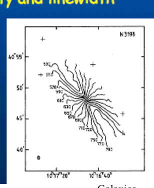

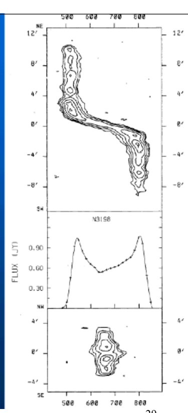

Trends with galaxy type - HI

- HI comprises ~half of total gas mass in typical spiral (vs ~50% H_2)
- HI gas fraction strong function of Hubble type
- $M_{HI}/M_{HI+stars}$ ranges from 0.0 to 0.9 from types E to Irr

Roberts & Haynes 1994, ARAA, 32, 115

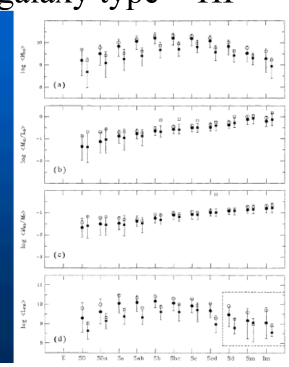

Molecular Gas

- Most molecular gas is in form of H_2, but cold H_2 gas has no observable emission lines (no dipole moment).
  - most information comes from millimeter rotational transitions of CO molecule, with supplemental information from CO isotopic lines and other molecules (HCN, OH…)
  - primary CO transition at 2.7 mm (J = 1 --> 0)
  - again, data on external galaxies come from a combination of single-disk and aperture synthesis measurements
- H_2 predominantly found in massive cold clouds (10^4 M_o and up), highly optically thick in CO mm transitions
  - mass of H_2 inferred <u>empirically</u> from correlation with CO brightness temperature (intensity) *controversial subject!*

$N(H_2)$ $(cm^{-2}) \sim 3 \times 10^{20}$ I(CO) (K km s^{-1})

CO distribution

- in spiral galaxies CO tends to follow distribution of stars more closely, especially young stars
  - little/no CO beyond optical radius
- in many low-mass galaxies (S, Irr), CO is systematically weak compared to young stars and HI
  - may reflect breakdown of CO/H_2 conversion factor and change in molecular cloud properties

Regan et al 2001, ApJ, 561, 218

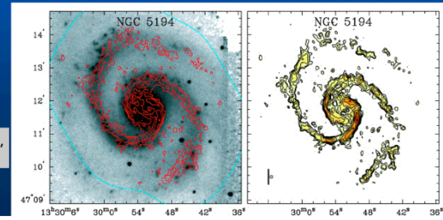

BIMA SONG Survey

Regan et al. 2001, ApJ, 561, 218

Helfer et al. 2003, ApJS, 145, 259

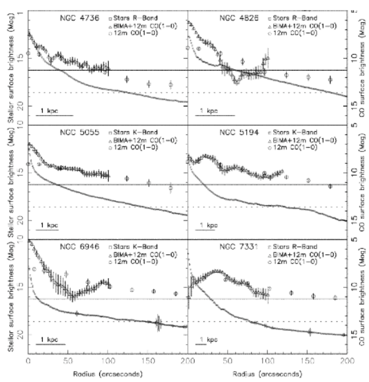

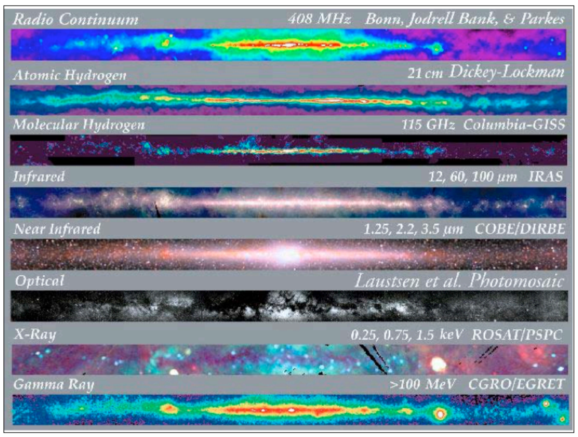

Radial distribution of gas in the (MW) Galaxy

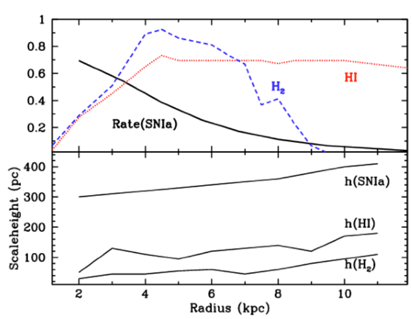

Trends with galaxy type: CO

- Molecular gas tends to be dominant phase in early-type spirals, with H_2 fraction decreasing in later type, lower luminosity galaxies
- role of physical trends vs changes in CO/H_2 factor uncertain
- strong increase in total gas fraction (atomic + molecular) with type

Young & Scoville 1991, ARAA, 29, 581

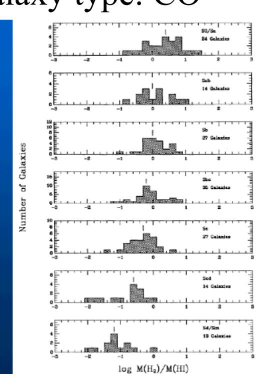

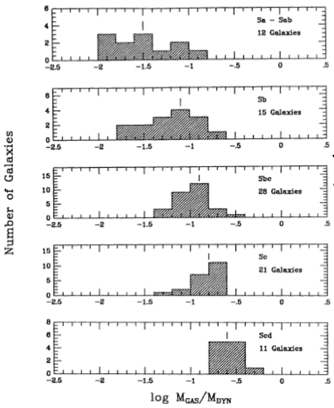

M-gas versus M-dynamical

Young & Scoville 1991, ARAA, 29, 581

Interstellar Dust

- Approximately 1% of ISM is in form of solid grains, which tie up ~50% of heavy elements in ISM
- Grains typically absorb ~40% of bolometric energy of galaxies in local universe
  - can study via modeling of extinction in visible, UV (difficult!)
  - dust grains re-emit energy in mid-far infrared (5 - 300 μm), can map structure directly
- Milestones
  - <1983: extinction modeling, fragmentary FIR data
  - 1983: IRAS all-sky survey, total fluxes of 14,000 galaxies at 12, 25, 60, 100 μm
  - 1995: ISO mission, maps of galaxies at 7, 15 μm, low-res mapping to 240 μm
  - 2003: SIRTF mission, maps at 3.5 - 160 μm, spectral maps, subject is being revolutionized!

Dust Emission

- Integrated spectrum of our Galaxy (below) is characteristic of galaxies generally
  - dust emission much broader than single temperature compone but can be fitted with ~4 distinct components
    - T ~ 15 K (100 - 300 mm) cold dust in molecular clouds
    - T ~ 20-30K (100-150 mm) dust in diffuse clouds, "IR cirrus"
    - T ~ 60 K (50 mm) warm grains in star forming regions
    - T ~ 300 K (10 mm) PAH band emission in small grains
- IR morphology traces optical dust lanes, star-forming regions
- Strong trend in relative emission with type

Cox et al. 1986, A&A, 155, 380

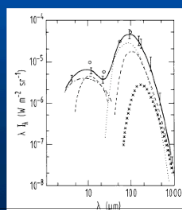

Dust spectrum

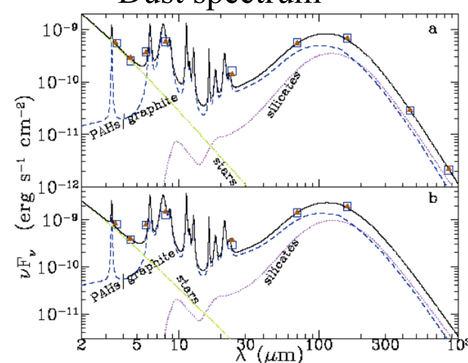

Regan et al. 2004, ApJS, 154, 204

Hot Ionized (Coronal) ISM

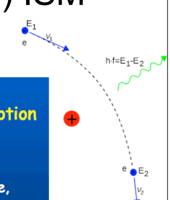

- Primarily traced via soft X-ray bremsstrahlung emission (1-10 keV) or high-ionization UV absorption lines (e.g. OVI)
- Characteristic $T \sim 3\text{-}5 \times 10^5$ K, $n \sim 10^{-3}$ cm^{-3}
  - high temperatures require kinetic heating (supernovae, stellar winds, cloud-cloud collisions)
- Several types of structures
  - diffuse coronae in/around massive E/S0 galaxies, bulges
  - diffuse disk emission from supernova remnants, stellar wind bubbles, supershells
  - extraplanar fountains, chimneys, "superwinds"
  - infalling clouds, cooling flows

CXO Images

http://www.chandra.harvard.edu

NGC 4649 = M60: E2
Randall & Sarazin 2001, unpub

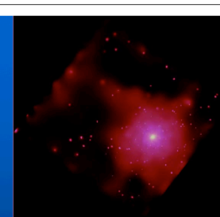

NGC 4631: Sc
Wang et al. 2001, ApJ, 555, L99

Relativistic Particles, Fields

- Radio continuum emission of galaxies at cm wavelengths is primarily non-thermal synchrotron radiation, from relativistic electrons in the Galactic magnetic field
  - thus radio emission (distribution, polarization) traces high-energy processes and structure/strength of interstellar magnetic field
  - B field probably plays critical role in large-scale structure of ISM, and possibly in Galactic evolution, but poorly understood
  - B fields also traced via Zeeman measurements, optical/UV polarization of starlight (via grain alignment)

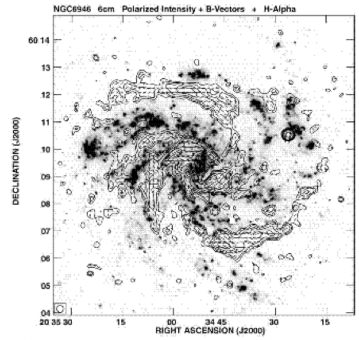

Figure 4. Polarized radio emission and **B**-vectors of the spiral galaxy NGC 6946 at λ6 cm, combined from observations with the VLA and Effelsberg telescopes (from Beck *et al.*, 1996) and overlaid onto an Hα image of Ferguson *et al.* (1998). The angular resolution of the radio image is 15 arc sec.

Beck 2001, Space Science Revs, 99, 243

Radio-FIR Correlation

- Low-frequency radio continuum (dominated by synchrotron emission) and far-infrared emission strongly correlated
- Correlation suggests coupling of energetic particle production with dust heating, possibly via star formation (and supernova rate)
- Correlation also *suggests* possible coupling of energy densities of CRs/magnetic fields with ISM

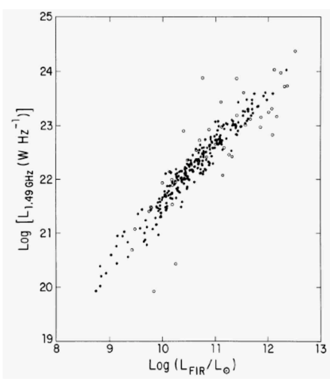

Condon et al. 1991, ApJ, 376, 95

Interstellar media

- Overview of Milky Way ISM

• Overview: the Galactic ISM

Component	f_V	$\langle n_H \rangle$	T_e	f_M	Probes
Hot ICM	0.5	0.005	500,000	0.001	X-rays, OVI
WIM	0.5	0.3	8,000	0.05:	Ha, IS abs lines
Warm HI	0.05:	1:	8,000	0.05:	HI, IS abs lines
HI Clouds	0.05	5-20	10-100	0.4	HI 21cm line
H_2 Clouds	0.005	>100	5-30	0.5	CO, HCN, (H_2)
HII Regions	0.001	10-10000	10,000	0.02	Ha, radio cont
Dust	~1		5-60	0.01	IR, extinction
Particles/Fields	1.0				radio cont, γ-rays

Galaxies

Lecture 11: Disc dynamics

- Circular rotation: Oort's Constants
- Epicycles
- Vertical z motions
- Radial/Azimuthal motions
- Resonances
- Density Waves

Circular Rotation: Oort's Constants

- In the 1920s theorist Bertil Lindblad (Swedish) and observer Jan Oort (Dutch) studied the rotation of the Milky Way disc.
- From the moving sun's location, nearby stars appear to move systematically as a function of galactic longitude.
- Two parameters, Oort's A & B, help parameterize the local velocity field.
- For the radial and tangential velocities, we find: $V_r = A\,r\,\sin 2l$

$$V_t = B\,r + A\,r\,\cos 2l$$

- Where Oort's constants A and B are given by (R_0 = solar radius):

$$A = \frac{1}{2}\left(\frac{V_c}{R} - \frac{dV_c}{dR}\right)_{R_0} = -\frac{1}{2}R\left(\frac{d\Omega}{dR}\right)_{R_0}$$

$$B = -\frac{1}{2}\left(\frac{V_c}{R} + \frac{dV_c}{dR}\right)_{R_0} = -\frac{1}{2}R\left(\frac{d\Omega}{dR} + \frac{2\Omega}{R}\right)_{R_0}$$

- Oort's A expresses **local shear**, while
- Oort's B expresses **local vorticity**, ie local rotation: $\Omega_{loc} = \nabla \times \mathbf{V}$ (curl **V**)

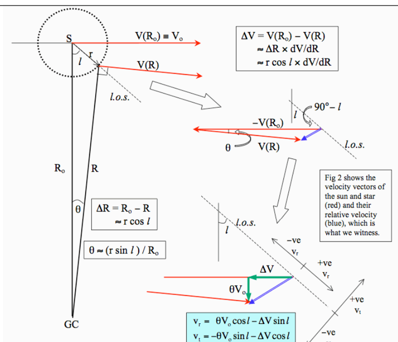

Fig 2 shows the velocity vectors of the sun and star (red) and their relative velocity (blue), which is what we witness.

Fig 1 shows the global situation: a circular rotation velocity field of amplitude V(R) about the GC with the sun at S. Consider a star at galactic longitude l, distance r from the sun: it subtends $\theta \approx (r \sin l) / R_o$ at the GC, and its velocity also subtends θ w.r.t. the solar velocity. It is closer to the GC by $\Delta R \approx r \cos l$ and differs in V by ΔR×dV/dR.

Fig 3 zooms into the difference velocity (blue). We want to find its projection parallel (v_r: doppler) and transverse (v_t : proper motion) to the line of sight (*l.o.s.*). To do this, make use of its (green) components parallel and perpendicular to the solar velocity (amplitudes ΔV and θV_o).

Radial velocity components projected onto the line of sight:

$$\boxed{v_r} = \theta V_o \cos l - \Delta V \sin l = \frac{V_o}{R_o} r \sin l \cos l - \frac{dV}{dR} r \sin l \cos l$$

$$= r \sin l \cos l \left(\frac{V_o}{R_o} - \frac{dV}{dR}\right) = \boxed{A\,r \sin 2l}$$

where $A = \frac{1}{2}\left(\frac{V_o}{R_o} - \frac{dV}{dR}\right)_{R_o}$ is Oort's first (sheer) constant.

Transverse velocity components projected onto the sky (proper motion):

$$\boxed{v_t} = -\theta V_o \sin l - \Delta V \cos l = -\frac{V_o}{R_o} r \sin^2 l - \frac{dV}{dR} r \cos^2 l$$

$$= -\tfrac{1}{2}\left(\frac{dV}{dR} + \frac{V_o}{R_o}\right) r\,(\cos^2 l + \sin^2 l) - \tfrac{1}{2}\left(\frac{dV}{dR} - \frac{V_o}{R_o}\right) r\,(\cos^2 l - \sin^2 l)$$

$$= -\tfrac{1}{2}\left(\frac{dV}{dR} + \frac{V_o}{R_o}\right) r + \tfrac{1}{2}\left(\frac{V_o}{R_o} - \frac{dV}{dR}\right) r \cos 2l = \boxed{B\,r + A\,r \cos 2l}$$

where $B = -\frac{1}{2}\left(\frac{V_o}{R_o} + \frac{dV}{dR}\right)_{R_o}$ is Oort's second (rotation) constant.

A measures the local sheer: the degree to which stars slide past each other. E.g. solid body has no sheer, since dV/dR = V/R, so A = 0. Note a flat rotation curve (dV/dR = 0) does have sheer, with A = ½ V/R.

B measures local rotation, or vorticity. It comes from the curl of the velocity field: B = ½ ∇× **V**. E.g. solid body is pure rotation, at the angular velocity of the disk: B = –V/R.

Here are some examples of circular disk rotation, with full velocities shown on the left (red vectors), and the differential velocity on the right (blue vectors). Each pair is for a particular rotation curve gradient near the sun (dV/dR). The galactic center is at y = –8.5 kpc, and V_{sun} = 220 km/s. The circle is 1 kpc in radius.

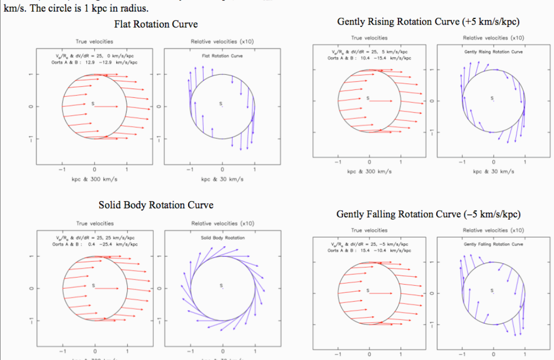

Oort's constants

- Current best (Hipparcos) estimates for Oort's A and B are:
  A = 14.8 +- 0.8 km/s/kpc and B = -12.4 +- 0.6 km/s/kpc
- Note: dimensions are velocity gradients; also frequencies
  - E.g. using psm units: A = 0.0148 km/s/pc 0.014 Myr^{-1} = 14.8 Gyr^{-1}
- From definition interesting properties of MW rotation measured:

$$A + B = \left(\frac{dV_c}{dR}\right)_{R_0} = +2.4 \text{ km/s/kpc}$$

$$A - B = \left(\frac{V_c}{R}\right)_{R_0} = \Omega(R_0) = 27.2 \text{ km/s/kpc}$$

- The first of these confirms that the rotation curve is fairly flat near the sun (gently rising).
- The second yields an **orbital period for the sun**:
  $P(R_0) = 2\pi / \Omega(R_0) = 2\pi / 27.2\ Gyr^{-1} = 0.23$ Gyr = 230 Myr

epicycles

- when coupled with an estimate for the galactocentric distance, R_0, the previous slide yields an **orbital velocity**: $V_c(R_0) = 218\ (R_0\ /\ 8\ \text{kpc})$ km/s
  - Which agrees fairly well with radio VLBI measurements of from proper motion of Sgr A^*
    $V_c(R_0) = 241\ (R_0\ /\ 8\ \text{kpc})$ km/s
- This analysis assumes the sun and stars are all on circular orbits.
  - In truth, this is only approximately true: the stars are in fact perturbed from circular orbits.
- This kind of motion can be analyzed using the concept of **epicycles**.

epicycles

- Disk stars have approximately circular orbits with small deviations : As with the Ptolemaic system: star orbits can be described by superposition of:
  - Circular orbit along **guiding center** (= deferent), radius R_g, angular velocity Ω_g
  - Smaller elliptical **epicycle**, angular velocity κ, **retrograde**

An intuitive way to understand the origin of the epicyclic motion:

- Consider star at *guiding center* (GC) and give it a kick radially **outwards**
- Conserving AM = mrv_ϕ, since r increases, v_ϕ decreases -> w.r.t. the guiding center, the star moves **backwards**
- Consider the new balance between gravity and centrifugal forces: Under AM conservation, $F_{centrifugal} \sim v_\phi^2 / r \sim r^{-3}$ while F_{grav} falls more **slowly** than r^{-3} -> at larger radii $F_{grav} > F_{centrifugal}$ and the star gets pulled back **inwards**
- As it falls in, r decreases so v increases and the star moves **forward** relative to the GC
- But now $F_{centrifugal} > F_{grav}$ and the star moves **outwards** again -> the cycle repeats, and we have a small **retrograde epicycle**

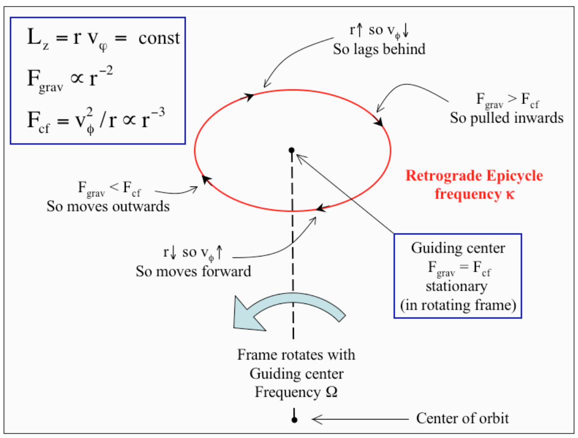

epicycles

- For a Keplerian potential, the orbit and epicycle frequencies are the **same**, $\kappa_g = \Omega_g$ The full orbit is **closed**: we have an off-centred Keplerian ellipse.
- However, in general Ω_g and κ are different so orbits don't close... Unless they are observed from frame rotating at Ω_g - 1/2κ :
  - orbits then appear **closed ellipses**, centered on galactic centre.
- lets briefly anticipate the relevance of epicycles for spiral arms:
  - For epicycle phases which vary systematically with radius: nested elliptical orbits may crowd in a spiral pattern this is called a **kinematic density wave**
  - Orbits are in turn perturbed by the spiral density pattern, this modifies the simple epicycles
  - Self-consistent solution is a **density wave** gas reponse causes shocks and star formation visible spiral arms

Epicycles: characteristics

- Consider a smooth axisymmetric flattened mass distiribution with potential Φ(R,z)
- Since we have no azimuthal forces AM is conserved, and we have :

$$\ddot{\mathbf{r}} = -\nabla\Phi(R,z)\ ; \quad L_z = R^2\dot{\phi} \ = \ const$$

- Separating the Equations of motion into components in cylindrical coordinates (R, Φ, z):

$$\ddot{R} - R\dot{\phi}^2 = -\frac{\partial\Phi}{\partial R}\ ; \quad \frac{d}{dt}(L_z) = 0\ ; \quad \ddot{z} = -\frac{\partial\Phi}{\partial z}$$

Epicycles: Vertical z Motions

- Take first the z motion about the plane z = 0; since the disk is symmetric about z = 0, then the z-force at z = 0 is zero

$$\left(\frac{\partial\Phi}{\partial z}\right)_{z=0} = 0$$

- consider small motion above and below the plane, we simply expand the z-force linearly for small z:

$$\ddot{z} = -\left(\frac{\partial\Phi}{\partial z}\right)_{z=0} - z\left(\frac{\partial^2\Phi}{\partial z^2}\right)_{z=0} = -z\left(\frac{\partial^2\Phi}{\partial z^2}\right)_{z=0} = -\nu^2 z$$

- This gives Simple Harmonic Motion (SHM), with frequency ν, where $\nu^2 = (\partial^2\Phi\ /\ \partial z^2)_{z=0}$

$$z(t) = Z\cos(\nu t + \psi_0)$$

- For Milky Way disk near the sun, $\nu^2 = 4\pi\ G\ \rho_o$, which gives ~ 0.096 Myr^{-1}, vertical oscillation period $2\pi/\nu$ ~ 6.5 x 10^7 yr ~ 1/3 circular period.

Epicycles: radial motions

- First consider the circular guiding orbit (R = const) : it has radius R_g, circular velocity V_c and angular velocity Ω_g defined by

$$\left(\frac{\partial \Phi}{\partial R}\right)_{R_g} = \frac{V_c^2}{R_g} = R_g \Omega_g^2$$

- For non-circular orbits, the radial acceleration is given by (centrifugal - gravity):

$$\ddot{R} = R\dot{\phi}^2 - \frac{\partial \Phi}{\partial R}$$

- However, since $L_z = R^2\, d\phi/dt$, then this can also be written as

$$\ddot{R} = -\frac{\partial \Phi_{\rm eff}}{\partial R} \quad \text{where} \quad \Phi_{\rm eff} = \Phi(R,z) + \frac{L_z^2}{2R^2}$$

- Where the **effective potential**, $\Phi_{\rm eff}$, allows us to describe the radial motion in 1-D form

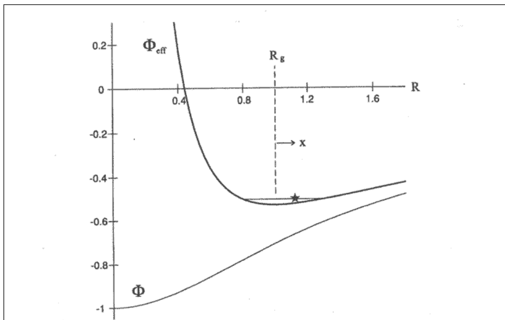

Figure 3.7 Effective potential $\Phi_{\rm eff}$ (upper curve) for a star with angular momentum $L_z = 0.595$, orbiting in a Plummer potential Φ_P (lower curve). The scale length $a_P = 1$; L_z is in units of $\sqrt{G\mathcal{M}a_P}$; units for Φ and $\Phi_{\rm eff}$ are $G\mathcal{M}/a_P$. The vertical dashed line marks the guiding center R_g; the star oscillates about R_g between inner and outer limiting radii.

Epicycles: radial motions

- Typically, $\Phi_{\rm eff}$ has a minimum, rising steeply at small R and slowly at large R
- This inner steep term imposes an **angular momentum (or centrifugal) barrier**
- At the minimum in $\Phi_{\rm eff}$, we recover the circular guiding orbit of radius R_g

$$\left(\frac{\partial \Phi_{\rm eff}}{\partial R}\right)_{R_g} = 0 = \left(\frac{\partial \Phi}{\partial R}\right)_{R_g} - R_g\dot{\phi}_g^2 = \left(\frac{\partial \Phi}{\partial R}\right)_{R_g} - \frac{V_c^2}{R_g}$$

- Other orbits will oscillate in radius, about R_g. Consider the potential at $R = R_g + x$

$$\ddot{R} = \ddot{x} = -\left(\frac{\partial \Phi_{\rm eff}}{\partial R}\right)_{R_g} - x\left(\frac{\partial^2 \Phi_{\rm eff}}{\partial R^2}\right)_{R_g} = -x\left(\frac{\partial^2 \Phi_{\rm eff}}{\partial R^2}\right)_{R_g} = -\kappa^2 x$$

- This gives SHM about the guiding radius $\quad x(t) = X\cos(\kappa t + \phi_0)$

  with frequency κ, where

$$\kappa^2 = \left(\frac{\partial^2 \Phi_{\rm eff}}{\partial R^2}\right)_{R_g} = \left(\frac{\partial}{\partial R}\left(\frac{\partial \phi}{\partial R}\right)\right)_{R_g} + \frac{3L_z^2}{R_g^4} = \left(R\frac{d\Omega^2}{dR} + 4\Omega^2\right)_{R_g}$$

Epicycles: azimuthal motions

- Since $L_z = R_g^2\,\Omega_g = R^2\Omega =$ const, changes in R yield changes in Ω (recall $\Omega = d\phi/dt$)

$$\dot{\phi} = \frac{L_z}{R^2} = \frac{L_z}{(R_g + x)^2} \simeq \frac{L_z}{R_g^2}\left(1 - \frac{2x}{R_g}\right) = \Omega_g\left(1 - \frac{2x}{R_g}\right)$$

- Integration gives :

$$\phi(t) = \Omega_g t - \frac{2\Omega_g X}{\kappa R_g}\sin(\kappa t + \phi_0)$$

- Thus, $\phi(t)$ follows the guiding center with small amplitude SHM superposed. Taking the y-axis in the forward direction with origin on the guiding center, we have

$$y(t) = -\frac{2\Omega_g}{\kappa} X\sin(\kappa t + \phi_0)$$

- the oscillation of frequency κ is the same as in x, but out of phase by $90^{\rm o}$

Epicycles: azimuthal motions

- Taken together, (and setting the initial phase $\phi_0 = 0$), we have

$$x(t) = X\cos(\kappa t)$$
$$y(t) = -\frac{2\Omega_g}{\kappa} X\sin(\kappa t)$$

Some properties of this motion are:

- **elliptical** epicycle with radial/azimuthal axis ratio = $\kappa / 2\Omega$
- epicyclic motion is **retrograde** w.r.t. orbit (c.f. Ptolemy's were prograde)
- For **Keplerian** potential: $\Omega \sim R^{-3/2}$ we get $\kappa = \Omega$
  - epicycle axis ratio 2:1 (cf Ptolemy's were 1:1 circles)
  - full orbit is closed ellipse, centered at the ellipse focus, e.g. (next slide)
- For **flat rotation curve**: $\Omega \sim R^{-1}$ we get $\kappa = \Omega$sqrt(2)
- For **solid body rotation**: Ω= const (harmonic potential):
  - $\kappa = 2\Omega$ giving **circular** epicycles and **closed** oval orbits
- In general, $\Omega < \kappa < 2\Omega$ so $\kappa > \Omega$
  - epicycle completed **before** rotation
  - from inertial frame, orbits don't close, but regress

epicycles

- In the case of a Keplerian potential, the epicycle has aspect ratio 2:1 with frequency equal to the orbital frequency.
- Hence the path traced out is **closed** in a stationary frame, and approximates an ellipse with focus at the gravitational center.
- This, and the harmonic potential, are the only to central force fields for which the orbit is closed.

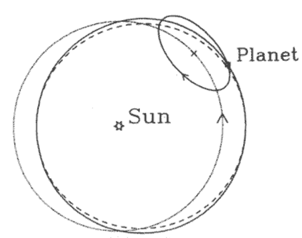

Figure 3-6. An elliptical Kepler orbit (dashed curve) is well approximated by the superposition of retrograde motion at angular frequency κ around a small ellipse with axis ratio $\frac{1}{2}$, and prograde motion of the ellipse's center at angular frequency Ω around a circle (dotted curve).

Values near the solar neighbourhood

- We can express the epicyclic and orbital frequencies at the solar radius, κ_0, Ω_0, in terms of Oort's constants:

$$\kappa_0^2 = -4B(A-B) = -4B\Omega_0 \,; \quad \kappa_0 = 37 \text{ km/s/kpc}$$

$$\Omega_0 = A - B = 27 \text{ km/s/kpc}$$

- The ratio κ_0 / Ω_0 ~1.3 -> Solar neighborhood stars make 1.3 epicyclic rotations per orbit.
- The ratio $\kappa_0 / 2\,\Omega_0$ ~0.7
  - Epicycles have radial/azimuthal extent of ~0.7
  - Stars with $R_g = R_0$ have velocity dispersions $\sigma_R / \sigma_\phi = \kappa_0 / 2\Omega_0$ ~0.7
  - However, at R_0, velocity dispersions are in fact $\sigma_R / \sigma_\phi = 2\Omega_0 / \kappa_0$ ~1.5 … because stars found at R_0 tend to have $R_g < R_0$ (more stars at smaller radii)
- Epicycle **sizes** are ~ σ/κ , so for σ_R ~ 30 km/s, we find ~ 1 kpc excursions
- Similarly, for σ_z ~ 30 km/s and ν ~0.096 Myr^{-1} we find vertical excursions ~ 300 pc.

epicycles

- Simple simulation of 2.5 orbits of the sun around the galaxy, with epicyclic frequency κ = 1.3 Ω
- The epicycle completes before the orbit, so the orbit appears to "regress"
- [In this case, the epicycle is circular (rather than elongated by ratio 1.3) and has roughly twice the size is should.]

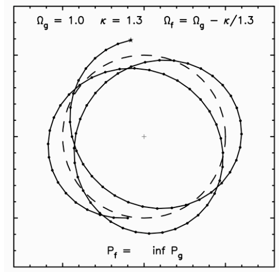

epicycles

- For the sun, z ~ 40pc and Ω ~ 7 km/s, so we expect modest vertical excursions.
- An amusing (speculative) theory is that disk crossings coincide with terrestrial craterings and/or extinctions -> The higher stellar densities perturb the Oort comet cloud, causing more impacts (!):

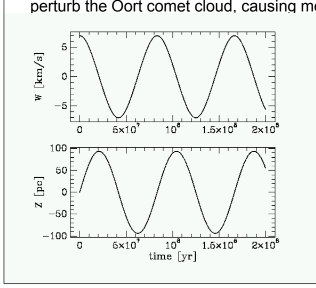

Resonances: Rotating patterns

- there can be regions of **enhanced stellar density** in the disk
- These can have the shape of spiral and bar **patterns**
- These patterns are neither stationary nor move with the disk stars,
- Instead they move at some *intermediate angular velocity*, Ω_p, called the **pattern speed**
- The interaction of these patterns with the epicyclic motion can lead to **resonances**:

co-rotation radius:

First consider a star which orbits **at the pattern speed**

- we have $\Omega_* = \Omega_p$ or $\Omega_p - \Omega_* = 0$
- Such stars experience a **persistant** non-axisymmetric perturbation, and their response builds up

Linblad resonances (ILR, OLR)

- Consider stars which complete exactly 1 epicycle between the passage of each arm
  - Their interaction with the spiral arm is **resonant**
  - Epicyclic amplitude is amplified and wave propagation is strongly modified
- Where do such resonances occur in the galaxy?

The angular frequency of the star w.r.t. the pattern is $\Omega_p - \Omega_*$

… There are two cases :
  - -ve if $\Omega_* > \Omega_p$; star moves past arms
  - +ve if $\Omega_p > \Omega_*$; arms move past stars
- The angular frequency of encountering **each** arm in a 2 armed spiral is $2(\Omega_p - \Omega_*)$

So the condition for resonance is:
  - $2(\Omega_p - \Omega_*) = \pm\kappa$ or $\Omega_p - \Omega_* = \pm\kappa/2$ ($\pm\kappa/m$ for an m-armed spiral)

Linblad resonances (ILR, OLR)

- There are two classes of resonance:
  - $\Omega_p - \Omega_* = -\kappa / 2$: **Inner Lindblad Resonance** (stars move past pattern)
  - $\Omega_p - \Omega_* = +\kappa / 2$: **Outer Lindblad Resonance** (pattern moves past stars)
- To establish the radii of these resonances, one needs to know (see next slide):
  - The pattern speed: Ω_p
  - The rotation curve, $V_c(R)$, which gives $\Omega(R)$ and $\kappa(R)$
  - E.g., for a 'Plummer sphere' often used to model GCs or other stellar systems $\Phi_P(r) = -\frac{GM}{\sqrt{r^2 + a^2}}$,
- Depending on $V_c(R)$ and Ω_p there may be 0,1,2,.... resonances (there can also be 0,1,2 **inner** Lindblad resonances)

- For a Plummer sphere, one can calculate the rotation curve, $V_c(R)$ or $\Omega(R)$ and from this $\kappa(R)$ [$= (R\, d\Omega^2/dR + 4\Omega^2)^{1/2}$].
- The figure shows $\Omega(R)$ and the two curves $\Omega + 1/2\,\kappa$ and $\Omega - 1/2\,\kappa$. If we now imagine a pattern speed, with frequency Ω_p (which is independent of radius), then we can ascertain the radii at which the inner and outer Lindblad radii occur, as well as corotation.
- Notice in this example there are, in fact, **two** inner Lindblad resonance

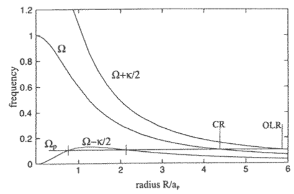

Figure 5.29 Frequencies $\Omega(R)$ and $\Omega \pm \kappa/2$ in the Plummer potential of Equation 3.11. For pattern speed Ω_p, the $m = 2$ inner Lindblad resonances are marked by vertical ticks, the corotation radius is labelled 'CR', and the outer Lindblad resonance 'OLR'. If the pattern speed had been twice as large, the inner Lindblad resonances would be absent.

Importance of resonances - several reasons:

- Density waves: (see below)
  - Can only survive in between the ILR and OLR (where we find arms)
  - Cannot pass an ILR (they are absorbed, like waves on a beach)
  - -> Important in allowing/preventing propagation across the disk through the center
- Orbit **shapes** change across the resonances:
  - Bars don't extend beyond CR, stop close to it
  - Bars probably rotate with pattern speed $\Omega_p \sim \Omega(R{=}CR)$
  - Expect stellar **rings** to form at CR and OLR (as found)
- Gas driven **inwards** to ILR and **outwards** to ILR
  - often find gas rings/disks/starformation near ILR
  - For the *Milky Way*, estimates are (for m=2): ILR at ~3kpc, CR at ~14kpc, and OLR at ~20kpc, with $\Omega_p \sim 15$ km/s/kpc

Density Waves

- **Kinematic Density Waves**: In general, orbits are **not closed** (~1-2 epicycles per orbit)
  - However, they **are** closed in a frame which rotates at Ω_g - 1/2κ
  - In this frame, orbit is closed ellipse with Galactic centre at the centre.
- Consider set of orbits whose epicyclic phases vary **monotonically** with radius (i.e. PA of ellipses rotates with increasing R)

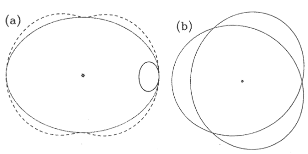

Simple **orbit crowding** will generate a two arm spiral pattern.
This is called a **kinematic density wave**

Figure 6-9. The appearance of elliptical orbits in a frame rotating at $\Omega_p = \Omega - n\kappa/m$. (a) $(n, m) = (0, 1)$, solid line; $(1, 2)$, dotted line; $(1, -2)$, dashed line; (b) $(n, m) = (2, 3)$.

- For a set of orbits with epicycles, we have a pattern which rotates with Ω- 1/2 κ.
  - If the phases are all the same, we have the pattern on the left.
  - If the phases increase systematically with radius we find a spiral pattern, where the oval orbits bunch up.
- Density wave theory envisions a situation in which the very density enhancements caused by the synchronized epicycles perturb the orbits in just the way needed to maintain these same epicycles.
  - Hence the entire system is stable and long-lived.

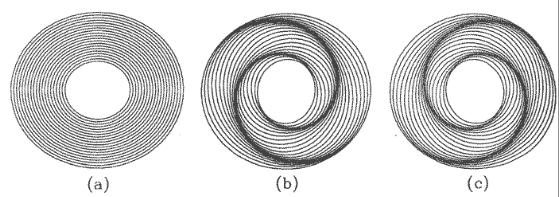

Figure 6-11. Arrangement of closed orbits in a galaxy with $\Omega - \frac{1}{2}\kappa$ independent of radius, to create bars and spiral patterns (after Kalnajs 1973).

Density Waves

- **If** Ω- 1/2 κ is roughly independent of radius (roughly true for flat rotation curve):
  - the pattern is **fixed** and rotates at $\Omega_p = \Omega_g$ - 1/2 κ = **pattern speed**
  - In fact, for V_c = const, pattern speed varies **slowly** with R, so spiral slowly **winds up**
- However, including **self-gravity** can yield a **different** Ω_p which is almost **independent of radius**
  - this is a result from "density wave theory", to which we now turn:

Lin-Shu (QSSS) Density Wave Theory

Sketch of Approach:

- The generation of **kinematic** spirals assumes **axisymmetric** potential
  - However, orbit crowding yields a **non-axisymmetric** spiral perturbation
  - Star (and gas) orbits are **modified** by the spiral perturbation
  - Their new orbits define a **new** surface density and associated potential.
- We need to look for a **self consistent** solution: response to input potential gives **same** potential The analysis is difficult (Lin & Shu 1964, 1966 and much subsequent work)
  - Considers **waves** propagating in a differentially rotating disk
  - Derive a **dispersion relation**: $\omega = f(k)$, with phase velocity, ω/k, and group velocity, $d\omega/dk$.
  - Look for **Quasi-Stationary Steady State** solution (QSSS).

Lin-Shu (QSSS) Density Wave Theory

- **Results:** Solutions are found with
  $\Omega_p = \Omega - (d\omega/dk) \times 1/2\kappa$
  which is ~ independent of R
- Pitch angles $\psi(R)$ ~ const, yielding **logarithmic spirals**
- Waves **survive** between ILR and OLR
- Waves are **absorbed** at ILR.
- Waves weaker in disks with higher velocity dispersion
  – need cold component to be replenished via star-formation (c.f. S0 disks don't have arms)

Lin-Shu (QSSS) Density Wave Theory

- Gas response:
  – Non-linear, leading to collisions/shocks above a threshold response
  – Gas runs into itself (c.f. traffic jams) creating **narrow gas features** (as observed)
  – Predict **velocity streaming** in vicinity of arms, roughly as found:
  – Geometry of density wave & strength of shock depend on both central concentration & V_c
    - explains correlation of pitch angle with bulge/disk ratio
    - explains lack of dwarf-spirals: need threshold V_c to form disk and arms.

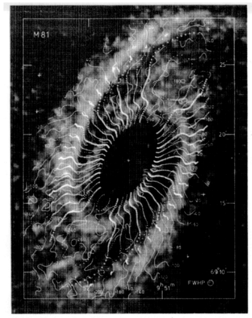

Figure 6-23. Constant-velocity contours of HI in the spiral galaxy M81. Solid lines represent observations made at the Westerbork Synthesis Radio Telescope, while chains of symbols represent predictions of a model based on the Lin-Shu hypothesis (Visser 1980). The contours are superimposed on an artificial photograph in which brightness is proportional to HI column density. The shaded circle at lower right represents the spatial resolution of the observations.

Alternative Sources of Global Density Waves

- It is unclear how often the QSSS density wave theory is applicable: (see Kormendy & Norman 1979 ApJ 233 539)
- Some galaxies have spiral arms within the region where V_c~ r (solid body):
  – arms don't wind up in this region.
- Many galaxies are **flocculent**, with no clear density wave pattern
- Many galaxies have an **alternative** source of density wave:
- There are two other obvious sources of density waves, both are m = 2.
- **(i) Tides from companions**
  – Tidal field of passing neighbor creates a strong m = 2 perturbation: [image]
  – This drives a strong kinematic density wave.
  – Self gravity enhances this perturbation.
  – However, these spirals are **transient**.
- **(ii) Bars and Oval Distortions**
  – Bars are another source of m = 2 perturbations
  – Sanders & Huntley (1976) find even weak bars can generates strong spiral arms
  – However, the mechanism needs **viscosity** (ie gas dissipation) to work.
  – Oval distortions may have a similar (though weaker) effect.

Galaxy flybys make spiral arms, tails, and bridges

Flyby Creation of Density Wave

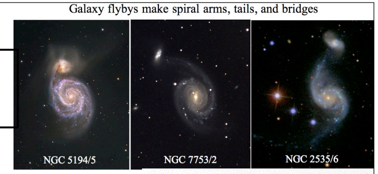

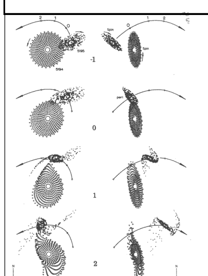

Figure 6-25. Model of the M51 system (Fig. 6-1) in which the spiral arms are caused by a recent passage of NGC 5195. The scenes on the left are viewed from the Sun, and those on the right are viewed from the side. See Toomre and Toomre (1972) and Toomre (1978).

114 CHAPTER 18. THEORIES OF SPIRAL STRUCTURE

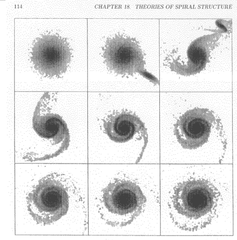

Figure 18.3: Self-consistent response of a disk galaxy to the passage of a smaller companion.

Galaxies 37

Galaxies

Lectures 12-13: Spiral galaxy dynamics; Introduction to the Local Group; further applications of Jeans equations

- **Disk galaxy instabilities and bars.**
- Intro to the Local Group of galaxies
- Tidal friction
- Tidal evaporation
- Tidal radius
- Galaxy interactions
- Asymmetric drift
- Mass to light ratios (dSph's)

Disk Instabilities and Their Amplification

- For the significant number of **flocculent** spirals, a different mechanism may be at work
- This involves the tendency of stars and gas within a disk to clump up gravitationally and form stars
- These clumps then get pulled into spiral arm fragments by differential rotation

NGC2997

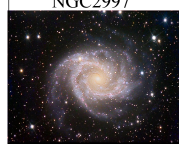

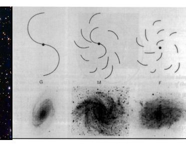

NGC5055

Local Disk Stability: Toomre's Q Parameter

- When are self-gravitating disks vulnerable to **local** gravitational instabilities ?
- Instabilities can arise from a competition between:
  - gravity causing overdense regions to collapse
  - stellar dispersion which inhibits the collapse
  - angular momentum which inhibits the collapse
- Toomre (1964) found the conditions for instability: $Q < 1$ where $Q \sim \kappa\sigma / (3\, G\, \Sigma)$
  - Where σ is the stellar velocity dispersion and Σ is the local surface density

Local Disk Stability:

simplified derivation based on a **modified Jeans analysis**:

- Consider overdense region radius R in a **non-rotating** disk
- The collapse time is $t_{coll} \sim R / V$ where V ~ gravitational velocity ~ $(G M / R)^{1/2}$
- So $t_{coll} \sim R / (GM / R)^{1/2} \sim (R^3 / GM)^{1/2} \sim (R / G\Sigma)^{1/2}$ (Σ is surface density)
- The time for stars to escape the region is : $t_{esc} \sim R / \sigma$ (σ is dispersion)
- So collapse occurs if $t_{coll} < t_{esc}$ ie $(R / G\, \Sigma)^{1/2} < R / \sigma$
- The critical size **for stability** due to dispersion is therefore: $R_J < \sigma^2 / G\, \Sigma$

Local Disk Stability:

- Now consider a **rotating** disk:
  - The **local** angular velocity is Oort's constant B
  - The region is **stable** if $F_{centrifugal} > F_{gravity}$
  - In this case $R\, B^2 > GM / R^2 = G\, \Sigma$
    The critical size **for stability** due to rotation is therefore : $R_{rot} > G\, \Sigma / B^2$
- Combining these: the disk is **unstable** in the range $R_J < R < R_{rot}$
- And therefore the disk is locally **stable** if $R_J > R_{rot}$
- ie $\sigma^2 / G\, \Sigma > G\, \Sigma / B^2$ or $\sigma B / G\, \Sigma > 1$
- Recall that $B = \kappa^2 / 4\, \Omega$ and ~ 1-2 so $B \sim \kappa/3$

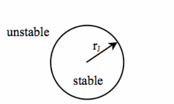

Collapse time vs Escape time

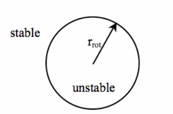

Rotation support vs Gravity

Local Disk Stability:

- The final condition for disk **stability** is therefore

$$Q \equiv \frac{\sigma |B|}{G\Sigma} \cong \frac{\sigma\kappa}{3G\Sigma} > 1$$

- [A similar relation for gravitational stability for a **gas** disk is: $Q = V_s\, \kappa / 3\, G\, \Sigma > 1$]
- Factors which promote gravitational **instability** (i.e. promote spiral structure) are:
  - low stellar velocity dispersion σ
  - high surface mass density Σ
  - low epicyclic frequencies (and/or low local rotation, i.e. low |B|).
- Solar neighborhood : $\sigma \sim 30$ km/s ; $\Sigma \sim 50$ M pc^{-2} ; $\kappa \sim 36$ km/s/kpc
  - these give Q ~ 1.4 and so the MW disk is locally stable near the sun

Swing amplification

- Some circumstances allow a powerful amplification of spiral patterns (eg Toomre 1981)

(i) The Swing Amplifier

- If we have a **leading** spiral density wave, then
- Differential rotation will gradually rotate it into a **trailing** spiral wave (see next slide)
- The rotation of the pattern is **retrograde**
- The timescale for rotation is ~ κ
  - Epicyclic motion approximately **follows** the arm
  - **Long** perturbation duration so epicycle amplified
  - The emerging trailing pattern is strongly **amplified**

- Sketch of the orbital progression, right to left, of a leading arm-fragment that becomes a trailing arm-fragment.
- Notice that the rotation of the arm-fragment is **retrograde**, which is the **same** as the direction of the epicycles.
- Hence the epicycles are perturbed for a long period of time, and respond strongly.

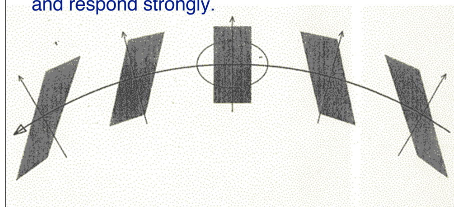

Figure 18.1: Evolution of an overdense perturbation in a shearing disk. The disk rotates counter-clockwise, as indicated by the heavy arc; a typical star moves around an elliptical epicycle in a clockwise direction. The perturbation (grey patch) initially has the form of a *leading* spiral (right), but is sheared into a *trailing* spiral (left) by the differential rotation of the disk. The epicycle and the perturbation rotate in the same direction, so stars stay in the perturbation longer than they would under other conditions.

- Similar sketch previous slide, although here the orbital progression (which in reality is right to left) is shown left to right.
- Again, stars whose epicyclic phase place them in the feature are perturbed for a long time as the epicycle progresses, so does the arm.

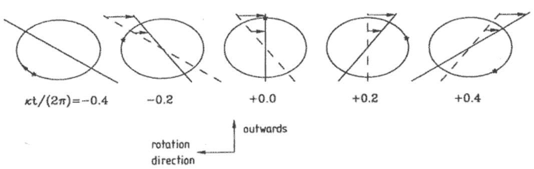

Figure 6-18. Schematic diagram showing the reason for swing amplification. The panels show the motion of a star in its epicycle and the motion of an unwinding material arm in a Mestel disk. The dashed and solid straight lines show the movement of the material arm between panels. The interval between panels is 0.2 times the epicycle period. Note the temporary similarity of angular speeds of the arm and the star: between $\kappa t/(2\pi) = -0.2$ and $+0.2$ the arm and the star swing around at roughly the same rate, so that the gravitational field of the arm can steadily attract the star.

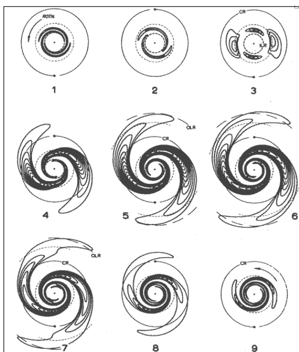

Figure 6-17. Evolution of a packet of leading waves in a stellar Mestel disk with $Q = 1.5$ and $f = 1$. Contours represent fixed fractional excess surface densities; since the calculations are based on linear perturbation theory, the amplitude normalization is arbitrary. Contours in regions of depleted surface density are not shown to minimize confusion. The time interval between diagrams is one-half of a rotation period at corotation. From Toomre (1981), by permission of Cambridge University Press.

- Density contours of a leading arm unwinding to become a trailing arm.
- The swing amplifier boosts the arm strength considerably.

Swing amplification

(ii) Feedback for the Amplifier

- For this to work, we need a source of **leading** spiral waves
- However, these are not normally generated in rotating disk
- Instead, look for **feedback**: trailing waves converted into leading waves.

- Waves **reflected** from outer edge experience 180deg phase shift (trailing ->leading)
  - unlikely to operate in real galaxies: edges too soft
- Trailing waves passing through the central regions emerge as leading waves (see next slide)
  - This can only occur when we have no ILR (which blocks wave passage)

Feedback: Swing amplification

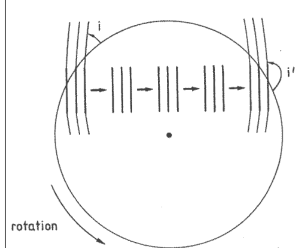

Figure 6-20. A graphical argument that suggests why trailing waves that propagate through the center of a disk emerge as leading waves. A small patch of three incoming trailing waves with inclination $i < 90°$ is shown on the left. The patch propagates through the center as a plane wave and emerges with a pitch angle $i' = 180° - i$. Since $i' > 90°$ the merging wave is leading.

- If trailing waves can pass through the central regions of a galaxy then they emerge as leading waves on the other side.
- These leading waves are then subject to the swing amplification.

Bar Instability and its Suppression

- N-Body simulations of disks seem to form bars **remarkably easily** (see next slide)
  - Indeed, it is difficult to devise stable disk models **even with Q > 1**
  - Reality of this **bar instability** has been verified using analytic methods
- Swing Amplification helps explain the instability:
  - Recall: leading waves are strongly amplified into trailing ones
  - Nothing happens unless there is a source of leading waves
  - Trailing waves pass through center and emerge as leading
  - Hence **feedback** keeps the amplifier going
    -> bar grows quickly.

Bar Instability and its Suppression

- Initially axisymmetric disks will develop a strong bar.
- This **bar instability** is quite severe and is strengthened in part by the swing amplification feedback of trailing waves passing through the central regions to become leading waves.

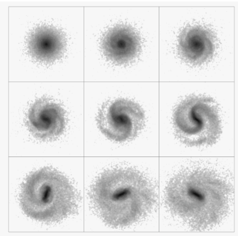

Figure 19.1: Bar instability in a model disk galaxy. This model is similar to the one shown in Fig. 18.2, but here the disk comprises 75% of the total mass.

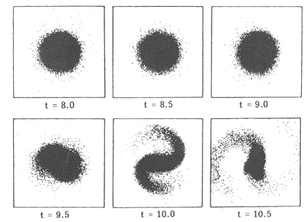

Figure 6-16. Evolution of the disk in Figure 6-15 without the constraint that the disk remain axisymmetric. The initial condition is the disk in Figure 6-15 at $t = 8.0$. Reprinted from Hohl (1971), by permission of *The Astrophysical Journal*.

Bar Instability and its Suppression

- Early work (Hohl 1971, Ostriker & Peebles 1973) noted the severity of the bar instability
  - As you might expect, increasing stellar **dispersion** can calm instability
    - found disks were stabilized against bar formation for KE(σ) / KE(rot) > 5
    - Note that for the MW disk near the sun, KE(σ) / KE(rot) ~ 0.15
      -> so our disk should be highly unstable to bar formation!
- What might suppress the bar instability in real galaxies? …
  - Put mass in a dark halo: this acts like a high dispersion component
    - More of historical interest: ~1973, any evidence for dark halo promoted
    - However, dynamics of the inner regions ***not*** influenced much by the halo
    - The halo may nevertheless help stabilize disks at larger radii.
  - Achieve the same by having a high dispersion bulge or inner disk
    Ingoing waves are damped before they pass though the centre:
    cuts feedback
  - An ILR will shield the centre and cut the feedback: A large central bulge mass yields an Ω(R) with an ILR

The Local Group

The Local Group

- The local group (LG) of galaxies is dominated by the bright spiral galaxies, the Milky Way and Andromeda (M31).
- The LG may be defined as all galactic systems bound gravitationally to the MW and M31.
- This can be difficult to demonstrate for all galaxies out to a radius of 1 Mpc of the MW/M31 barycentre (observationally)
- Therefore, a purely radial cut of 1 Mpc can also be applied.
- The LG provides a close up view of galaxy related physics in action, e.g. interactions, mergers, star formation and globular cluster formation.

The Local Group

Taxonomy of members

- The LG is dominated in terms of luminosity (mass) by the giant spirals M31 (Andromeda) and the MW.
- Then comes a small gap in the luminosity distribution before including the spiral M33 (Triangulum) and the LMC (large magellanic cloud).
  - Note that some researchers classify the LMC as a barred spiral (SBm) and others classify it as an irregular galaxy.
    - … an example of the subjective nature of morphological classification.
- Dwarf Elliptical/Irregular galaxies can be defined as $-18 < M_V < -14$.
- Dwarf Spheroidal galaxies range $-14 < M_V < -4$!

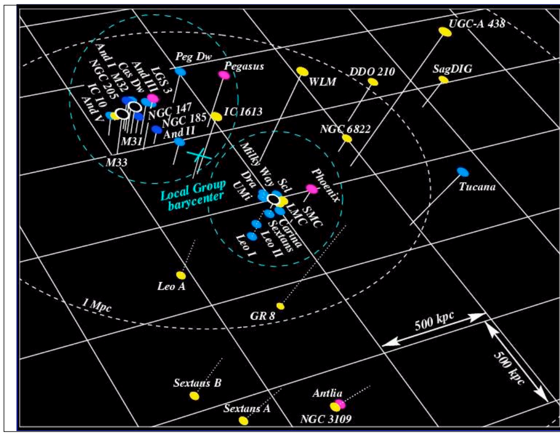

Name	Alias	DDO Type	$(m-M)_0$	M_V	l (deg)	b (deg)	D (kpc)	$\cos\theta$
M31	NGC 224	Sb I–II	24.4	−21.2	121.17	−21.57	760	0.88
Milky Way	Galaxy	S(B)bc I–II:	14.5	−20.9:	000.00	00.00	8	−0.15
M33	NGC 598	Sc II–III	24.5	−18.9	133.61	−31.33	795	0.73
LMC	...	Ir III–IV	18.5	−18.5	280.19	−33.29	50	−0.80
SMC	...	Ir IV/IV–V	18.85	−17.1	302.81	−44.33	59	−0.61
M32	NGC 221	E2	24.4	−16.5	121.15	−21.98	760	0.88
NGC 205	...	Sph	24.4	−16.4	120.72	−21.14	760	0.88
IC 10	...	Ir IV:	24.1	−16.3	118.97	−03.34	660	0.94
NGC 6822	...	Ir IV–V	23.5	−16.0	025.34	−18.39	500	0.29
NGC 185	...	Sph	24.1	−15.6	120.79	−14.48	660	0.91
IC 1613	...	Ir V	23.3	−15.3	129.73	−60.56	725	0.47
NGC 147	...	Sph	24.1	−15.1	119.82	−14.25	660	0.92
WLM	DDO 221	Ir IV–V	24.85	−14.4	075.85	−73.63	925	0.32
Sagittarius	...	dSph(t)	17.0	−13.8::	005.61	−14.09	24	−0.04
Fornax	...	dSph	20.7	−13.1	237.24	−65.66	138	−0.25
Pegasus	DDO 216	Ir V	24.4	−12.3	094.77	−43.55	760	0.76
Leo I	Regulus	dSph	22.0	−11.9	225.98	+49.11	250	−0.44
And I	...	dSph	24.55	−11.8	121.69	−24.85	810	0.86
And II	...	dSph	24.2	−11.8	128.91	−29.15	700	0.78
Leo A	DDO 69	Ir V	24.2	−11.5	196.90	+52.41	690	−0.14
Aquarius[a]	DDO 210	Ir V	25.05	−11.3	034.04	−31.35	1025	0.40
Sag DIG[a]	...	Ir V	25.7:	−10.7:	021.13	−16.23	1300:	0.22
Pegasus II	And VI	dSph	24.45	−10.6	106.01	−36.30	830	0.83
Pisces	LGS 3	dIr/dSph	24.55	−10.4	126.77	−40.88	810	0.71
And III	...	dSph	24.4	−10.2	119.31	−26.25	760	0.86
And V	...	dSph	24.55	−10.2	126.22	−15.12	810	0.87
Leo II	...	dSph	21.6	−10.1	220.14	+67.23	210	−0.26
Phoenix	...	dIr/dSph	23.0	−9.8	272.19	−68.95	395	−0.30
Sculptor	...	dSph	19.7	−9.8	287.69	−83.16	87	−0.06
Tucana	...	dSph	24.7	−9.6	322.91	−47.37	870	−0.44
Cassiopeia	And VII	dSph	24.2	−9.5	109.46	−09.95	690	0.98
Sextans	...	dSph	19.7	−9.5	243.50	+42.27	86	−0.65
Carina	...	dSph	20.0	−9.4	260.11	−22.22	100	−0.85
Draco	...	dSph	19.5	−8.6	086.37	+34.71	79	0.77
Ursa Minor	...	dSph	19.0	−8.5	104.88	+44.90	63	0.66

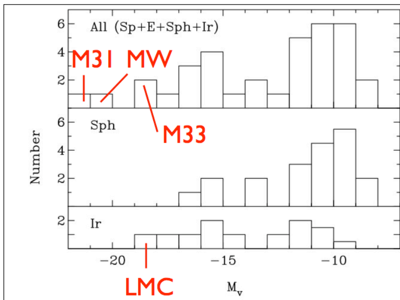

FIG. 1.—Histogram of the luminosity distribution of Local Group members, with absolute magnitude data taken from Table 1. The top panel gives the luminosity distribution for all Local Group members, and the middle and bottom panels show the luminosity distributions for Ir/dIr and Sph/dSph morphological types. Four galaxies appear in the top panel but not in the lower panels: the spirals M31, the Milky Way, and M33; and the elliptical M32. The galaxies Pisces and Phoenix (dIr/dSph) are counted with weight 0.5 in each of the lower two panels.

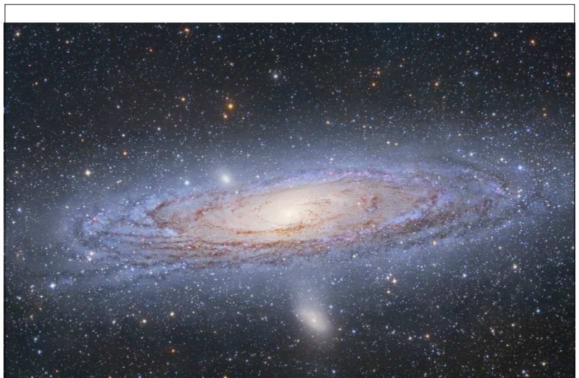

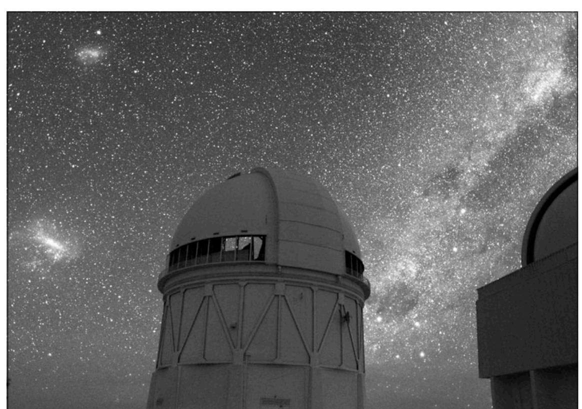

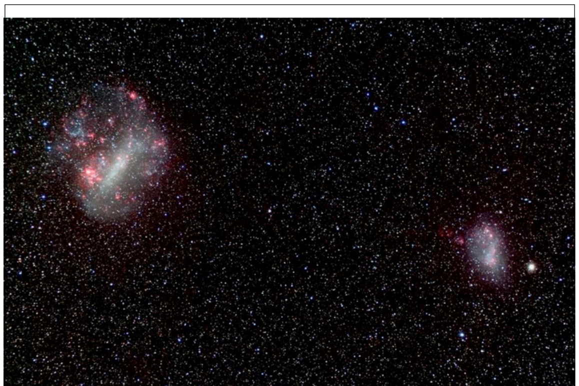

M32 and NGC205: Low-Mass E Galaxies

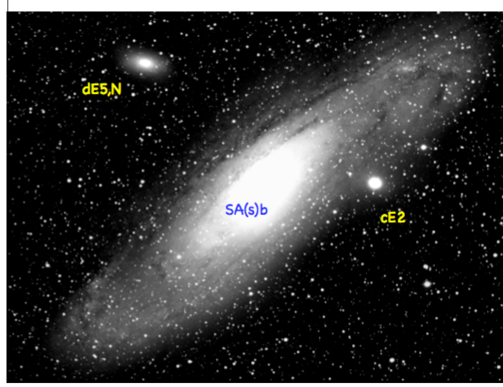

The Local Group

- Dwarf Elliptical/Irregular galaxies can be defined as $-18 < M_V < -14$.
  - Irrespective of where the exact line is drawn the important consideration is whether such dwarf galaxies are physically distinct compared to giants.
  - Recall, this does appear to be the case with the giant and dwarf ellipticals.
  - dSph's are different once again!
  - The SB profiles of giant ellipticals are well described by de Vaucouleurs profiles.
  - However, dwarf ellipticals show lower central surface brightnesses and overall start to be better fit by exponential profiles.
  - dSph's well fit by King profiles or exponentials

The Local Group

- A more physically continuous description of the SB profiles is provided by the Sersic profile parametrised by the effective radius Re and the radial fall-off n.
  - Taking n = 4 generates a de Vaucouleurs profile, while n = 1 is an exponential profile.
  - Furthermore, HST ACS observations indicate that as one considers fainter ellipticals the rate of occurrence of bright, central nuclei increases.
  - There do appear to be important structural differences, and thus clues to different formation histories and formation mechanisms, between giant and dwarf ellipticals, and dSphs.

The Local Group

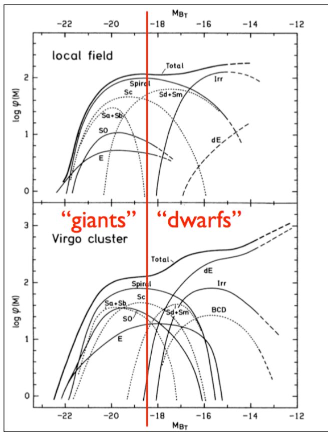

31

The Local Group

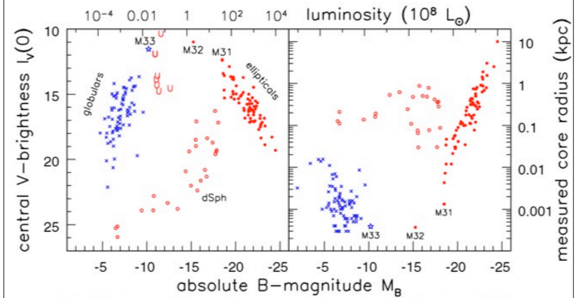

Galaxies

32

Scaling relations for red-seq galaxies

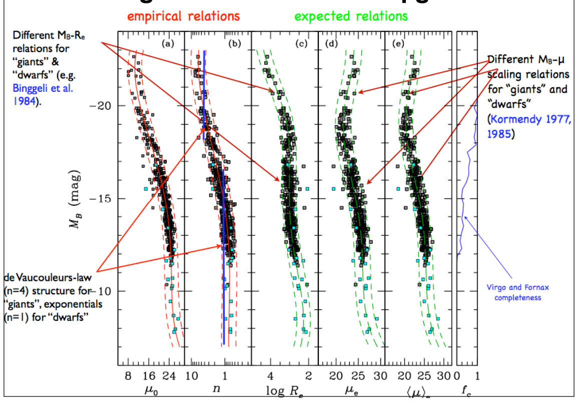

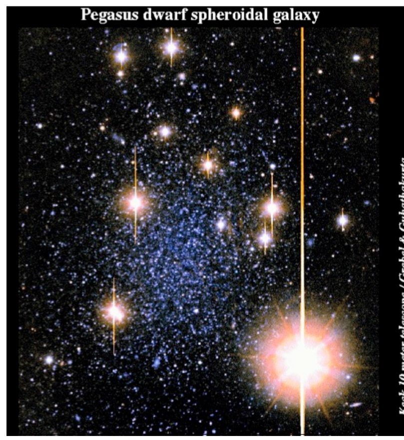

1Mpc distant

34

1Mpc distant

35

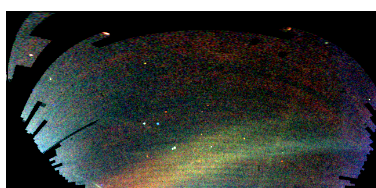

Belokurov et al. 2006

- **MW dsph's** found down to Mv < -3.5
- But only ~1/3 of sky covered.

Mv=8 Mv=6 Mv=5 Mv=4

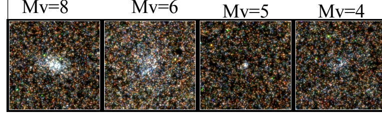

36

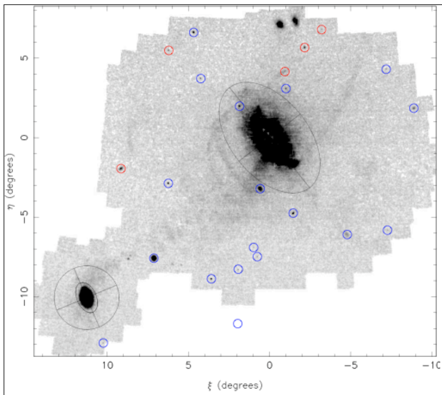

dSph galaxies viewed 'complete' for the first time in the Local Group in the M31 subgroup: (Irwin+)

However, only complete down to Mv<-6

GC's as simple stellar systems

- Difference from dSph galaxies is essentially in DM content (none versus >100 M/L)

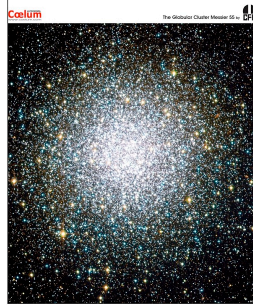

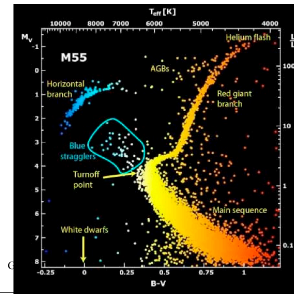

Multiple stellar pops in the Carina dSph galaxy

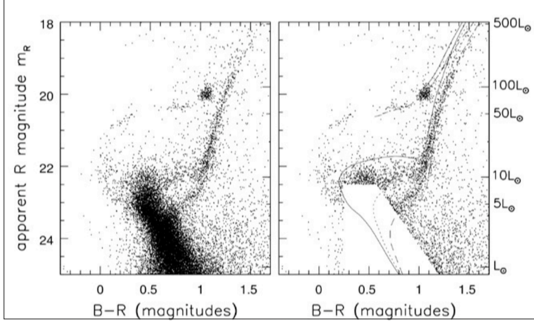

Sgr dSph (Ibata et al. 1994)

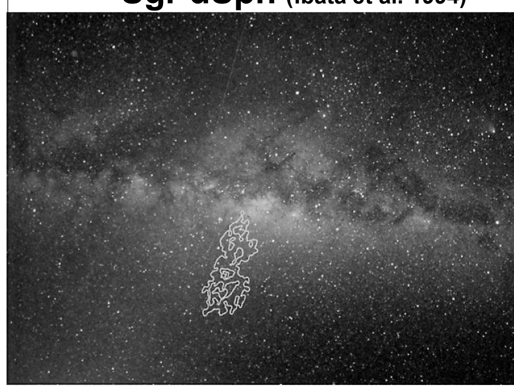

Sgr dSph (Ibata et al. 1994)

- Star counts to find a new merging dSph satellite of the MW!

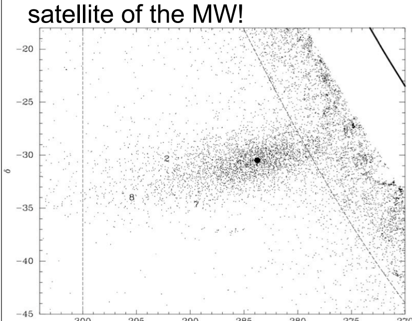

Similarly in M31

- Ibata et al. (2002), Irwin et al. (2005)

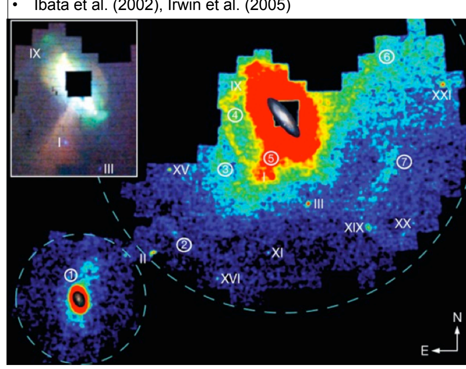

Tidal streams in the MW

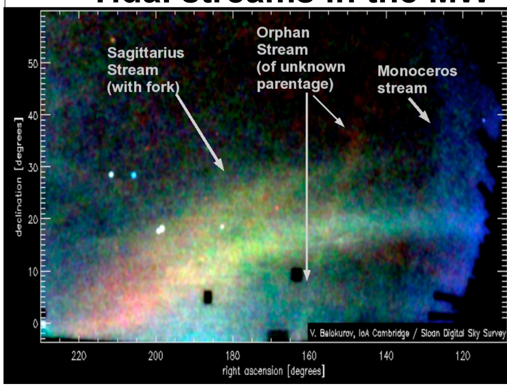

The Local Group

- L* galaxy stellar halos (MW, M31) could be built up mostly from 'tidally evaporated' dwarf galaxies, accreted over a Hubble time.
- Need to understand (with help from Jeans equations):
  - Dwarf galaxy M/L and dark matter haloes
  - Tidal friction
  - Galaxy encounters
  - Tidal evaporation

The Local Group

Galaxies

Lectures 13: galaxy interactions

- Different classes of interactions
- Tidal friction
- Tidal evaporation (tidal tails)

Galaxy Interactions

- Galaxy-Galaxy interactions are **important in understanding many aspects galaxy evolution:**
  - Morphological and dynamical structures
  - Star formation and starburst histories, with associated chemical enrichment history
  - AGN creation and fuelling
  - Elliptical galaxy formation
  - Formation of **all** galaxies in the Heirarchical merging scenario.

Galaxy Interactions

several different regimes:

- Strength of interaction:
  - **Weak** and/or distant encounters: flyby with associated tides satellite orbit decay due to dynamical friction tidal evaporation of orbiting satellite tidal or gravitational shocks
  - **Strong** and/or close encounters: can lead to mergers more global gravitational effects become important
- Relative size of merging galaxies:
  - major mergers: roughly equal sized galaxies
  - minor (eg satellite) mergers: one galaxy is significantly smaller than the other
- Hubble type of interacting/merging galaxies:
  - disks: dynamically cold (tend to generate narrow tidal tails)
  - spheroids: dynamically hot (tend to generate wider tidal fans)

Galaxy Interactions

- Different galaxy constituents:
  - these can respond quite differently during a merger and can play quite different roles
    - stars: a collisionless system
    - gas: dissipational; star formation; feedback
    - dark matter: extended collisionless reservoire for absorbing Energy and AM
- Relics:
  - Visible effects can survive long after the main merger (or interaction) has ended, particularly at large radii where relaxation times are very long:
    - Polar rings or shells
    - HI at large radii, possibly raining back down on the remnant
    - Kinematically distinct cores
    - Elliptical galaxies (may be merger relics!)

Galaxy Interactions: Analytic Tools

- We first consider four regimes which are analytically tractable as well as dynamically important.
- They also develop our ability to interpret numerical simulations of more complex regimes.
  - **(a)** A small system moving through a larger one (dynamical friction)
  - **(b)** Tidally driven evaporation: the Jacobi (Roche) Limit
  - **(c)** "Slow" encounters, where $V_{internal} >> \Delta V_{encounter}$ (adiabatic approximation)
  - **(d)** "Fast" encounters, where $V_{internal} << \Delta V_{encounter}$ (impulse approximation; tidal shocking)
- Unfortunately, major mergers do not conform to any of these regimes; They cannot be treated analytically and require numerical simulation

Dynamical Friction

- Consider a mass M moving at speed V through a population of stars with uniform space density n.
- The stars have mass m (<<M) velocity distribution f(v) (expressed as # per v)
- Gravitational focussing creates a wake behind the moving mass which pulls back on it

• This retarding force is called **dynamical friction**

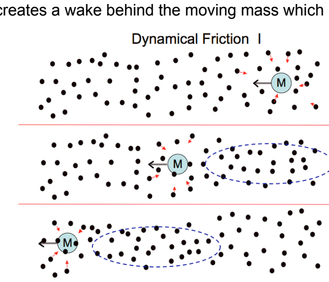

Dynamical Friction II

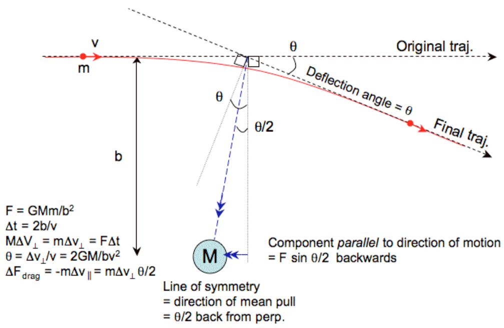

Dynamical Friction

- The basic idea behind dynamical friction is that a moving mass attracts objects to it, but because of its motion, the objects tend to gather **behind** the mass, pulling it backwards.
- To calculate the retarding force, it is best to think of a single object passing the mass on a Keplerian hyperbolic trajectory (i.e. jump to a frame moving with the mass).
- A simple analysis (next slides) approximates the full Keplerian solution.
- A small deflection angle θ defines the direction of symmetry for the orbit which is tilted by $\theta/2$ to both incoming and outgoing asymptote.
- Thus, while momentum transfer occurs throughout the flyby, it can be approximated by the force at closest approach multiplied by the flyby time (roughly, $2b/v$) in the direction of symmetry.
- Integrating over all encounters, the force perpendicular to the trajectory averages to zero, while the force parallel to it doesn't.

Dynamical Friction

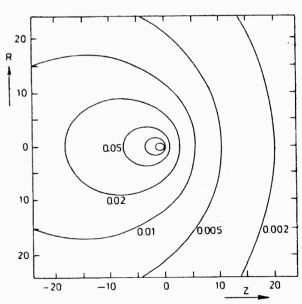

Figure 7-3. A mass travels from left to right at speed v through a homogeneous Maxwellian distribution of stars with one-dimensional dispersion $\sigma = v$. Deflection of the stars by the mass enhances the stellar density downstream more than upstream. Contours of equal stellar density are labeled with the corresponding fractional density enhancement. (From Mulder 1983.)

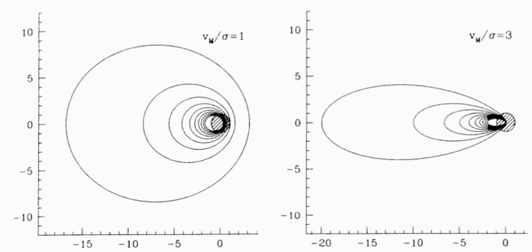

Figure 8.2 A mass M travels from left to right at speed v_M, through a homogeneous Maxwellian distribution of stars with one-dimensional dispersion σ. Deflection of the stars by the mass enhances the stellar density downstream, and the gravitational attraction of this wake on M leads to dynamical friction. The contours show lines of equal stellar density in a plane containing the mass M and the velocity vector $\mathbf{v}_M$; the velocities are $v_M = \sigma$ (left panel) and $v_M = 3\sigma$ (right panel). The fractional overdensities shown are $0.1, 0.2, \ldots, 0.9, 1$. The unit of length is chosen so that $GM/\sigma^2 = 1$. The shaded circle has unit radius and is centered at M. The overdensities are computed using equation (8.148), which is based on linear response theory; for a nonlinear treatment see Mulder (1983).

Derivation of the Retarding Force

- Consider a **single** star passing with impact parameter b
  - It experiences a force towards M of $F_p \sim GMm/b^2$ for a time $\Delta t \sim 2b / V$
- After passing by, the impulse has imparted a perpendicular velocity:
  $\Delta v_p \sim \Delta t\, F_p/m = 2GM / bV$
- The (small) angle of deflection is therefore
  $\tan\theta \sim \theta \sim \Delta v_p / V = 2GM / bV^2$
  - (this approximates the hyperbolic Kepler/Coulomb solution)
- The encounter has symmetry about the vector of closest approach i.e. the line $1/2\theta$ backwards from the original perpendicular impact parameter vector
- Newton's 3rd law demands that the impulse felt by m is equal and opposite to the impulse felt by M: $m\Delta v = M\Delta V$

Derivation of the Retarding Force

- We are interested in the component of the force **parallel** (and backwards) to the motion of M
  - (the perpendicular component will average to zero when summing over all stars)
  - So, we have for a single star's retarding force:
- $\Delta F_{drag} = -m\Delta v = -m\ 2GM/bV \tan 1/2\theta = -2G^2M^2m / b^2V^3$
- Integrating over all impact parameters ($2\pi b\, db$) and over the encounter rate nV, we get:

$$F_{\rm drag} = -\frac{4\pi G^2 M^2 nm \ln\Lambda}{V^2} = -\frac{4\pi G^2 M^2 \rho \ln\Lambda}{V^2}$$

- Here, $\Lambda = b_{max} / b_{min} = b_{max}V^2 / GM$ is the usual Coulomb logarithm, where b_{min} is defined when $\Delta v \sim V$ and b_{max} is the effective size of the region
- Note also that *nm* is simply the total density: ρ

Derivation of the Retarding Force

- Approximately, we have for ln Λ: Open clusters (6); Globular Clusters (11); L^* E galaxy (22); Galaxy clusters (7)
- Allowing for an (isotropic) field star velocity distribution, f(v), we get the **Chandrasekhar (1943) dynamical friction formula**:

$$F_{\rm drag} = -\frac{4\pi G^2 M^2 m \ln\Lambda}{V^2}\int_0^V 4\pi v^2 f(v)dv$$

- Note the approximations used in this derivation:
- M >> m the object significantly outweighs the field stars
- M << M_{sys} the responding field distribution is ~symmetric about the object
- the field stars have an isotropic velocity field
- we have ignored the self gravity of the wake

- Despite these approximations, the equation works well in a wide range of situations.

Special Cases

- if M moves **slowly** compared to the stars: V << v: we replace f(v) with f(0) to get:
  F_{drag} = $-(16/3)\,\pi^2 G^2 M^2 m \ln\Lambda\, f(0)\, V$
  - only stationary stars contribute to the wake, the rest quickly leave the area
  - Since $F_{drag} \sim V$, this resembles Stokes's law for motion through a viscous fluid.
- if M moves **fast** compared to the stars: V >> v: the integral converges, and we recover the simple equation abo e
  F_{drag} = $-(4\,\pi\, G^2 M^2 \rho \ln\Lambda) / V^2$
  - **all** stars contribute to the wake
  - since with $F_{drag} \sim V^{-2}$, the drag **decreases** for faster moving masses

Special Cases

- for a **Maxwellian** f(v), with dispersion σ, we obtain:

$$F_{\rm drag} = -\frac{4\pi G^2 M^2 nm \ln\Lambda}{V^2}\left[\mathrm{erf}(X) - \frac{2X}{\sqrt{\pi}}\exp\left(-X^2\right)\right]$$

- where X = V / σ sqrt(2) (y=erf(x)- 2x/sqrt(pi) exp($-x^2$) : 0 for X = 0 and 1.0 for X > 2.4)
- Note that the star masses enter as *nm*, ie the total mass density ρ
- the drag is therefore independent of *m*, and the equation works for a spectrum of masses
- $F_{drag} \sim M^2$: gravitationally focussed mass ~M so force ~M^2
- $F_{drag} \sim V^{-2}$: fast objects **don't** experience much drag.

Applications of Dynamical Friction

Satellite in Circular Orbit: For an isothermal galaxy with flat rotation curve V_c = const, we have: $\rho(r) = V_c^2/ 4\pi G r^2$; dispersion σ = V_c/sqrt(2) (ie X = 1); giving $F_{drag} = -0.43 \ln\Lambda\, GM^2/ r^2$

- As the satellite spirals inwards, its angular momentum is always: $L = MV_c r$ so, the rate of change of L is given by the torque:
  $dL/dt = F_{drag} r = -0.43 \ln\Lambda\, GM^2/ r$

and we get

$MV_c r\, dr/dt = -0.43 \ln\Lambda\, GM^2$

Solving ODE from initial radius r_i (at t=0) down to r=0 at t_{infall}, we get

$1/2\, r_i^2 = 0.43 \ln\Lambda\, GM / V_c\, t_{infall}$

Using as fiducials, numbers appropriate for a Globular cluster orbiting the MW:

$M = 10^6$Msun; V_c = 250 km/s; $b_{max} = r_i$ = 2 kpc; (so lnΛ ~10)

This gives:$t_{infall} \sim 2.6\text{x}10^{11}$ yr $(\ln\Lambda)^{-1}\, r_{2kpc}^2\, V_{250}\, M_6^{-1}$

so although most GCs at large radii have not significantly changed their orbits, GCs with initial radii r <1.5 kpc may have already settled to the MW center.

Applications of Dynamical Friction

Massive Galaxy Encounter

- Although this case is not strictly legitimate (M ~M_{system}) it is nevertheless instructive:
- for M ~10^{10} Msun ; r_i~20 kpc; V~V_c
- we get:
- r_{infall} ~ $2\text{x}10^8$ yr ~ 1 orbital period
- Clearly, massive galaxies entering each other's halos experience strong dynamical friction.

Applications of Dynamical Friction

- **Large and Small Magellanic Clouds**
  - For LMC, Msun 2~10^{10} M, r~60 kpc (so lnΛ~ 3) giving t_{infall}~$3\text{x}10^9$ yr, suggesting LMC should have **already** spiralled inwards
  - <u>However</u>: This assumes a circular orbit. A more thorough analysis (Murai & Fujimoto '80) requires:

  (a) that LMC & SMC have **remained bound to each other** in the past

  (b) their orbital plane includes the HI Magellanic stream (next slide)
- They find:
  - the LMC+SMC orbit is elongated with pericenter/apocenter ratio ~0.5
  - they are currently near pericenter○their orbit has decayed by x2 in radius over the past 10^{10}yr
  - the Magellanic stream came from the SMC following a close encounter with the LMC $2\text{x}10^8$ yr ago
  - the LMC and SMC will tidally separate when they come within 30 kpc of the galaxy
  - they will finally settle to the galactic center in further 10^{10} years.

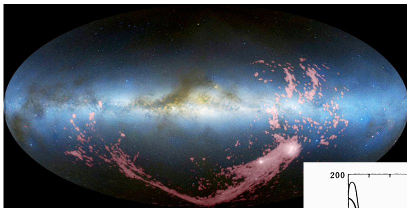

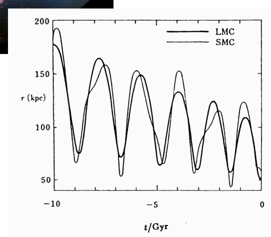

Figure 7-4. The decay of the orbit of the Magellanic Clouds around our Galaxy according to the model of Murai and Fujimoto (1980).

Tidally Driven Evaporation: Trunction and Disruption

- The outer luminosity profiles of globular clusters are **often sharply truncated**
- Naively, this is puzzling since stellar systems don't naturally have "edges"
- The reason: outer stars become more bound to the galaxy than to the GC potential This is an example of **Tidal Stripping** or **Tidal Truncation**

  (Similar effects are seen in some cluster galaxies)

Tidal Radius

- Number counts (with King profile fit), showing a steep cutoff beyond the tidal radius

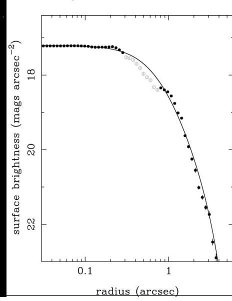

(i) Tidal (Jacobi/Roche) Limit

- How far must a star "wander" from its satellite before it is lost to the galaxy ?
  - If you answer: "where the r^{-2} force of the satellite and galaxy are balanced" you would be **wrong**
  - You forgot to include the fact that the satellite is **also orbiting the galaxy**
  - The satellite and galaxy are "fixed" only in a **rotating frame**, in which **pseudo-forces** are also important.
- In this rotating frame, the star's energy $E = 1/2\mathbf{V}^2 + \Phi(\mathbf{r})$ **is not conserved** (recall, space probes can use planets to gain energy in a "gravitational slingshot")
- Instead, the **Jacobi Integral** $E_J = 1/2\mathbf{V}^2 + \Phi_{eff}(\mathbf{r})$ **<u>is</u> conserved**; where we have again introduced the **effective potential** in a rotating frame:

  $$\Phi_{eff}(\mathbf{r}) = \Phi(\mathbf{r}) - 1/2 \mid \Omega \times \mathbf{r} \mid^2$$

  where Ω refers to the satellite's orbit and $\mathbf{r}$ has origin at the Centre of Gravity (~ galaxy center)

(i) Tidal (Jacobi/Roche) Limit

- contour plot of $\Phi_{eff}(\mathbf{r})$ for two point masses:

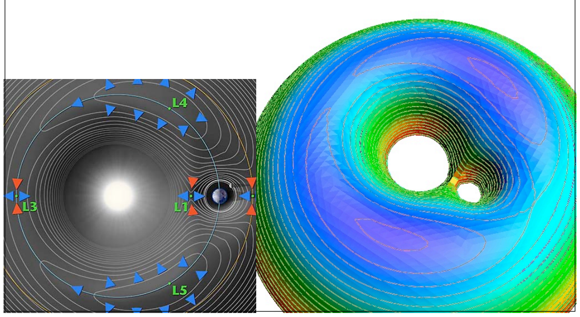

(i) Tidal (Jacobi/Roche) Limit

- Note the 5 **Lagrange points**: maxima in Φ_{eff} where stars are **stationary** (in the rotating frame)
  - L1 is the deepest; L1, L2, L3 are **unstable**; L4, L5 are **stable** (although L4, L5 are maxima, coriolis force keeps objects in a slow "epicyclic orbit" around them)
- Consider the simplest case: two point masses: a small satellite in circular orbit about a massive galaxy (ie m<<M)
  - evaluate Φ_{eff} along a line connecting m and M (separation R), with origin at m:

  $$\Phi_{eff}(x) = - GM / |R - x| - Gm / |x| - 1/2\ \Omega^2(x - R)^2$$

- Now find the turning points :
  - substitute for $\Omega^2 = GM / R^3$; differentiate w.r.t. x; set to zero and solve for $x = r_J$:
- $r_J = R(m / 3M)^{1/3}$ is the **Jacobi Limit** (also called the tidal or Roche radius, or Hill radius)

(i) Tidal (Jacobi/Roche) Limit

- If we re-calculate for the case of a galaxy with isothermal (flat V_{rot}) galaxy halo, we get:
  $r_J = R(m / 2M)^{1/3}$
- In general, a useful approximation is that r_J marks the point at which:
  – the orbital period of the satellite about the galaxy is similar to
  – the orbital period of a star about the satellite (in the absence of the galaxy).
- In practice, measured tidal radii agree **only roughly** with our simple expression for r_J.
  – The derivation should be considered as indicative rather than predictive.

(ii) Satellite Evaporation and Possible Destruction

- The value of Φ_{eff} at r_J divides stars into those which can escape from those which cannot
  – Consider a satellite star with E_J moving away from the satellite: V is decreasing as the star approaches the contour $\Phi_{eff} = E_J$, V approaches zero and the star turns around
  – Clearly, if $E_J > \Phi_{eff}(r_J)$ then the star **crosses the critical contour**
  – **If** this happens to be near L1 (or L2), the star proceeds "down hill" **and is lost from the satellite**
  – Thus, over time we expect to lose all stars with $E_J > \Phi_{eff}(r_J)$
- The satellite **evaporates**, in the sense that it is losing stars with the highest energy
  – Unlike the slow evaporation of an isolated cluster, when stars scatter into orbits with $V > V_{esc}$ tidal evaporation is **independent of scattering within the cluster**:
  – even **bound stars** (ie E < 0 for an isolated satellite) can have $E_J > \Phi_{eff}(r_J)$ and can be lost

(ii) Satellite Evaporation and Possible Destruction

- For a satellite which is **approaching** a galaxy, r_J and $\Phi_{eff}(r_J)$ continually decrease:
  – the cluster may lose an ever increasing number of stars.
- Recall from elliptical galaxy lectures that **most** stars are marginally bound (ie N(E) peaks near E~0):
  – a small decrease in $_{eff}(r_J)$ can result in the loss of many stars.
- Nice examples of tidal evaporation
  – MW globular cluster Palomar 5: (next slides)
  – simulation of the tidal destruction of a dwarf satellite by Kathryn Johnston

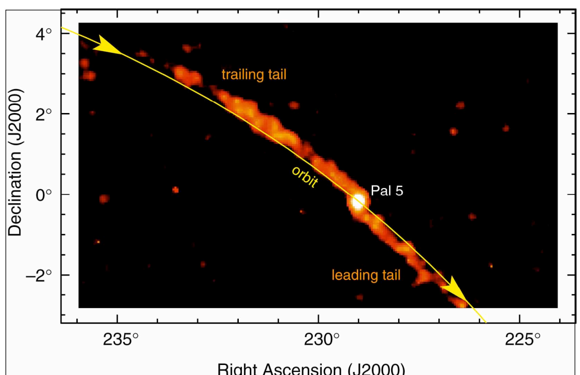

Satellite evaporation

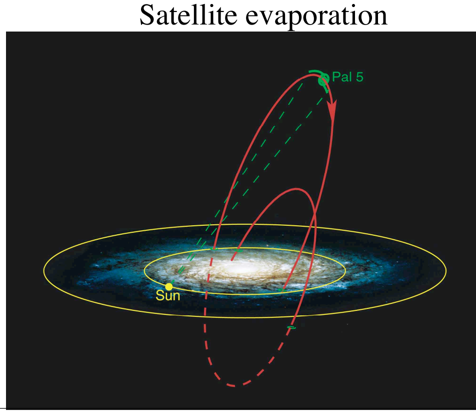

Galaxy Interactions

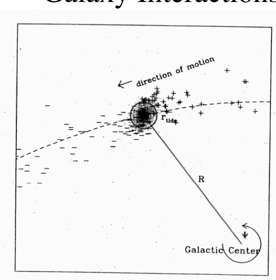

Fig. 3.— Snapshot of particle positions in the orbital plane of a simulation of a tidal encounter. The dots label particles still bound to the satellite, and the "-" and "+" signs label those unbound on orbits with lower and higher energy than the satellite orbit respectively. The dashed line shows the satellite's path. The bold circle shows the physical scale calculated from equation (3). JOHNSTON (1998)

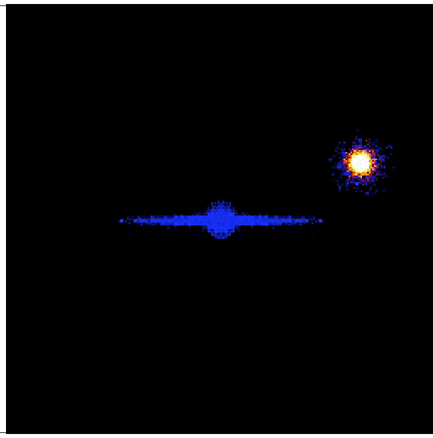

Adiabatic Approximation (Slow Encounter)

- During a tidal encounter, the orbits of many stars are significantly affected.
  - However, some orbits are **not** greatly affected: those for which $t_{orbit} << t_{encounter}$
  - As the tidal field slowly changes, the orbit responds slowly and **reversibly**
    - cf the response of the moon's orbit during the year as the Earth's distance to the sun changes
  - This type of response is called **adiabatic**
- If the encounter is a "flyby", the tidal field first grows, then decays
  - the rapid orbits slowly modify, but then **return to their original form**
  - Thus, stars on rapid orbits near galaxy centers are **not greatly affected** by tidal encounters (unless, of course, the encounter proceeds to become a merger)

Impulse Approximation (Fast Encounter: Tidal Shocks)

- The opposite extreme occurs when $t_{orbit} >> t_{encounter}$ This occurs when $V_{internal} << \Delta V_{encounter}$
- In this case **stars don't move much during the encounter**
  - no change in PE : $\Delta PE \sim 0$
- However, they do feel **an impulse**, (ie a force acting over a short time)
  - changes in both global and internal velocities: $\Delta \mathbf{V}_{CM}$ and $\Delta \mathbf{V}_{internal}$ (B&T p434-435)
  - so internal KE **does change**: KE ~ 1/2 $\Sigma m \, \Delta V_{int}^2$ (note: always +ve)
  - The effect of the tidal shock is to **heat** the stars
- We say the system has experienced a **tidal shock**

Impulse Approximation (Fast Encounter: Tidal Shocks)

How does the system respond (relax) **after** experiencing the tidal shock ?

- Loosely speaking: the increased KE causes the system to **expand** and **cool** (self gravitating star systems have -ve specific heat: eg, Collapsing gas cloud radiates energy, collapses further, and **heats up.**)
- More formally: using subscripts o="original", i="initially after encounter", and f="finally after relaxation"
- Virial theorem applies to the original and final relaxed systems: $E_o = -KE_o$ and $E_f = -KE_f$
- immediately following the encounter we have: $KE_i = KE_o + \Delta KE$ and $E_i = E_o + \Delta KE = -KE_o + \Delta KE$
- following relaxation, we have: $E_f = E_i$ -> $-KE_f = -KE_o + \Delta KE$ giving $KE_f = KE_o - \Delta KE$
- from original to final, the system has indeed **cooled**, by an amount ΔKE
- since the shock **heats** the original system by ΔKE, then **during relaxation** (i to f) the system cools by $-2\Delta KE$ (ie $KE_f = KE_i - 2\Delta KE$)
- of course, the system has also **expanded**, increasing the final PE by ΔKE

Negative Specific Heat

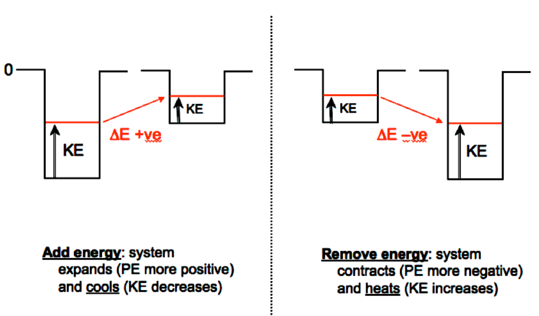

Impulse Approximation (Fast Encounter: Tidal Shocks)

- Since the stars receive energy, some may become **unbound** (E > 0)
  - these are lost from the system: they **evaporate**
  - If there are **repeated** tidal shocks, a cluster may be disrupted and **disintegrate**
- Finally, if the encounter is distant, the "tidal approximation" applies: (B&T p 437-438)
- *eg*, a spherical system (mass M, size r) is passed by a mass m at distance b with speed V
  - the change in its energy is $\Delta E \sim (4 G^2 M^2 m \, r^2) / (3 b^3 V^4)$
  - it is left elongated, long axis pointing to the point of closest approach (cf lunar tides)

Impulse Approximation (Fast Encounter: Tidal Shocks)

Examples

- Open clusters are shocked by the passage of Dense Molecular Clouds (DMCs)
  - there are very few old open clusters
  - most have evaporated from repeated shocks on a timescale ~5×10^8 yr.
- Globular Clusters are shocked when they pass through the MW disk
  - can lead to evaporative disruption (depends on where in the disk)
  - eg for GC with σ = 5 km/s, r = 10pc, V_p = 170 km/s crossing at ~3.5 kpc,
  - disruption timescale is 6×10^9 yr

Impulse Approximation (Fast Encounter: Tidal Shocks)

- Tidal shocking of galaxies in clusters is termed: **galaxy harassment**
  - disks are **heated** they get thicker and Toomre's Q parameter increases (see lecture12)
  - spiral arm formation is therefore suppressed
  - appear to have **earlier** Hubble types (eg Sb Sa)
- Also, stars and dark matter expand and are lost to the galaxy but join the cluster
- Gas, however, loses AM and goes to the center to trigger a starburst (next slide shows process in action):

Impulse Approximation (Fast Encounter: Tidal Shocks)

- Left column shows the path of a single galaxy through the galaxy cluster.
- As it is subject to tidal shocks passing the other galaxies, the stars and dark matter are heated and some are lost to the tidal field of the entire cluster.
- The evaporated stars and dark matter form a long tail.
- Right column zooms in on the **gas** in the galaxy, which steadily evolves via shocks and cooling and gravitational torques, into a compact nuclear disk.
- This disk likely gives rise to a high star formation rate.

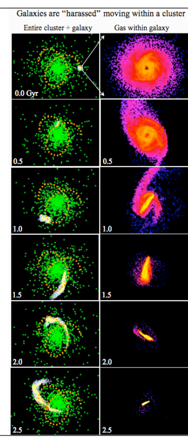

Impulse Approximation (Fast Encounter: Tidal Shocks)

- Ring galaxies are formed from tidal shocks
  - Perturber passes rapidly through & close to center of a disk galaxy ($V \gg V_c$)
  - shock induces $\Delta V_r \sim \pi V_c(V_c / V)$ radially inwards for **all stars**
  - this sets up **synchronised** epicyclic motion
  - (recall, velocity perturbations to orbiting stars yield epicyclic motion)
  - the response is an **expanding circular density wave** -> a ring !
  - these density waves can, of course, trigger star formation …. The most famous is the "cartwheel":

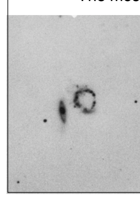

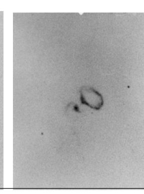

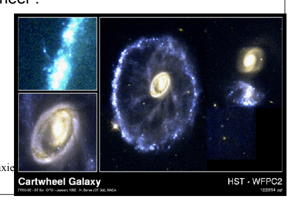

Impulse Approximation (Fast Encounter: Tidal Shocks)